UNIVERSITA' DEGLI STUDI DI VERONA

DIPARTIMENTO DI

Patologia e Diagnostica

SCUOLA DI DOTTORATO DI

Scienze Biomediche Traslazionali

DOTTORATO DI RICERCA IN

Biomedicina Traslazionale

CICLO XXIV

TITOLO DELLA TESI DI DOTTORATO:

GUIDED NANOPARTICLES FOR TUMOR IMAGING AND THERAPY

S.S.D. MED/04

Coordinatore: Prof. Cristiano Chiamulera

Tutor: Dott. Giulio Fracasso

Dottoranda: Dott.ssa Anita Boscaini

ANNO ACCADEMICO 2011-2012

Acknowledgements:

My special thanks to:

Dr. Giulio Fracasso (Dep. Pathology, Università degli Studi di Verona) for giving me the opportunity to follow the PhD course and for the useful suggestions, materials and techniques provided to develop my research.

Professor Marco Colombatti (Dep. Pathology, Università degli Studi di Verona) for being always open for discussion and supportive in sharing his experience and ideas.

Dr. Cristina Anselmi (Dep. Pathology, Università degli Studi di Verona) for her help and support during these three years.

Riassunto:

L'immunoterapia passiva basata sull'utilizzo di anticorpi monoclonali ha recentemente migliorato la risposta terapeutica e la sopravvivenza in neoplasie ematologiche e solide. Alcuni pazienti non manifestano però risposta a questi trattamenti ed inoltre possono altresi' insorgere meccanismi di resistenza; per questi motivi sono attualmente in studio clinico numerosi coniugati di anticorpi a molecole citotossiche o radionuclidi. Poiché nella terapia delle neoplasie la prognosi è fortemente influenzata dalla possibilità di una diagnosi precoce vi è la necessità di metodiche diagnostiche ad alta sensibilità e specificità; sono percio' motivo di interesse nuovi protocolli basati sull'immuno-imaging.

Nell'ottica quindi di implementare il trasporto a livello delle lesioni tumorali di elevate quantità di farmaco e di molecole trackers, le nanotecnologie possono offrire valide soluzioni. I nanosistemi presentano la caratteristica di concentrarsi a livello delle lesioni neoplasiche grazie all' "EPR Effect"; l'accumulo e la ritenzione a livello delle lesioni puo' essere implementata coniugando le nanoparticelle con molecole veicolanti quali anticorpi o fattori di crescita. Combinando quindi la nanomedicina con la tecnologia degli anticorpi ricombinanti è possibile incrementare notevolmente la specificità dei trattamenti antitumorali, permettendo quindi anche la diminuzione delle dosi utilizzate e aumentare la sensibilità dei sistemi diagnostici attualmente in uso (MRI).

Il presente lavoro di tesi, svolto in collaborazione con il gruppo del Prof. Meneghetti (Università di Padova) e con i gruppi del Prof. Mancin e del Prof Papini (Università di Padova) nell'ambito del progetto europeo Nanophoto, descrive la generazione e caratterizzazione di diverse tipologie di nanocomposti e il loro possibile impiego nell'imaging e nella terapia antitumorale.

La prima parte dello studio è stata incentrata sulla sintesi e caratterizzazione di nanoparticelle metalliche, oro e ossido di Fe, non guidate. L'oro è un materiale utilizzato in medicina per la sua biocompatibilità e per le sue particolari proprietà chimiche e ottiche. Tra queste è interessante la possibilità di produrre segnale Raman, che può essere amplificato piu' di 108 volte se caricate con molecole SERS. Abbiamo dimostrato che è possibile quantificare mediante spettroscopia Raman la quantità di NPs incorporata dalle cellule. Questo risultato pone le basi per un sistema ultrasensibile di rivelazione della quantità di nanosistemi veicolati a livello delle lesioni neoplastiche. Mediante l'applicazione di nanoparticelle di FeOX (nanoparticelle magnetiche) abbiamo evidenziato che: a) è possibile utilizzate le NP mag-

netiche per il sorting di popolazioni cellulari modificate (vd. Cellule caricate con FeOX-NPs adsorbite con SiRNA o cDNA) b) è possibile, mediante campi magnetici esterni, direzionare ai siti di interesse specifiche popolazioni cellulari (es. Cellule T anti-tumore o macrofagi, caricati con FeOX-NPs).

La seconda parte dello studio si è focalizzata sull'analisi del targeting di nanoparticelle d'oro e di silice, coniugate ad anticorpi monoclonali specifici per TAA, al fine di implementarne l'accumulo a livello del sito d'interesse. La specificità di legame e l'internalizzazione di questi nanocomposti è stata dimostrata "in vitro" e "ex vivo" utilizzando cellule antigene positive e negative e tessuti espiantati da modelli murini singenici (topi C57/B16 iniettati sc con cellule B16 trasfettate con gli Ags di interesse). E' stato inoltre valutato "in vitro" il potenziale terapeutico sia di nanoparticelle d'oro caricate con un agente chemioterapico, la doxorubicina, sia di nanoparticelle di silice caricate con l'agente fotosensibilizzante Foscan®. In entrambi i casi, i risultati ottenuti sono promettenti; si è evidenziata, infatti, una tossicità del 60% e 40% maggiore rispetto alle NP non caricate, utilizzando rispettivamente NP caricate con Doxorubicina e Foscan®. Abbiamo inoltre dimostrato che è possibile rilevare singole cellule Ag positive ed inoltre è possibile sviluppare protocolli di imaging multi-target, mediante spettroscopia Raman e nanosistemi d'oro veicolati con diversi mAbs e caricati con molecole SERS.

Abstract

The passive immunotherapy based on the use of monoclonal antibodies has recently improved the therapeutic response and survival in hematologic and solid tumor. However, some patients show no response to these treatments, moreover a resistance mechanism can rise up. For these reasons many conjugates of antibodies and radionuclides or cytotoxic molecules are currently in clinical trials. As in the cancer treatment, the prognosis is strongly influenced by the possibility of an early diagnosis; there is the neccesity of diagnostic methods with high sensitivity and specificity. Therefore in the last years new protocols based on immunoimaging are object of interest. In order to increase the transport of a large amount of drug and tracker molecules at tumor lesions site, nanotechnology can offer effective solutions. The nanosystems have the characteristic to focus in neoplastic lesions thanks to the EPR effect; the accumulation and the retention in the injury sites can be implemented by conjugating nanoparticles with targeting moieties such as antibodies or growth factors. Combining nanomedicine together with recombinant antibody technology, it is possible to increase the

specificity of cancer treatments greatly, thus allowing the decrease of therapeutic doses and increasing the sensitivity of diagnostic tools currently used (MRI).

This thesis work was done in collaboration with the reaserch group of Prof. Meneghetti (University of Padua) and the groups of Prof. Mancin and Prof. Papini (University of Padua) in the context of the European project “Nanophoto”. The work describes the production and characterization of different types of nanoconjugates and their potential use in imaging and cancer therapy.

The first part of the study was focused on the synthesis and characterization of metal nanoparticles, gold and iron oxide, not targeted. Gold is a material used in medicine thanks to its biocompatibility and its unique chemical and optical properties. Among these, the ability to produce Raman signal is interesting, this can be amplified more than 108 times by using SERS dies. We have shown that by Raman spectroscopy it is possible to quantify the amount of NPs uptaken by the cells. This result provides the basis for an ultrasensitive method that can detect the amount of nanocompound conveyed at neoplatic lesions. By applying FeOX-MNPs (magnetic nanoparticles) we have shown that: a) magnetic NPs can be used to sort modified cell populations (see cells loaded with FeOX-MNPs coated with siRNA or cDNA) b) it is possible to direct into the site of interest specific cell populations by external magnetic field (see anti tumor T cells or macrophage, loaded with FeOX MNPs).

The second part of the study was focused on the analysis of the targeting of gold and silica nanoparticles, conjugated to monoclonal antibodies specific for TAAs, in order to increase the accumulation in the site of interest. The binding specificity and internalization of these nanocompounds has been demonstrated “in vitro” and “ex vivo” using antigen positive and negative cells and tissue harvested from syngenic mouse models (C57/B16 mice injected sc with B16 cells transfected with the Ags of interest).

It was also assessed “in vitro” the therapeutic potential of both gold nanoparticles, loaded with a chemoterapeutic agent, doxorubicin, and silica nanoparticles loaded with the photosensitiser Foscan®. In both cases the results are promising: it is highlighted a toxicity of 60% and 40% greater than not loaded NPs, using NPs loaded with doxorubicin and Foscan® respectively. We have also proved that it is possible to detect single antigen positive cells and develope multi-target methods, by using Raman spectroscopy and gold nanoparticles conjugated with different mAbs and loaded with SERS dies.

INDEX:

Abbreviations used:

Ab/Abs	Antibody/antibodies
Ag	Antigen
APC	Allophycocyanin
AuNPs	Gold nanoparticles
BSA	Bovine Serum Anbumin
CaP	Prostate carcinoma
cpm	Counts per minutes
Doxo	Doxorubicin
DMSO	Dimethyl sulfoxide
DTT	Dithiothreitol
EDTA	Ethylenediaminetetraacetic Acid
EGFR	epidermal growth factor receptor
FDA	Food and Drug Administration
FCS	FITC Fluorescein isothiocyanate
hr/hrs	Hour/hours
Ig	Immunoglobulin
LASiS	Laser Ablations Synthesis in Solution
mAb	Monoclonal antibody
MBS	3-Maleimidobenzoic acid N-hydroxysuccinimide ester
MG	Malachite green
MFI	Medium Fluorescence Intensity
MNPs	Magnetic nanoparticles
MRI	Magnetic Resonance Imaging
mTHPC	meta-tetra (hydroxyphenyl) chlorine

NIR	Near InfraRed
NPs	Nanoparticles
O_2•	Reactive singlet oxygen
o.n.	overnight
PDT	Photodymanic therapy
PEG	Polyethylene glycol
PBS	Phosphate Buffered Saline
PMA	Phorbol 12 myristate 13 acetate
PSA	Prostatic Specific Antigen
PSCA	Prostate Stem Cell Antigen
PSMA	Prostate Specific Membrane Antigen
QDs	Quantum Dots
ROS	reactive oxygen species
rpm	Revolutions per minute
RT	Room temperature
RT PCR	Real time PCR
SERS	Surface enhanced resonant Raman scattering
SiO_2-NPs	Silica nanoparticles
SDS	Sodium dodecyl sulfate
SPDP	N-Succinimidyl-3-(2-Pyridylthio)Propionate
SPR	Surface plasmon resonance
TAA	Tumor Associated Antigen
TEM	Transmission electron microscope
TR	Texas red
^{3} HTdr	Triziate-Thymidine
2 IT	2 iminothiolane

INTRODUCTION

1. CANCER IMMUNOTHERAPY

The term "cancer" refers to the uncontrolled proliferation of tissue as a result of mutations in the portions of DNA that control cell growth (genes for growth factors and their receptors, intracellular transducers genes, genes for nuclear transcription factors). Further alterations may confer upon cells the ability to degrade the basal lamina constituents such as collagen, proteoglycans and glycosaminoglycans, in order to evade the immune system and to ignore the contact with cells of different tissue: in these cases you realize the characteristics of invasive surrounding tissue and spread away from the site of onset, typical of cancer "evil" [*Wikipedia. org*].

The extent and grade of disease progression are described, for most cancers, with the TNM (Tumor Node Metastasis) staging system [*Robbins 1999*] developed by the American Joint commits on Cancer (AJCC). According to this protocol, tumor characterization must be defined through a careful history and appropriate techniques of investigation. This type of characterization has a high prognostic value and impact, before other factors, driving the choice of which treatment approach to adopt.

In general we can say that the surgical removal of the tumor is the first-line treatment of localized solid tumors and radiotherapy or chemotherapy adjuvanted protocols are applied to decrease the risk of recurrence.

Chemotherapy can also be performed before surgery as neoadjuvant or primary therapy in order to facilitate tumor removal. Radiation therapy is useful in case of locally advanced tumors. In the later stages due to the presence of metastases, the best treatment is chemotherapy for its systemic action. Given the high toxicity, it alters the "performance status" (a measure of quality of life of the patient) and current lines of research are intended to identify the best protocols to combine the efficacy and tolerability of treatment. The chemotherapeutic agents are drugs with low therapeutic index, given their high potential to cause serious side effects, using them in effectively and safely manner requires a deep knowledge of the pharmacokinetics, pharmacodynamics and drug interactions. In the recent years many re-

sources are designed to improve not only the aspect of prevention, but also the therapeutic strategies are aimed at finding new ways to implement the poor results of current treatments in patients in advanced stages. Among these, one of the most promising is the immunotherapy. At the beginning of the 20th century, scientists suggested the potential for using the body's own defence systems treating cancer. In 1968, Porter and Edelman managed to identify and structurally characterize a class of serum proteins that could bind a virtually unlimited variety of molecular targets with high specificity: the immunoglobulins. Few years later, in 1975, immunoglobulins became available as tools for research and clinical purposes thanks to the development of the hybridoma technology by Köhler e Milstein, which allowed the custom generation and large-scale production of monoclonal antibodies (mAbs) of murine origin [*Köhler and Milstein, 1975; Schrama et al., 2006*].

Since the early 80's more than 200 mAbs with anti-cancer potential have been investigated in clinical trials by academic and private institutions. Although the first attempts failed to provide a clear evidence of beneficial effects on patients, antibody-based drugs (immunotherapeutics) have, by now, become important tools in the treatment of an increasing number of human malignancies. To date twelve mAbs have been FDA approved and marketed for cancer treatment [*Reichert et al., 2005; Reichert and Valge-Archer, 2007*].

Cancer immunotherapy can be divided into active and passive immunotherapy:

- The passive immunotherapy consists of in the administration to the patient of immunological effectors directed to a target antigen: they can be molecules such as monoclonal antibodies (mAb) alone or conjugated to toxins or cytokines (eg IL-2) or cells such as tumor-specific T lymphocytes isolated from the patient, expanded ex vivo and subcultured;
- The active immunotherapy involves the stimulation of the patient's immune response against tumor cells (vaccination) through the administration of antigen (Ag) in various shapes (eg recombinant proteins, cDNAs inserted into a plasmid and / or a viral vector, peptides) or by using tumor cells unable to replicate (apoptotic or necrotic) or by loaded immune cells..

Immunotherapy can act through one or more mechanisms:

1. Stimulating host antitumor response by increasing the number of effector cells or by producing one or more soluble mediators.
2. By reducing the immunosuppressive mechanisms of the host

3. Altering tumor cells to increase their immunogenicity or to make them more susceptible to be damaged by effector cells.

The major impediment in the clinical use of mAb is that they are xenogeneic proteins, because typically produced in mice; this leads rapidly to the onset, after a few doses of an antibody response against the murine Ab (HAMA, human anti-mouse antibody). The problem of immunogenicity, together with the difficulty of identifying possible tumor-specific targets, has been for a long time the greatest obstacle to the spread of the mAb in clinical practice.

The immunogenicity problem has been approached with different strategies:

- Transformation of human B-lymphocytes with Epstein Barr virus: a herpes virus that infects and immortalizes B-lymphocytes specifically human. However, this technique is not yet widely used because it has several drawbacks (eg. high probability that the donor has already contracted EBV, therefore the cytotoxic T lymphocytes specific against EBV can attack and kill the new B cells just trasformed with EBV, preventing their immortalization);
- Chimeric Ab: obtained by linking the variable domain of heavy and light chains (VL, VH) of murine origin to the constant domains (CL, CH1-CH2-CH3) of human immunoglobulins using recombinant DNA techniques;
- Humanized Ab: obtained by transferring the binding region (CDR1-2-3-) from mouse mAb to the molecular structure of a human immunoglobulin;
- Human Ab: human Ab fragments (Fab or scFv) isolated by selection from phage display libraries or produced by transgenic mice (Xenomouse) then linked with costant domain of human immunoglobulin. This type of Ab has the undoubted advantage over previous ones, to be fully human and thus completely overcome the problems of immunogenicity. [*N. Stricker et al., 2001; L.L.Green 1999; M. Little et al.,2006; A.Cecilia Roque et al., 2004*].

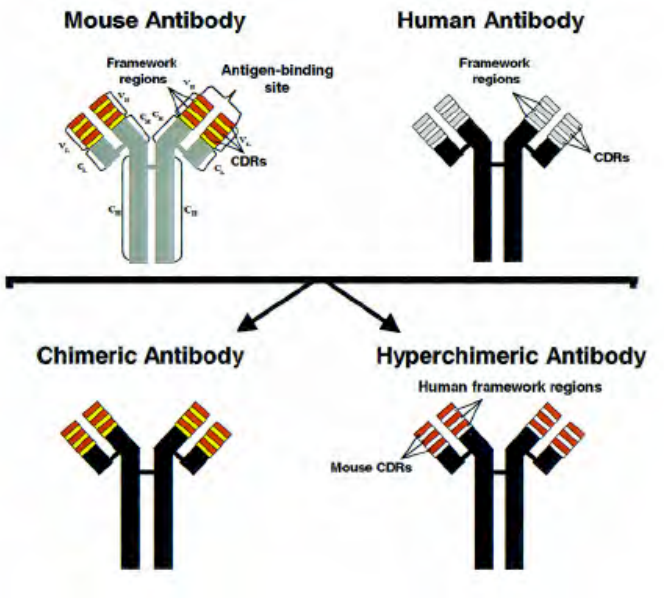

Fig 1: Graphical representation of murine Ab, chimeric and hyperchimeric.

The effector functions of a naked Ab (non-conjugated to other molecules) can be:

- Antibody-mediated cellular cytotoxicity (ADCC): its target is triggered by the interaction between the Fc region of an Ab bound and the receptor for the Fc region located on the membrane of effector cells (macrophages, neutrophils and natural killer cells) in order to mediate phagocytosis and lysis of the target cell;
- Complement-mediated cytotoxicity: in this case IgM and / or IgG bound to target cells trigger an enzymatic cascade (the complement system) which, through a series of proteolytic cleavage and association of molecules, that finish with the formation of membrane attack complex (MAC), and in the osmotic lysis of the cell;
- Signal trasduction interference: mAb may play anti-cancer activity blocking the cellular signaling pathways involved in cell proliferation or resistance to apoptosis, these pathways can be triggered either by contact mechanical or by receptors such as those for growth factors (eg EGFR). [Adams and Weiner, 2005; Sharkey and Goldenberg, 2006]

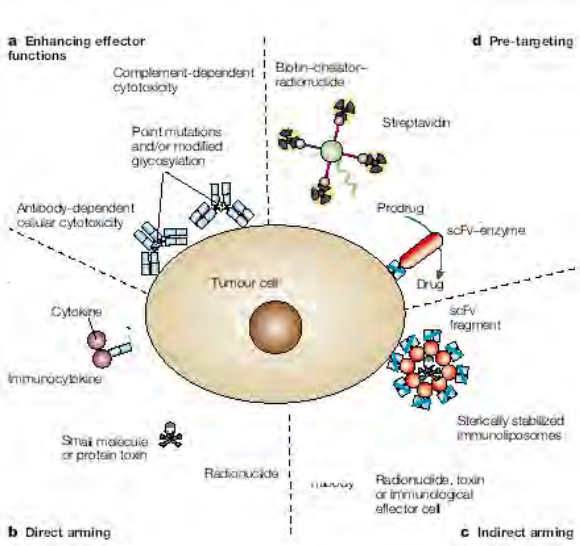

Fig 2: Representation of the possible use of mAb naked in order to increase their cytotoxic potential**.**

In some cases these effector functions are not sufficient because malignant cells can be very resistant to the induction of apoptosis and the immune system of the patient can be defective in triggering responses like ADCC. Furthermore naked antibodies attack only antigen-positive cells so bystander effect cannot be exploited.

Some options have been investigated to improved the killing efficacy of mAb in cancer therapy:

- directly armed Ab obtained by the covalent bond with toxins, Ab used as chelating agents for radionuclides or chemotherapeutics. The directly armed Ab are a good way to overcome the tumor escape mechanisms; [*Pastan et al., 2006; Wu and Senter 2005*]
- indirectly armed Ab: Ab fragments such, as scFv are chemically bonded to the surface of liposomes loaded with chemotherapeutic agents or toxins, in this way it can be carried a great amount of drug, protecting it from the attach of immune system.
- pre-targeting, by means of prodrugs or radionuclides; in the first case using fragments of Ab bound to enzymes that activate prodrugs selectively in cancer tissues, in the latter case biotinylated Ab are used at first and then streptavidin complex + radionuclide, in order to reduce non-specific targeting and side effects. [*M. Little et al; 2006*].

Among the twelve monoclonal antibodies currently approved for use in immunotherapy, eight are naked antibodies, three are labelled with radionuclides and one is chemically conjugated to a toxic moiety, calicheamicin (fig 3) [*Reichert and Valge-Archer, 2007; Reichert et al., 2005*].

Since the high molecular size of the whole Ab makes difficult the penetration at the level of the tumor lesions (it is estimated that only 0.01% of the administered dose reaches the tumor

site) [*Epenetos A et al, 1986*] new recombinant Ab were produced by reverse transcription of mRNA of human mAb variable regions derived from peripheral blood B cells from pre-immunized or naive donors. The obtained cDNA is then amplified by PCR and inserted into appropriate vectors.

Generic name (trade name)	Description	First approval indication	Year (country) of first approval
Unconjugated mAbs			
Edrecolomab (Panorex)	Murine, IgG2a, anti-EpCAM	Colorectal cancer	1995 (Germany)*
Rituximab (Rituxan)	Chimeric, IgG1, anti-CD20	Non-Hodgkin's lymphoma	1997 (United States)
Trastuzumab (Herceptin)	Humanized, IgG1, anti-HER2	Breast cancer	1998 (United States)
Alemtuzumab (Campath)	Humanized, IgG1, anti-CD52	Chronic lymphocytic leukemia	2001
Cetuximab (Erbitux)	Chimeric, IgG1, anti-EGF receptor	Colorectal cancer	2004
Bevacizumab (Avastin)	Humanized, IgG1, anti-VEGF	Colorectal cancer Non small-cell lung cancer Advanced Breast cancer	2004 2006 2008 (United States)
Nimotuzumab (TheraCIM)	Humanized, IgG1, anti-EGF receptor	head/neck epithelial cancer	2005 (China)
Panitumumab (Vectibix)	Human, IgG2, anti-EGF receptor	Colorectal cancer	2006 (United States)
Immunoconjugates			
Gemtuzumab ozogamicin (Mylotarg)	Humanized, IgG4 k, anti-CD33, immunotoxin (calicheamicin)	Acute myelogenous leukemia (AML)	2000 (United States)
Ibritumomab tiuxetan (Zevalin)	Murine, IgG1, anti-CD20, radiolabelled (Y-90)	Non-Hodgkin's lymphoma	2002 (United States)
^{131}I-Tositumomab (Bexxar)	Murine, IgG2a, anti-CD20, radiolabelled (I-131)	Non-Hodgkin's lymphoma	2003 (United States)
^{131}I-ch-TNT	Chimeric, IgG1k, anti-DNA associated antigens, radiolabelled (I-131)	Lung cancer	2003 (China)

Table 1: Monoclonal antibodies approved for cancer therapy (updated from Reichert and Valger-Archer 2007; Sharkey et al 2008)

2. ANTIBODY AND TUMOR ASSOCIATED ANTIGEN

A very important input to the development of tumor immunotherapy was due to the discovery of several tumor antigens (nowadays over 2000, the updated list is available at the website http://www2.licr.org/CancerImmunomeDB/) able to generate a specific immune response against the tumors. Targeting TAA is emerging as a promising area for controlling and monitoring the immune responses to tumor cells in cancer patients and during immunotherapeutic protocols.

A good tumor antigen should be immunogenic (it should elicit an immunological response), and has a restricted expression pattern (expressed only or preferentially by tumor cells than by normal tissues) and be indispensable to tumor cells giving them an advantage of its proliferative characteristics or other tumoral features, in this way tumor cells can not limit the protein expression and carry out an immune escape.

Most of these antigens have been identified in melanoma, but in the recent years an increasing number of works have described TAA associated with the most common forms of tumor. It follows a brief description of TAA considered as target on this thesis.

- The PSCA (Prostate Stem Cell Antigen) is a 123 amino acids glycoprotein first identified in the LAPC-4 prostate xenograft mode of human CaP (Prostate cancer) [Reiter et al., 1998]. It is a member of the GPI anchored proteins, molecules joined to the plasma membrane by a glycosylphosphatidylinositol moiety. Its functions are still unknown, but given its homology with the Stem Antigen 2 (SCA-2) one might assume a role in signal transduction or in cell adhesion. This protein is normally expressed at low levels in a subpopulation of basal and secretory cells of some organs such as the colon, stomach, prostate, but PSCA overexpression was discovered in transitional cell carcinoma of the bladder, pancreatic adenocarcinomas, clear renal cell carcinoma and in prostate cancer. PSCA overexpression correlates with a high risk of recurrence and/or distant metastases and so cancer treatment often requires the use of external beam radiotherapy after primary therapy for human CaP. Furthermore its resctricted expression in normal tissue makes PSCA an interesting target for immunotherapy. Several anti PSCA mAb have been generated (4A10, 1G8, 3E6 etc…) conjugated to toxins or in combination with chemotherapics drug and are still studied in phase I clinical trials. [Reither *et al, 1998; Yong Li et al, 2009*]

- Recent studies have found an antigen, the PSMA (Prostate Specific Membrane Antigen), which could be an ideal target antigen. Contrary to other antigens associated with prostate tissue, such as PSA or prostatic acid phosphatase (PAP), which are released secreted protein, the PSMA is a glycoprotein expressed on the surface of both healthy and neoplastic prostate cells. Its expression increases substantially in primary carcinoma in metastatic disease and hormone-refractory prostate cancer, its level increases in relation to the severity of the disease (Gleason score). PSMA is also expressed by healthy prostate cells, small intestine, proximal renal tubules, salivary glands and in some brain areas, but the level of expression in these normal tissues is 100-1,000 times lower than the level observed in malignant prostate. It is also present in high levels in newly formed blood vessels infiltrating the tumor and not in vascular endothelium of normal tissues. [*S.S. Chang et al, 1999; R.S. Israeli et al, 1994; S.S. Chang, V.E. Reuter et al, 1999*). These data are very intriguing because it indicates that PSMA could be used as a target for antivascular therapies in some types of cancer, due the role that new vessels have for the development and survival of solid tumors. The PSMA is a type II protein of 110 kDa, with a short N-terminal cytoplasmic domain (19 aa), a hydrophobic transmembrane region (24 aa) and a large C-terminal extracellular domain (707 aa). PSMA gene was cloned, sequenced and mapped to chromosome 11p and it is composed of 19 exons that encode a type II transmembrane protein. Some variants of this molecule have been identified, whose presence is supposed to be due to alternative splicing events. There are studies that suggest for PSMA multiple functions. Structurally, its highly glycosylated extracellular region has 54% homology with the transferrin receptor, and the fact that it is internalized through clathrin-coated endocytic vesicles may indicate that it is a receptor for an unknown ligand. Internalization is mediated by the 5 aa N-terminal tail (MWNLL) and the deletion of this amino acid tail inhibits the process of endocytosis; the internalization motif (L-L) also present in the transferrin receptor are not critical for internalization. [*S.S. Chang et al, 2004; M.I.Davis et al, 2005*]

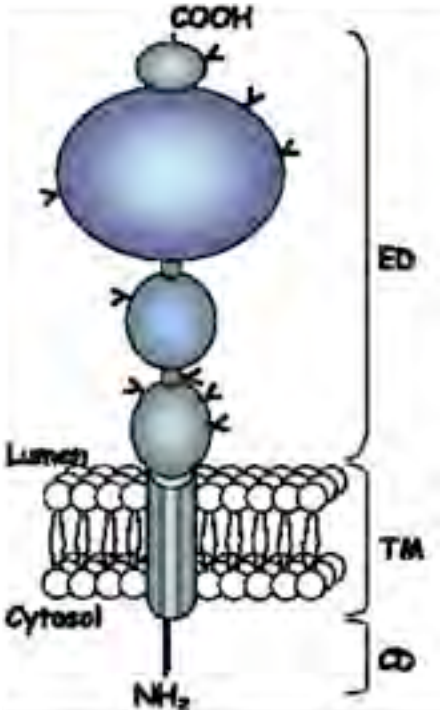

Fig 3: Representation of PSMA structure ED: extracellular domain TM: transmembrane region CD: cytoplasmatic domain. [Am J Physiol Cell Physiol, 2005].

It remains unclear the role of PSMA in the physiology of prostate cancer. It has been proposed that enzymatic activity of folate hydrolase could be involved in the mechanisms of resistance to methotrexate. It also seems to have carboxypeptidase activity, so it may be implicated in the neuroendocrine regulation of growth and differentiation of prostate cells. The peptidase activity may also trigger a cascade of signals involved in the survival, proliferation and cell migration. [*Sven et al, 2007*]

The interaction of PSMA with filamin A, a phosphoprotein devoted to stabilize many membrane receptors and to regulate cell adhesion and mobility, indicates its possible involvement in cell migration. Furthermore our group has demonstrated that the cross linking of cell surface PSMA with specific antibodies activates an enzymatic cascate, with an increased expression of IL6 and CCL5 gene as final downstream effect. IL6 and CCL5 are involved in LNCaP proliferation. The novel role attribuited to PSMA have a relevant influence on the survival and proliferation of prostate tumor cells. All these conclusions are confirmed by observation that PSMA overexpression is related to a worse prognosis. [*Colombatti et al, 2009*]

PSMA was originally identified and characterized by 7E11c mAb, which was subsequently approved by FDA for diagnostic applications. However recognizing 7E11c an intracellular

epitope is unable to bind viable cells but only necrotic or apoptotic cells within a tumor mass. Therefore a new series of monoclonal antibody, J591, J415, J533, E99 were developed which recognize epitopes in the extracellular domain of PSMA and therefore are able to bind viable cells. In particular, mAb J591 is currently investigated in numerous studies and clinical trilas for diagnostic and therapeutic purpose. Humanized recombinant mAb J591 has been genetically modified to replace certain regions of the mouse protein with human sequenze that are less likely to induce the possibility of human anti mouse antibody (HAMA) response.

Humanized J591 was administered conjugated to the radionuclides I^{131}, Y^{90}, Lu^{177} and to the chemotherapic drug DM1. The results of these studies in terms of therapeutic effectiveness were encouraging. Phase I clinical trials have shown little toxicity, specific targeting to CaP lesions, and therapeutical activity in patients. Phase II clinical trials are currently under way to further evaluate the efficacy of these treatments. [*A. Ghosh et al, 2005; S. Chang et al, 2001: RT. Kipp et al, 2007: Bander et al, 2002*]

- EGFR (epidermal growth factor receptor) was identified firstly in 1980 by the Nobel Prize Stanley Cohen. This receptor is a member of the family receptor called ErbB, with intrinsic tirosin Kinase activity. It is a transmembrane glycoprotein of 170 KDa. The structure of the receptor ErbB family shows a common structure that is schematized in three separated region: 1) an extracellular domain, binding site for different growth factor. 2) a trans membrane domain, membrane anchoring site. 3) an intracellular domain, responsible for the activation of the receptor and the intracellular signaling cascade.

  The EGFR is activated by binding of its specific ligands, including epidermal growth factor (EGF), TGF-α (Trasforming Growth Factor-α), amphiregulin, HB-EGF (Heparin Binding EGF), betacellulin, epiregulin, epigen, neuregulins 1,2,3 and 4 [*Lafky et al., 2008*].

  Upon activation by its growth factor ligands, EGFR undergoes a multistep process that facilitates the transmission of signals from the extracellular environment to the nucleus such as: 1) receptor dimerization due to a conformational change induced by binding receptor-ligand complex and formation of homodimers or heterodimers with ErbB-2. 2) the tyrosin kynase domain phosphorylates tyrosine residue present in the tail of its C terminal dimerization partner in a process called autophosphorylation. 3) the recruitment of cytosolic adapter proteins, responsible for signal transduction. This activity is subject to strict controls, if a malignant transformation is going on the controls fail with conse-

quences such as increased proliferative activity, inhibition of apoptosis, the triggering of angiogenetic processes, and metastatic invasion of the sorrounding tissues.

The receptor is also internalized after binding to his ligand by endocytosis through clathrin-coated vesicles. It was proposed that inside these vesicles the receptor is degraded. In this way the cytosolic domain is able to reach the nucleus and act as a transcription factor. Alternatively the entire receptor once activated and associated with EGF can move directly into the nucleus. These results explain the tumor resistance to drugs that act only by blocking the trasduced signal from the receptor. [*Thariat et al., 2007*]

The healthy cells express normal levels of EGFR between 40,000 and 100,000 molecules/cell [*Zimmermann et al., 2006*] while in many tumors it is an overexpression of EGFR and an increased production of its ligand. Particulary the EGFR is overexpressed in adenocarcinomas, especially colorectal cancer, non-small cell lung cancer (NSCLC) and squamous cancers of head and neck, where high levels of EGFR mRNA and proteins are found in 80 to 90% of patients.

Numerous studies indicate that blockade of the EGFR pathway by an anti EGFR antibody results G1 phase arrest, in inhibition of invasion, and /or in activation of apoptosis in metastatic CaP cells (in vitro and in vivo experiments). So several therapeutic strategies have developed that target this receptor and its effector pathways, either individually or in combination with chemotherapy. Some anti EGFR drugs are currently FDA approved or in clinical trials, including small inhibitory molecole, as well as antibodies such as Cetuximab.

Cetuximab, trade name Erbitux ®, is an IgG1 chimeric monoclonal antibody recognizing the extracellular domain of EGFR, with an affinity 5-10 times higher than that of the endogenous ligands [*Sato et al; 1983*]. The U.S. Food and Drug Administration (FDA) [www.fda.gov/Drugs] approved the use of cetuximab, alone or in combination with other standard chemotherapeutic drug, for the first time in February 2004, for treatment of patients with metastatic colorectal cancer (mCRC). Erbitux is now able to potentiate the effects of both antineoplastic chemotherapy and radiation therapy; it is indicated for the treatment of patients with colorectal cancer and for the treatment of patients with head-neck squamous cell carcinoma.

Antigen	Preclinical studies	Clinicals Trials
PSA : *prostate specific antigen*	Negative	Left
PSMA: *prostate specific membrane antigen*	Positive	On going
PSCA: *prostate stem cell antigen*	Positive	On going
HER/2: *prostate stem cell antigen*	Positive	Left- new mAb considered
EGFR: *epidermal growth factor receptor*	Positive borderline	Blocked
VEGF: *prostate stem cell antigen*	Positive	On going
MUC1	Positive	On going

Table 2: Prostate tumor associated antigen (TAA) actually used in immunotherapy.

3. PROBLEMS AND LIMITATIONS OF IMMUNOTHERAPY

Cancer diagnosis and treatment are of great interest due to the widespread incidence of the diseases, high death rate, and recurrence after treatment. Current diagnostic and prognostic classifications do not reflect the whole clinical heterogeneity of tumor and are insufficient to make prediction for successful treatment of patient out come. In Europe there were an estimated 3.2 million new cases of cancer and 1.7 million deaths from cancer in 2008. The most common cancers were colorectal cancers (436,000 cases, 13.6% of the total), breast cancer (421,000, 13.1%), lung cancer (391,000, 12.2%) and prostate cancer (382,000, 11.9%). The most common causes of cancer death were lung cancer (342,000 deaths, 19.9% of the total), colorectal cancer (212,000 deaths, 12.3%), breast cancer (129,000, 7.5%) and stomach cancer (117,000, 6.8%). [*Ferlay et al; 2010*]

Most current anticancer agents do not greatly differentiate between cancerous and normal cells, leading to systemic toxicity and adverse effect. Consequently systemic application of these drugs often causes severe side effects in other tissues (such as bone marrow suppression, cardiomyopathy, and neurotoxicity), which greatly limit the maximal allowable dose of the drug. In addition, rapid elimination and widespread distribution into nontargeted organs and tissues require the administration of a drug in large quantities, which is not economical and often complicated owing to nonspecific toxicity.

The use of immunotherapy like monoclonal antibody can differentiate between cancer and normal cells, reducing systemic toxicity and side effects. But despite their broader use as targeting tool, mAbs based terapies still present several problems that have to be resolved completely: immunogenicity, selectivity and penetration into solid tumours. The problem of immunogenicity has been quite resolved by now, thanks to the enormous progress in mAb engineering, even if execept for few mAbs, the other FDA approved mAbs have at least CDR sequences derived of murine origin. To increase the mAb selectivity and thereby to reduce unspecific toxicity, new tumor antigens and respective mAbs have to be identified.

Besides to affect solid tumor, the therapeutic agent must overcome several obstacles, including the vascular endothelium, stromal and epithelial barriers and the high interstitial pressure, these limitations cause the low penetration of administered antibodies around tumor tissue. Moreover renal clearance and uptake and degradation by immune system effectors decrease their penetration further. Furthermore cancer cells can down regulate class I major histocompatibility complex, which inhibits recognition by cytotoxic T lymphocytes, similary cancer cells can mutate or downregulate surface targets for antibody recognition. In addition, solid tumors are quite heterogeneous and it is therefore difficult to target them completely. Side effects and safety issues era common and unavoidable in antibody therapy, the possible toxicities are either antibody-antigen binding mechanism dependent, including cardiac dysfunction, infusion reactions, infections and transitori lymphocyte B depletion, or mechanism indipendent such as hypersensitivity reactions, fever, chill, headache and hypotension. Another limit finally consists in the small amount of ligand (drugs, trackers, toxins) that can be cojugated to an antibody; furthermore most of the chemoterapeutic agents are poorly water-soluble and are formulated with toxic solvent.

This problem can be overcome by incorporating the anticancer drugs into various hydrophobic nanocarriers to improve solubility of lipophilic compounds.

Nanotechnology offers a more targeted approach and could thus provide significant benefits to cancer patients. In fact, the use of nanoparticles for drug delivery and targeting is likely one of the most exciting and clinically important applications of cancer nanotechnology. Nanomedicine combinated with the use of mAb as targeting moieties has the potential to increase the specific tratment of cancer cells while leaving healthy cells intact throught the use of nanoparticles to seek and treat cancer in the human body. [Young-Eun *Choi et al, 2010; Shuming et al, 2007*]

4. NANOSCIENCE AND NANOTECHNOLOGY

Nanoscience definition given by Royal Society & The Royal Academy of Engineering (UK) is: *"Nanoscience is the study of phenomena and manipulation of materials at atomic, molecular and macromolecular scales, where properties differ significantly from those at a larger scale"* and *"Nanotechnology is the design, characterisation, production and application of structures, devices and systems by controlling shape and size at nanometre scale".*

In the latest years nanoscience has become one of the most exciting area in science. In literature there are a great number of definitions for the term nanotechnologies. A common definition for nanotechnology is: " the design, characterization, production and application of materials, devices and systems by controlling shape and size of the nano scale", where nano scale is consensually considered to cover the range from 1 to 100 nm. [*Ramsden, 2009*]

Fig 4: Nanotechnology is the meeting point of different scientific disciplines. (from: www.Keralaevents.com)

The history of nanotechnology began in 1959, when Richiard Feynman offered a prize for the first person to built a working electric motor with an overall size not exceeding 1/64th of an inch. In the same year Feynman gave a talk at the California Insitute of Technology and said: "A biological system can be exceedingly small. Many of the cells are very

tiny, but they are very active; they manufacture varius substances; they walk around; they wiggle; and they do all kinds of marvelous things- all on a very small scale. Also they store information. Consider the possibility that we also can make a thing very small which does what we want- that we can manufacture an object that maneuvers at the level". [*Ramsden, 2009*]

The second approach to the nanoscale world was with the construction of microscope, although the word nanotechnology was conied by Norio Taniguchi in 1983, talking about engineering. Since 1980 there have been many inventions and discoveries in nanotechnology. [*Ramsden, 2009*]

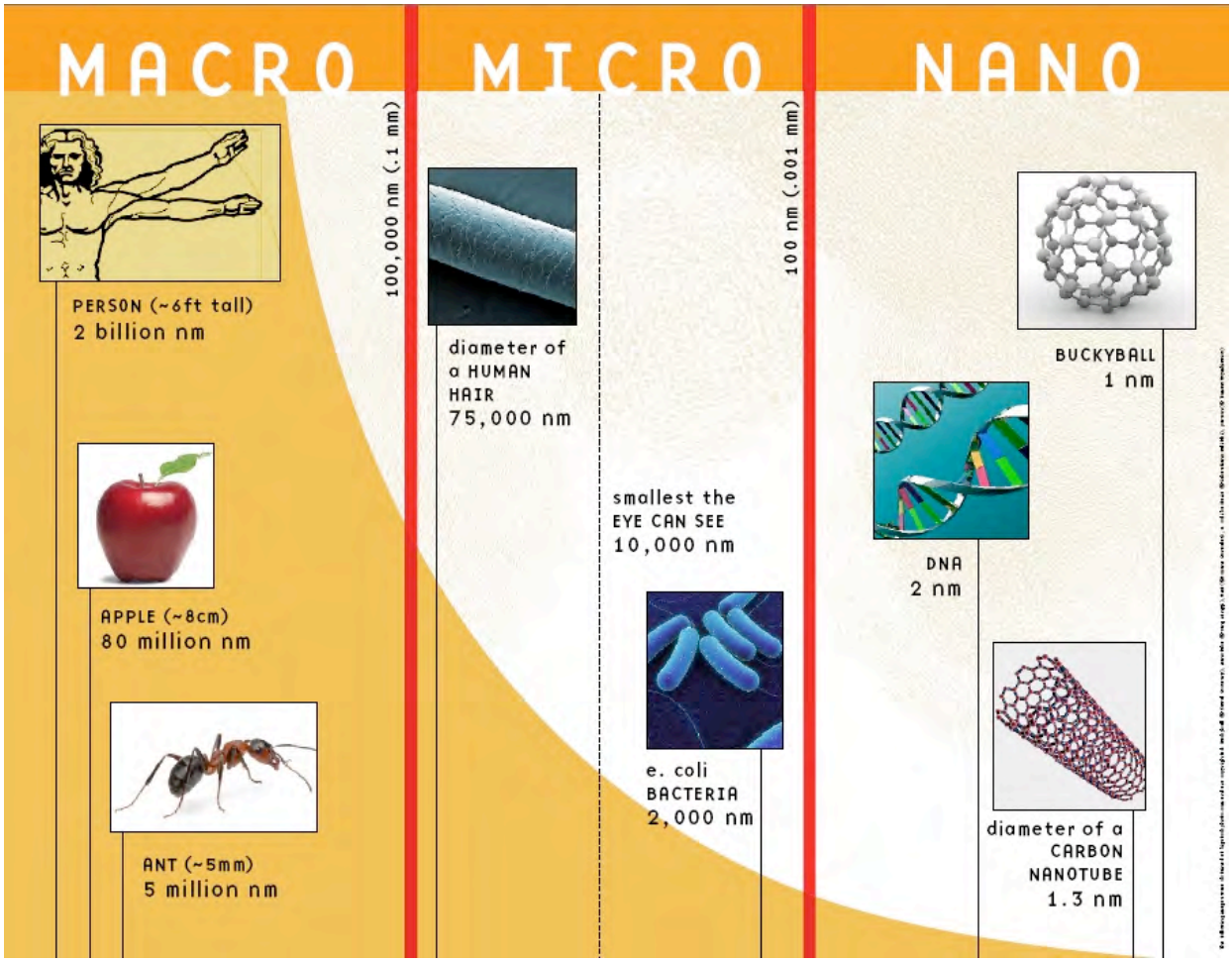

Fig 5: (source: Silicon Valley Toxics Coalition)

In 1998 the White House created the Interagency Working Group on Nanoscience, Engineering and Technology to recognize the importance of this new scientific branch. In 2001 the USA have allocated a budget of $ 497 million for the National Nanotechnology Initiaitve (NNI), and made it a top scince and technology priority. [*Bhushan 2010*]

The applications of nanotechnology range from chemistry to biomedicine, from construction to information technology, in order to sustain a development of new systems for energy saving. Two main approaches are used in nanotechnology: one is a "bottom-up" approach where materials and devices are built from molecular components which assemble themselves chemically using principles of molecular recognition; the other one being a "top-down" approach where nano-objects are constructed from larger entities without atomic-level control.

The impetus for nanotechnology has stemmed from a renewed interest in colloidal science, coupled with a new generation of analytical tools such as the atomic force microscope (AFM) and the scanning tunneling microscope (STM). Combined with refined processes such as electron beam lithography, these instruments allow the deliberate manipulation of nanostructures, and in turn led to the observation of novel phenomena.

The revolutionary perspectives associated with nanotechnology stems from the fact that at these dimensions the behavior and material characteristics change drastically and nanotechnologies represent a radical new way to produce materials, structures and devices with improved properties and functionalities or completely new.

In summary, nanotechnology is likely to have a profound impact on our economy and society, comparable to that of the industrial revolution. According to the 2nd Census AIRI / Nanotec IT, published in 2006, between organizations/structures (companies, research institutes, university departments, institutes, etc.) active in nanotechnology, 60% refers to public research and 40% to private companies and organizations listed in the 6989 Census have resulted in scientific publications almost all of which (6795) were published in international journals. [*Gelain 2007*]

Particular interest in nanotechnology has been in the healthcare area, where nano medicine has emerged as a new research field, which could have deep effect in the current treatment paradigms for various diseases. So NANOMEDICINE is defined as the application of nanotechnology to healthy, and hence is virtually synonymous with nanobiotechnology considering health as applied biology [*Ramsden, 2009*].

NANOPARTICLES (NPs) are defined as particulate dispersion or solid particles with a size in the range of 10-100 nm. The dimensions of nanoparticles are similar to biomolecules such as protein (1-20 nm) virus (20 nm) and cell surface receptors (10 nm). Therefore, using these new nanostructures to study and explore biological complex system, highly sophisticated theoretical experimental tools are required. In particular the visualization, the characterization, and manipulation of materials and devices require sophisticated imaging and

quantitative techniques with spatial and temporal resolutions on the order of 10^{-6} (the size of a micron) and below to the molecular level. In addition these techniques are critical for understanding the relationship and interface between nanoscopic and mesoscopic/macroscopic scales, a particularly important objective for biological application. As such, further nanotechnological advances will need parallel progress of these physical characterization techniques. [*G.A. Silva; 2004*].

The National Cancer Institute (NCI) has recognized that nanotechnology offers the possibility to study the normal and cancer cells in real time, at the molecular scale. [*Patra et al; 2010*]

Nanoparticles can be prepared from a wide variety of materials such as proteins, polysaccharides and synthetic polymers. The selection of matrix materials is regulated to many factors including: (a) size of nanoparticles required; (b) in case of drug delivery inherent properties of the drug, e.g., aqueous solubility and stability; (c) surface characteristics such as charge and permeability; (d) degree of biodegradability, biocompatibility and toxicity; (e) drug release profile desired; and (f) antigenicity of the final product. [*Mohanraj et al 2006*]

Different methods for the synthesis of nanoengineered materials and devices can accomodate precursors from solid, liquid, or gas phases and encompass a tremendously varied set of experimental techniques. In general, however, most synthetic methods can be classified into two main approaches: " top down" and " bottom up" approaches and combinations thereof.

- "Top down" techniques begin with a macroscopic material or group of materials and incorporate smaller-scale details into them.
- Bottom up" approaches, or self-assembly, on the other hand, involve gradual additions of atoms or group that have the ability to self-assemble or self-organize into higher order mesoscale and macroscale structures. The physical mechanisms that drive these molecules to selfassemble into organized structures, are due to thermodynamics and competing molecular interactions including hydrophobic/hydrophilic forces, hydrogen bonding, and van der Waals interactions that aim to minimize energy states for different molecular configurations. [*G.A. Silva; 2004*].

Finally improvements in solubility are achieved through modification of the nanoparticle's outer layer; a large variety of chemical, molecular, and biological entities can be covalently or adsorbed to it. The linking of hydrophilic polymers as PEG to the NP surface greatly increases the hydration (i.e., solubility) of the nanoparticles and can protect attached proteins from enzymatic degradation when used for in vivo applications. Nanoparticles with hydrophilic polymers as PEG attached to their surface can act as a platform for lipophilic molecules and

overcome the solubility barrier. Insoluble compounds can be attached, adsorbed, or otherwise encapsulated in the hydrated nanoparticles. Solubility of the composite entity subsequently becomes a function of the nanoparticle carrier rather than being strictly dependent on the drug itself. Liposomes are perhaps the most common example of this application. [*S.E. McNeil, 2005*]

The surface coating with PEG ("pegylation") and other hydrophilic polymers also increases the "in vivo" compatibility of nanoparticles. When injected intravascularly, uncoated nanoparticles are rapidly cleared from the bloodstream by the reticuloendothelial system (RES): they are easily recognized by the body immune systems, and then they are cleared from the circulation by RES phagocytes. Their surface hydrophobicity regulates the amount of adsorbed blood components, mainly proteins (opsonins). Binding of these opsonins onto the surface of nanoparticles, called opsonization, enhances the uptake by phagocyte cells. [*V.J. Mohanraj, 2006*]

Nanoparticles coated with hydrophilic polymers have prolonged half-lives, due to decreased opsonization and subsequent clearance by macrophages. This represents a slight paradigm shift from classical pharmacology; plasma protein binding (e.g., to albumin and -acid glycoprotein) can be a desired attribute for traditional therapeutic drugs, as it serves to increase bioavailability by limiting first-pass hepatic extraction.

Several groups have also extended the ability to tailor the surface chemistry to the nanoparticle's zeta potential or overall charge by derivatizing the surface with cationic or anionic species. The particle's charge can influence its biocompatibility and ability to pass through biological barriers. Surface charge has also been implicated in the ability of nanoparticles to cross the blood-brain barrier and their distribution between the vascular and extravascular compartments of tumors [*S.E. MacNeil, 2005; V.J.Mohanraj et al, 2006*]

Currently there are about twelve of FDA approved nanodevices; the most common are liposome and polymeric NPs. In general nanoparticles are classified by chemical composition and shape. The main feature that distinguishes the various types of nanoparticles is the preparation with organic polymers and/or inorganic elements.

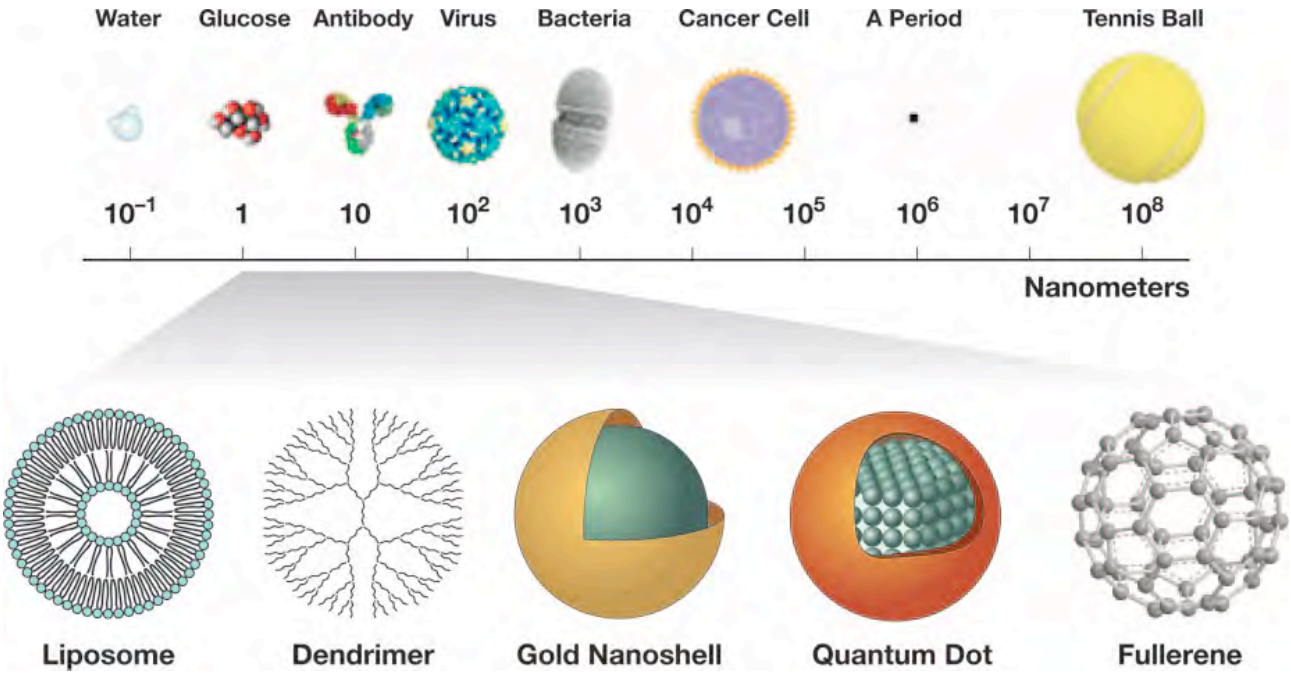

Fig 6: Relative size of nanoparticles compared with familiar items. [S.E: Mc NcNeil, 2005]

Next, we summarize the nanoparticles currently used in experimental and clinical trials:

- **Liposomes** are phospholipid vesicles, which can have variable size betwwen 50-100 nm. They usually have a bilayer membrane structure, made of a double layer of phospholipids or cholesterol and an internal aqueous phase. The spherical structures that contain no fat in an aqueous solution are called micelles. These sorts of compounds are usually classified according to size and number of layers into multi, oligo or uni lamellar. Thanks to their amphiphilic nature, they are promising in improving the trasport of many hydrophobic drugs within their aqueous core, and hydrophobic drug dissolved into the membrane. Owing to their physicochemical characteristics, liposomes have excellent biocompatility, circulation, and penetration. After rapture they are readly integrated into cell walls, so they are used to enhancing the transfer of therapeutics into cells and tissue, avoiding particular organs and enabling sustained release to reduce drug toxicity. Furthermore their surface can be chemically modified with ligans and/or polymer to increase drug specificy. Current clinical usage of stealth liposomal is in association with doxorobicin, reducing toxicity effect, increasing the amount released in situ. [*Sanvinces et al, 2008; K. Cho et al, 2008, N.G.Portney et al 2006*]
- **Dendrimers** are highly repeatedly branched synthetic polymers with layered architectures costituted of a central core, an internal region and numerous terminal groups

that determine dendrimer characteristics. In fact the properties of dendrimers are due to the functional groups present on the molecular surface. There are two methods to synthesize dendrimers: divergent and convergent synthesis. The divergent synthesis, assembles the molecule, starting from the core, extending radially towards the periphery, the convergent synthesis starts from the periphery and proceeds inward. The method used for the synthesis defines the dendrimer solubility and biological activity. Applications of dendrimers typically involve conjugating with other chemical species to the dendrimer surface through chemical modification of their terminal group for imaging-diagnosis or therapeutic scope. [*Sanvinces et al, 2008; K. Cho et al, 2008; N.G.Portney et al 2006*]

- **Silica nanoparticles** are also extremely versatile; the ease of synthesis allows the creation of complex structures through core shell architecture with multiple layers. Silica nanoparticles can be synthesized using different techniques; silanol groups can be functionalized through different procedures. The Stober process is the most common method for the synthesis of colloidal silica based nanopartilces with a 100 nm diameter. It is based on the hydrolysis of a silica alkoxide precursor, such as TEOS and then silica nanoparticles are formed after concentration of silicic acid produced during hydrolysis. The silica hydroxyl group can react with various reagents to introduce amine, carboxyl, or thiol groups. Silica surface modification is not limited to chemically mediated procedures. Passive adsorption of molecules such as avidin is commonly used. These nanoparticles (NPs) can be prepared with the desired size, shape and porosity. The porosity of their matrix allows the diffusion of molecules as well as singlet oxygen generated following the light-activation of the entrapped photosensitizer. In addition, when using SiO_2-NPs the entrapped photosensitizer shows its phototoxic effect without being released from the carrier and this may reduce significantly the phototoxic effects in the skin and eye caused by accumulation of the free photosensitizer. The use of silica particles loaded with a photosensitizer drug for PDT has been proposed by Prasad and co-workers which demonstrated cellular uptake and retained in vitro PDT activity of the nanocarriers as we see below.[*Ismail A.M. Ibrahim et al, 2010; Yu Shen Lin et al, 2010*]
- **Carbon nanotubes** are allotropes of carbon with a cylindrical nanostructure; they belong to the family of fullerenes and are formed of coaxial graphite sheets rolled up. Their name is derived from their long, hollow structure. These cylindrical carbon mol-

ecules have unusual properties: exhibit excellent strength, electrical properties and efficient heat conductivity. Thanks to these characteristics they are often used as biosensor. When they are in hydrophilic forms, obtained by surface functionalization, they are also used as drug carriers and tissue repair scaffolds. [*Sanvinces et al, 2008; K. Cho et al, 2008*]

- **Quantum dots** are promising nanoscale tools for biological application, thanks to their easy surface functionalization. They are colloidal fluorescent semicondutor nanocrystals (2-10 nm), with a central core made of cluster of semiconductor elements from II to VI of periodic system. They show a narrow bandwidth emission for multiple color imaging, broad absorption spectrum for single excitation sources, and superior photostability. Their surface is passivate by coating with several monolayers of larger band gap material, es ZnS, which also reduces leaching of damaging metal ions by oxidation from the surface. Furthermore they are resistant to photobleching and show excepional resitance to chemical degradation, so they are powerful class of trackers for biomedical imaging and detection. [*Sanvinces et al, 2008; Shuming Nie et al, 2007*]
- **Magnetic nanoparticles** are nanocrystal of 10-20 nm of size with iron/nickel/colbat core surrounded by dextran or PEG molecules. This class of nanoparticles can be manipulated using magnetic field; they have controlable sizes ranging from few nanometres up to tens nanometres. They can be coated with biological molecules in order to improve interaction with biological structures and so they are often used as nanocarriers. Finally the magnetic nanoparticles can be made to resonantly respond to a time varying magnetic field, with advantageous results related to the transfer of energy from the exciting field to the nanoparticle. For example, the particles can release adsorbed energy by heating, which leads to their use as hyperthermic agents. Chemotherapy efficacy can be improved by association thermo therapy and magnetic NPs, which increase the cells sensibility by warming. In addition their magnetic properties make them excellent agents to label biomolecules in bioassays, as well as MRI contrast agents. These will be explained in further detail below. [*Sanvinces et al, 2008; V.I.Shubayev et al, 2009; Q.A. Pankhurst et al, 2003*]
- **Gold nanoparticles** are the most used among the metallic nanoparticles. There are several reasons for the use of gold nanoparticles in medicine; first of all it is well estabilished that gold nanoparticles are biocompatible and non-toxic. Gold has been used long in medicine through the hystory of civilization, from Egyptians, to Greeks and

Chineses. Since 1927 gold has been used in clinic for the treatment of arthritis. Moreover their simple, economically cheap and safe synthetisis and their negative surface make them highly reactive for binding with targeting biomolecule. Also the strong interaction between the gold surface and thiol/amine containing molecules induces an easy surface modification. Gold nanoparticles can be prepared with different geometries, such nanospheres, nanoshells, nanorods. There are several synthesis methods, generally gold nanoparticles are produced in solution by reduction of chloroauric acid: Au+3 ions are reduced in citrate buffer that act as both a reducing and capping agent. If the solution is stirred vigorously enough, the particles will be fairly uniform in size. This formation of gold nanoparticles can be observed by a change in color since small nanoparticles of gold are red. These nanoparticles show localized surface plasmon resonance properties and this feature makes them excellent labels for biosensor, as it will be described later, because they can be detected by numerous techniques such as optic absorption, fluorescence and elettric conductivity. [*Sanvinces et al, 2008; Young Eun Choi et al, 2010*]

5. CANCER NANOTECHNOLOGY

Cancer nanotechnology is emerging as a new field of interdisciplinary research, spanning among the disciplines of biology, chemistry, engineering, and medicine, and is expected to lead to major advances in cancer detection, diagnosis, and therapy. Nanomedicine has emerged as a possible solution to many of the problem associated with the current treatment of cancer, as already described above, the early detection, and the excessive toxicity to the surrounding healthy cells. The progression of nanoparticle technology toward these problems solving is mainly the result of the properties of these devices. In designing nanoparticles as delivery system the major goals are to control particle size, surface properties and release of pharmacologically active agents, in order to achieve the site specific action of the drug at the therapeutically optimal rate and close regimen.

Cancer cells show peculiar characteristics as abnormal growth, and abnormal differentiation. Among these differences are included altered vasculature and endothelial systems. Solid tumors are unique as they grown approximately beyond 2 mm in size. They need to create their own system of blood vessels in order to deliver nutrients and oxygen to sustain further

growth. Moreover the rapid production of blood vessels, the vasculature tends to be highly permeable thanks to the leaky capillaries. The Enhanced Permeability and Retention (EPR) effect is the property by which molecules of certain sizes (typically nanoparticles, and macromolecular drugs) accumulate in tumor tissue much more than they do in normal ones. The cancerous cells produce factors such as VEGF and other angiogenic factors in order to cause an increased microvasculature density within the tumor. These newly formed tumor vessels are usually abnormal in form and architecture. They are poorly aligned and defective of endothelial cells, with wide fenestrations, lacking a smooth muscle layer, or innervation with a wider lumen. [*Wikipedia.org*] Furthermore, tumor tissues usually lack effective lymphatic drainage. All these factors will lead to abnormal molecular and fluid transport dynamics, especially for macromolecular drugs. As a result of these characteristics, concentrations of nanoparticle-drug conjugates in tumor tissue can reach levels 10 to 100 times higher than the resulting from the administration of the free drug with less toxicity to healthy tissue. [*Wikipedia.org; K.Cho et al, 2008; M.S. Arayne et al, 2006; R. Sinha et al 2006*]

Nanoparticles for their physical properties are keenly suited to exploit these unique tumor properties; this phenomenon is called **"passive" targeting**. Localization of nanoparticles by EPR was demonstrated by infrared-induced thermal ablation therapy in work by O'Neal [*N.G. Portney et al, 2006*]. Nanoparticles are usually taken up by the liver, spleen and Reticuloendothelial system dependending on their surface characteristics: a more hydrophobic surface facilatate liver uptake, followed by the spleen and lung. The optimal size should be less than 100 nm in diameter to maximixe half-life times and targeting ability. [*L.Brannon Peppas et al, 2004*]

An alternative passive targeting strategy is to utilize the unique tumor environment in a scheme called tumor activated prodrug therapy. The drug is conjugated to a tumor specific molecule and is administered in as inactive state and once it reaches its destination, the tumor environment is able to convert it to an active and volatile substance, so-called tumor-activated prodrug therapy. [*R. Sinha et al 2006*]

Other targeting approach exploit tumor new vasculature and angiogenesis process. Although passive targeting approaches form the basis of clinical therapy, they suffer from several limitations. Furthermore, it is not always possible to reach all the cells within the tumor mass because some drugs can not spread efficiently and is difficult to control the process due to the random nature of the approach. This absence of control can induce multiple-drug resistance (MDR), a situation in which patients fail chemotherapy treatment due to resistance tumor cell

against one or more drugs. This phenomenon occurs because the proteins involved in the expulsion of drug are over expressed on the surface of tumor cells. The expulsion of drugs inevitably lowers the therapeutic effect and quicky cancer cells develop resistance to a variety of drugs [*Dan Peer et al, 2007*]. The passive strategy is further reduced because some tumors do not show the EPR effect, and the permeability of blood vessels can not be the same within a single tumor mass [*O.C. Farokhzad et al, 2009; Dan Peer et al, 2007*].

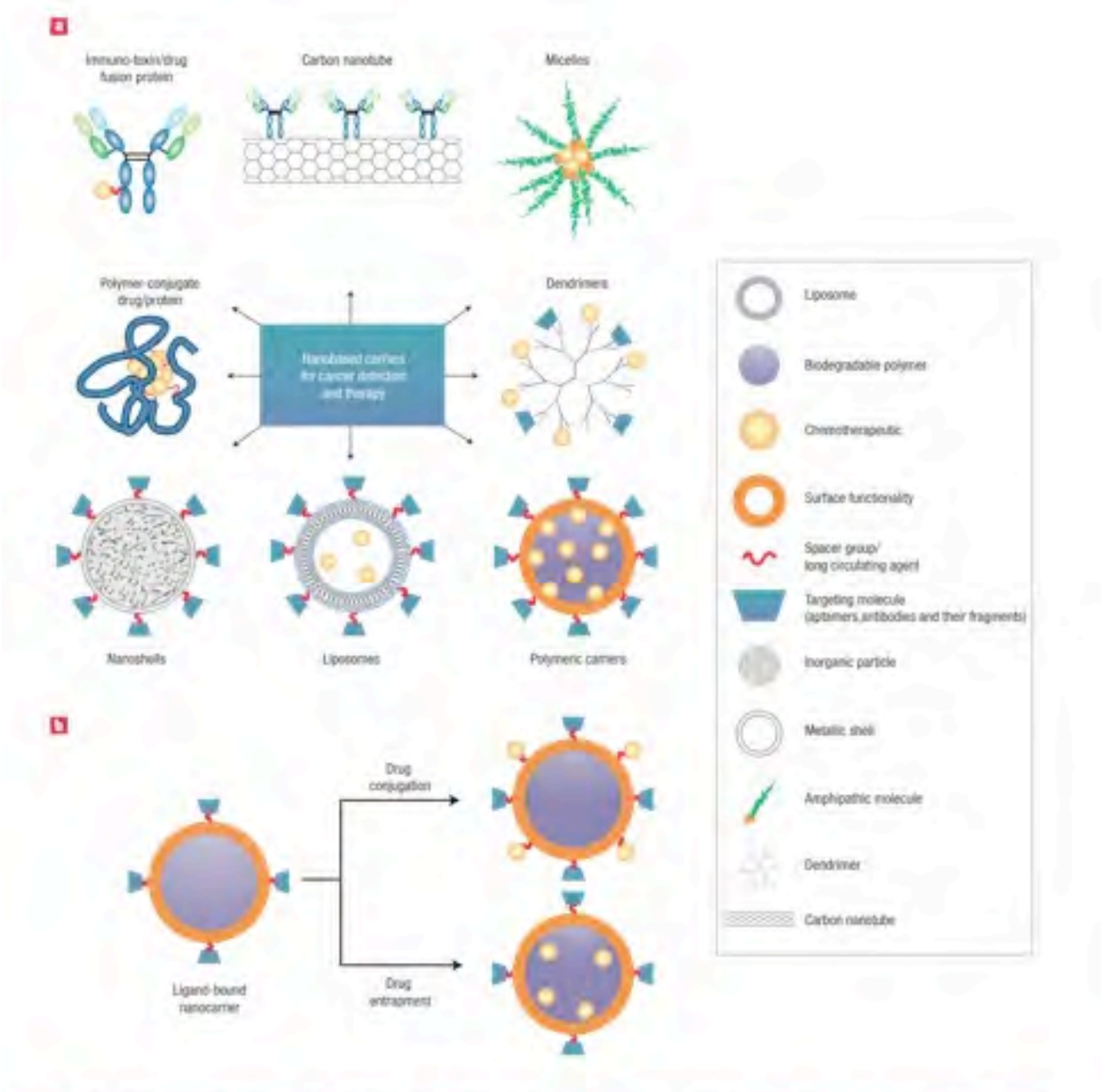

Fig 7: Examples of nanocarriers for targeting cancer. a) A whole range of delivery agents are possible but the main components typically include a nanocarrier, a targeting moiety conjugated to the nanocarrier, and a cargo (such as the desired chemotherapeutic drugs). b) Schematic diagram of the drug conjugation and entrapment processes. The chemotherapeutics could be bound to nanocarrier, as dendrimers and others particulate carriers, or they could be entrapped inside nanocarrier. [*Dan Peer; 2007*]

To overcome this problem the best solution is to functionalize nanocarriers so they actively bind to the target cells after extravasation: this strategy is called **"active" targeting**. This binding specificity may be achieved by linking targeting moiety on the NPs surface. In this way if targeted antigen is internalized after receptor binding, drug is released inside the cell. [*Dan Peer et al, 2007 R. Sinha et al 2006; Shuming Nie et al, 2007*]

Monoclonal antibody or monoclonal antibody fragments are good targeting vehicles for nanoparticles but other targeting molecules are successfully used (see folate, aptamers, luteinizing hormone releasing hormone, thiamine) [*S.E. McNeil, 2005*].

Antibodies have unique advantages compared with other ligands: higher specificity and affinity than the other small molecules, they have a chemical structure with a huge amount of NH_2 and COOH groups required for cross-linking reactions. Finally most of them are already approved by US FDA for cancer therapy, whereas none of the other ligands such as folate, are approved. So the development of targeted nanomedicines, which perfectly combine antibody engineering and nanotechnology, is becoming a challenge in nanomedicine research. The contribution that antibody engineering has given to nanomedicine development is remarkable, improving significantly the therapeutic effectiveness of conventional chemotherapy or gene therapy in cancer. Obviously to maximize specificity, a surface marker (antigen or receptor) should be overexpressed on target cells compared with normal cells. For example, to efficiently deliver liposomes to B-cell receptors using the anti-CD19 monoclonal antibody (mAb), the density of receptors should be in the range of 10^4–10^5 copies per cell [*Dan Peer et al, 2007*]. Less effectively targeted was observed with lower density. In a breast cancer model, a receptor density of 10^5 copies of ErbB2 receptors per cell was necessary to improve the therapeutic efficacy of an anti-ErbB2-targeted liposomal doxorubicin relative to its nontargeted counterpart. Moreover targeting antigen must be internalized and thus the nanocarrier, in order to increase the amount of drug inside the cell. Receptor mediated internalization is not required for targeted radionuclide therapy, because it can operate extracellularly. Moreover, targeting nanocarriers against non-internalizing receptors may sometimes be advantageous in solid tumours owing to the bystander effect, where cells lacking the target receptor can be killed through drug release at the surface of the neighbouring cells, where carriers can bind. Active targeting of solid tumors mediated by targeted nanomedicines armed with antibodies is more difficult, owing to a great number of hindrances, such as stability in the bloodstream (half life time), extravasation into the tissue and specific binding to the target cells, can impede the diffusion and penetration of targeted nanomedicines within the tumor

parenchyma. For solid tumours, it is clear that high binding affinity can decrease penetration of nanocarriers due to a 'binding-site barrier', where the nanocarrier binds to its target so strongly that penetration into the tissue is blocked. This observation increases the importance of designing suitable antibodies in order to achieve a rapid and complete tumor penetration; a high affinity binding interaction may be undesirable. In addition to enhanced affinity, multivalent binding effects (or avidity) may also be used to improve targeting. A collective binding in a multivalent interaction is much stronger than the monovalent binding. [*A.Z. Wang et al, 2008*].

Growth factor and vitamin are commonly used as targeting agents, as cancer cells often overexpress the receptors for nutrition to maintain their fast growing metabolism (es. the vitamin folic acid has been used for cancer targeting because the folate receptors are often overexpressed in some of tumors, for the same reason the Epidermal Growth Factor (EGF) has been shown to bind to the EGF receptor frequently overexpressed in patients). [*Dan Peer et al, 2007; Gao et al, 2010; V.J. Mohanraj et al, 2006*]

To conclude, recently, nanoparticles have been used to change and improve the pharmacokinetic and pharmacodynamic parameters of different drugs. They have been also used in vivo to protect the drug in the blood stream, to improve the specific distribution of the drug to target sites. So every nanoparticle vector would achieve long circulation time, low immunogenicity, good biocompatibility, selective targeting, efficient penetration of physiological barriers (e.g. vascular endothelium and the blood brain barrier), external activation or self regulating drug release, and have no toxicity effect. Universal procedures such as pegylation and immunolabelling become necessary requisite to improve circulation time and to enable selective targeting. [*N.G. Portney et al, 2006*]

Despite of significant progresses, there are still many significant challenges and outstanding issues for cancer therapy applications. The covalent conjugation procedures appear the only effective way to join antibodies irreversibly to nanoparticles. On the other hands it can affect the Abs functions. Moreover the right orientation of the antibodies on the nanoparticle surface is essential to preserve a good antibody activity and unfortunately it is not guaranteed. It cannot be well controlled, resulting in low antibody conjugation efficiency or impaired biological activity of antibodies.

In summary the advantage of using nanoparticles includes the following:

1. Particles size and surface characteristics of nanoparticles can be easily manipulated to achieve both passive and active drug targeting. Nanoparticles smaller than 20 nm can cross through blood vessel walls, they also offer the ability to penetrate the blood barrier or the stomach ephitelium, it is estimated that the threshold of first pass elimination by the kydneys is 10 nm diameters. Similarly to pass in the liver, the particles must be small enough to pass through the organ's 150-200 nm sized fenestrate. The size of nanoscale devices also allows them to interact readily with biomolecules on the cell surface and inside the cell, often in ways that do not alter the behavior and biochemical properties of those molecules. Despite their small size nanoparticles can accomodate tens of thousands of atoms or small molecules, such as magnetic contrast agent for MRI. [*S.E. McNeil, 2005; S. Dufort et al, 2011*]. Also nanoparticle circulation times can be fine tuned controlling their size and surface properties.
2. Drug release during the trasportation and the target site localization can be controlled and sustained; it is possible to change the site of localization and clearence of the drug in order to increase the therapeutic efficacy and to reduce the side effect.
   Controlled release and particle degradation characteristics can be readily modulated by the choice of matrix constituent. Drug loading is relatively high and drug can be incorporated into the system by means of chemical linkage or without any chemical reaction. Drug adsorbtion has the advantage to preserve drug activity, but with chemical bound the drug release is more controlled.
3. Site specific targeting can be achieved by linking targeting moieties to the NPs surface or by means of magnetic guidance.
4. The system can be used for various administration routes including oral, nasal, parental, and intraocular.
5. Multifunctional device: nanoparticles also offer a wide range of surface functional groups allowing chemical conjugation to multiple diagnostic and therapeutic agents. It is thus possible to design and develop multifunctional nanostructures that could be used for simultaneous tumor imaging and therapy. Furthermore, as already said, nanoparticles are sufficiently large to accomodate simultaneously multiple types of drug molecules, without changes in NPs pharmacokinetic.
6. Loaded drugs are located inside the particle, and so their type and number do not affect the pharcokinetic properties and biodistribution of the nanoparticle.

In spite of these advantages, nanoparticles have some limitations. For example, their small size and large surface area can lead to particle aggregation, making their handling in liquid and dry forms difficult. Furthermore the particle size affects the drug release: smaller particles have larger surface area. Therefore, most of the associated drug would be at or near the particle surface, leading to fast drug release. Whereas, larger particles have large cores, which allow more drug to be encapsulated and slowly diffuses out. Polymer degradation can also be affected by the particle size. It is thought that in smaller particles, degradation products of polymer formed can diffuse out of the particles easily while in large particles; degradation products are more likely remained within the polymer matrix for a longer period to cause autocatalytic degradation of the polymer material. Therefore, it was hypothesized that larger particles should contribute to faster polymer degradation as well as faster drug release.
These practical problems have to be overcome before nanoparticles can be used in clinic or made commercially available. [*VJ Mohanraj et al, 2006*]

6. APPLICATIONS IN CANCER

The main areas of **cancer applications** include:

1. *Prevention and control*: the development of nanoscale devices provides cancer prevention agents and the planning of anticancer vaccines multiple components;
2. *Early diagnosis and diagnostic imaging*: the development of intelligent platforms for simultaneous analysis of tumor associated antigens and the design of targeted contrast agents to optimize the resolution;
3. *Multifunctional therapies*: the creation of therapeutic devices able to control the release of specific anti-cancer drug. The nanoparticles are sufficiently large to contain multiple targeting ligands that can allow multivalent binding to cell surface receptors.

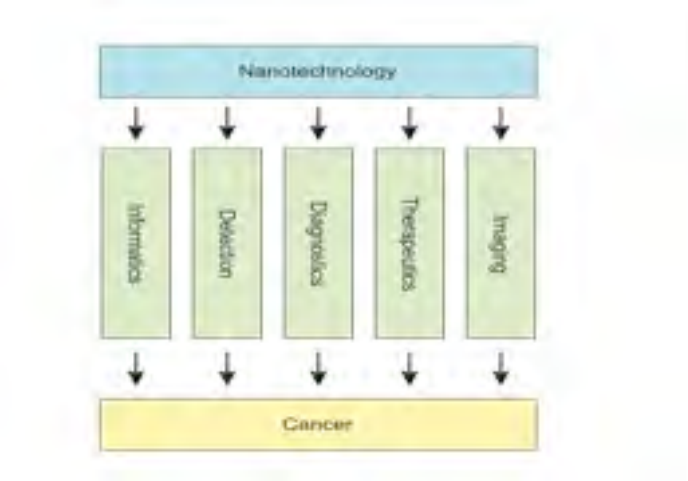

Fig 8: Schematic diagram showing Nanotechnology applications in cancer through molecular tumor imaging, early detection, molecular diagnosis, targeted therapy, and cancer bioinformatics. [*S.Nie et al, 2007*]

Thanks to the combination of modern instrumentation and nanomaterials, nanoparticles are being increasingly applied to molecular diagnostics and several technologies are in development. Currently gold NPs and QDs are the most widely used, but many other nanotechnology devices, such as nanobiosensors, are promising for their potential clinical applications. Semiconductor QDs are NPs with intense and stable fluorescence emission that can allow detecting cancer biomarkers in blood assays or on cancer tissue biopsies. They offer unique features that allow the detection of cancer markers in biological specimens at picomolar range concentrations. Biomarker is in general a substance used as indicator of a biological state of disease; studying molecolar profiling and cancer development discover most of cancer biomarker. It is characteristic of a specific state and therefore can be used as a marker for a target disease. By critically defining the interrelationship among these biomarkers, it could be possible to diagnose and prognosticate cancer based on a patient's molecular profile, leading to personalized and predictive medicine. Current technologies for molecular profiling, including RT PCR, gene chips, are not able to handle the highly heterogeneity of cancer sample. In this contest the development of nanodevices can provide the essential link by which biomarkers could be functionally correlated with cancer behaviour, detecting molecular changes even when they occur only in a small percentage of cells. Due to their unique optical, chemical, magnetic characteristics nanomaterials have been used for more sensitive and precise detection.

An example of this type of nanotechnology application is the *nanowire,* composed of repeating molecular units either organic or inorganic. These nanostructure can be engineered to sense

and pick up molecular markers of cancer cells. Nanowires can be coated with probe such as antibody that binds to target protein and relay the information via electrical connections. Molecular diagnostics has also been greatly benefited by the advent of AuNPs, which promises increased sensitivity and specificity, multiplexing capability and short turn around times. AuNP-based colorometric assays also show great potential in point-of-care testing assays. The widespread use of AuNPs as labels in diagnostics and detection is due to a unique combination of chemical and physical properties that allow biological molecules to be detected at low concentrations.

NPs as diagnostic agents

Type of nanomaterial	Diagnostic strategy	Advantages
AuNPs	The selectivity and specific affinity of aptamers is combined with spectroscopic advantages of AuNPs to detect diseased cells	For sensitive detection of cancer cells. Can easily differentiate between different types of target and control cells based on the aptamer
Magnetofluorescent particle systems	These bimodal contrast agents allows detection of cancer cells	Noninvasive diagnosis of breast cancer
AuNPs	Identification is based on the reaction of cell surface proteins with specific antibodies conjugated with AuNPs	Rapid identification and quantification of tumor cells
Semiconductor fluorescent QDs	These fluorescent biomarkers are analyzed by their resulting fluorescence and thus enables efficient cancer diagnostics	Enables fast and precise cancer diagnostics
Semiconductor QDs	Intense stable fluorescence enables the detection of cancer biomarkers	Useful for molecular diagnostics of cancer
Aptamer conjugated NPs	Aptamer-conjugated magnetic NPs can be used for selective targeting cell extraction and aptamer-conjugated fluorescent NPs can be used for sensitive cancer detection	Enables the collection and detection of multiple cancer cells
Fluorescent europium(III)-chelate-doped NP	Highly fluorescent europium(III)-chelate-doped NP labels, together with high affinity monoclonal antibodies (antihexon) coated on label particles and microtitration wells provides a sensitive adenovirus immunoassay	Has potential in sensitive screening of viral analytes

Table 3: The major nanoparticle devices used in diagnostic. [*S.Parveen et al*, *2011*]

In relation to the second point, nanoparticle contrast agent is being developed for tumor detection purpose. The development of an effective carrier system includes the execution of delivery, as well as the positive confirmation of the site-specific delivery of the drug. Consequently, the ability to track and image the fate of any nanomedicine from the systemic to the subcellular level becomes essential. Labeled nanoparticles and non-labeled particles are already being tested as imaging agents in diagnosis procedures such as computed tomography and nuclear magnetic resonance imaging. Furthermore NPs can be successfully exploited to improve the advantage of fluorescent markers for medical imaging and diagnostic purpose. Although various fluorescent markers, such as dyes (fluorescein, rhodamine, alexa fluors), are widely used in research and clinical diagnostic applications, current techniques have several

disadvantages, such as the requirement of color-matched lasers, fluorescence bleaching and lack of discriminatory capacity of multiple dyes. Fluorescent NPs can greatly overcome these problems and a major advance towards clinical applicability is the use of NPs to image tumors and other diseases in vivo. Nowadays there are several types of nanoparticle used in molecular imaging in cancer diagnosis such as liposomes, dye molecule doped silica nanoparticle, quantum dots, gold nanoparticles, and magnetic ones. Thus, different types of nanoparticulate systems can be efficiently used as in vitro and in vivo imaging agents for efficient diagnostics and therapeutics (see table 3). [*S.Parveen et al, 2011; N.G.Portneyet al 2006; L. Zhang et al, 2008*]

NPs as imaging agents

Type of nanomaterial	Diagnostic strategy	Advantages
Poly(alkyl cyanoacrylate) NPs	The fluorescent rhodamine B-tagged poly(alkyl cyanoacrylate) amphiphilic copolymer nanoparticles enables specific human brain endothelial cell imaging	These NPs can be used for human brain endothelial cell imaging,
AuNPs	NP bioconjugates coated with dithiol bearing hetero-bifunctional PEG (polyethylene glycol), and cancer-specific monoclonal antibody F-19 can be used to label sections of healthy and cancerous pancreatic tissue.	These NPs can be used for human brain endothelial cell imaging
AuNPs	Surface functionalized AuNPs with prostate-specific membrane antigen (PSMA) RNA aptamer that binds to PSMA enables specific imaging of prostate cancer cells that expresses the PSMA protein.	Multifunctional NPs that that enables combined prostate cancer imaging by computed tomography (CT) and anticancer therapy
Streptavidin NPs	Biotinylated anti-Her2 Herceptin antibody to provide tumor targeting, whereas a biotinylated DOTA chelator labeled with ^{111}In and a biotinylated Cy5.5 fluorophore to a streptavidin NP provides specific imaging of the tumor	Streptavidin NPs were effective for multimodality imaging of tumor in mice by fluorescence and nuclear detection
Multifunctional superparamagnetic iron oxide NPs	Folate provides specific targeting, and DOX-loaded superparamagnetic iron oxide NPs serve as a therapeutic agent as well as MRI contrast agent.	Promising candidate for treating liver cancer as well as monitoring the cancer using MRI
CNPs	Tumor targeted CNPs containing dual imaging agents (near-infrared fluorescent dye, Cy5.5 (20), and gadolinium (Gd(III)) ions) was designed as dual-modality cancer imaging agents	Effective as an optical/MR (magnetic resonance) dual imaging agent for cancer treatment
QD-loaded micelles	Lipid conjugated QDs together with herceptin enhances tumor cell uptake and thus can be used for simultaneous tumor therapy and imaging	Can be used for targeting, imaging and treatment of cancer in the early stages
Carboxyl-functionalized silica-coated QDs	The stable fluorescent property of QDs enables specific imaging	Monodisperse and stable in aqueous solution, provides specific targeting and are easy for bio-conjugation. Can serve as efficient targeting probes for cell imaging
Fluorescent silica NPs	Silica NPs can be loaded with fluorescent dyes for sensitive imaging of cancer cells. In addition, for targeting cancer cells, these can be conjugated to specific biomolecules overexpressed on cancer cells	Useful for cancer targeting and imaging
Polymer-Ag@SiO2 Hybrid Fluorescent NPs	Cationic surface and suitable size allows the nanocomposites to be rapidly internalized into cells, thus effective in cellular imaging	These nanoparticles show cytocompatibility and bright fluorescence and thus is especially useful for efficient cellular imaging

Table 4 The major nanoparticles used as imaging tools. [*S.Parveen et al, 2011*]

Many of the same techniques used to target imaging agent may also be used to target delivery of drugs to cancerous tissue, NPs have widespread use in drug delivery, increasing the number of highly effective therapeutic agents. The therapeutic applications of NPs are different, ranging from cancer therapeutics, antimicrobial actions, vaccine delivery, gene delivery and site-specific targeting to avoid the undesirable side effects of the current therapeutics. Drug can be loaded onto NPs by various methods such as encapsulation, surface attachment or entrapment. They are opening new therapeutic opportunities for therapeutic agents that cannot be used effectively as conventional drug formulations due to poor bioavailability or drug instability. Many chemotherapeutic drugs such as carboplatin, paclitaxel, doxorubicin and etoposide have been successfully loaded onto NPs and these nanoparticulate systems are very effective against various cancer cells while sparing healhy cells, as demonstrated by the studies of various research groups. In addition, multifunctional NPs with surface- functionalized biomolecules are also being synthesized and serve as potential therapeutic agents. Functionalized NPs are also being used for targeted gene silencing because these offer exciting prospects and have garnered the attention of researchers.

NPs as therapeutic agents

Type of nanomaterial	Encapsulant	Indicator	Therapeutic improvement
Polyisohexylcyanoacrylate NPs	DOX	Hepatocellular Carcinoma	Higher antitumor efficacy than native doxorubicin and can overcome multiple drug resistance phenotype.
PLGA NPs	Paclitaxel	Various cancers	Effective in chemotherapeutic and photothermal destruction of cancer cells
Gold NPs (AuNPs)	-	Various cancers	Effective as radiation sensitizers for cancer therapy
Chitosan NP (CNP)	siRNA	Ovarian cancer	Increased selective intratumoral delivery and significant inhibition of tumor growth compared to controls
Cetyl alcohol/polysorbate NPs	Paclitaxel	Brain tumor	Higher brain and tumor cell uptake, thus leading to greater cytotoxicity; also effective towards p-glycoprotein expressing tumor cells.
Lipid nanocapsules	Etoposide	Glioma	Greater cytotoxicity. Can overcome p-glycoprotein dependent multidrug resistance.
P (4-vinylpyridine) particles	-	Antimicrobial agent	These particles can be used to inhibit bacterial growth for various bacteria as biocolloids
Chitosan-alginate NPs	Carboplatin	Retinoblastoma	Enhanced antiproliferative activity and cytotoxicity of NPs in comparison with native carboplatin
Poly (3- hydroxybutyrate-co-3-hydroxyoctanoate) NPs	DOX	Various cancers	Effective in selective delivery of anticancer drug to the folate receptor-overexpressed cancer cells

Table 5: Nanoparticle devices used in cancer therapy**.** [*S.Parveen et al*, *2011*]

There are several nanoscaled systems for systemic cancer therapy already applied and their latest stage of development are summarized in table 5.

Several nanotechnology-based products that are being tested or have been approved

Product	Type of Nanomaterial	Indicator	Phase	Advantages	Company
Doxil	PEGylated liposome	Ovarian cancer and multiple myeloma	On Market	Enhanced circulation time and is up to six times more effective than free DOX.	Janssen
Abraxane	Albumin NPs	Lung Cancer Breast Cancer	On Market	Enhanced cytotoxicity, shorter infusion time, low dose required	Celgene Corporation/ Abraxis Biosciences
Aurimmune (CYT-6091)	AuNPs coupled to TNF and PEG-Thiol	Solid Tumors	Phase II	Selectively destroys cancer cells without harming healthy tissues	CytImmune Sciences
AuroShell	Gold-coated silica NPs	Solid Tumors	Phase I	Highly selective and rapid tumor destruction with minimal damage to surrounding healthy tissues	Nanospectra Biosciences
Combidex	Iron oxide NPs	Tumor Imaging	NDA Filed	Efficient for the detection of metastatic lymph nodes in various cancers	Advanced Magnetics
Cyclosert	Cyclodextrin NPs	Metastatic solid tumor	IND Filed	Very effective in preventing tumor progression	Insert therapeutics
ING N-401	Liposome	Metastatic lung cancer	Phase I	Suppresses tumor growth and inhibits metastasis of lung cancer	Introgen
MRX-952	Formulation of irinolecan metabolite	Oncology	Preclinical		ImaRx therapeutics
Nanoxel	Nanoparticlulate delivery system for paclitaxel	Breast Cancer Ovarian Cancer	On market	Cremophor free water-soluble formulation. Greater efficacy and decreased cytotoxicity	Dabur Pharma
TNT AntiEpCAM	Polymer-coated iron oxide	Solid Tumors	Preclinical	Provides targeted therapy. Selectively kills EpCAM positive cells	Triton BioSystems
Verigene platform	DNA functionalized AuNPs	Diagnostics	On market	AuNPs enable efficient diagnosis for methicillin-resistant *Staphylococcus aureus*	Nanosphere Triton BioSystems

Abbreviations: NDA, New Drug Application; IND, Investigational New Drug.
Source: http://www.accessdata.fda.gov/scripts/cder/drugsatfda/.

Table 6: List of the NPs in the market or in clinical trails. [*S.Parveen et al, 2011*]

6.1 Nanoparticles without targeting ligands

A representative example is Doxil (Ortho Biotech), a PEG liposome containing the cytotoxic drug doxorubicin, FDA approved. It was originally approved for the treatment of AIDS related Kaposi's sarcoma and is now approved for use in ovarian cancer and multiple myeloma. Liposomes carrying chemotherapeutic drugs have been approved for cancer since in the mid 1990s, and are mainly used to solubilize drug. The problem with this type of nanoparticles is the absence of control for the time of drug release, and in most cases does not achieve effective intracellulary delivery. To overcome this problem, doxorubicin may be encapsulated by means of an ammonium sulphate gradient, allowing a stable drug entrapment. However Doxil circulated in the body as a nanoparticle and has a half-life 100 times longer than free drugs, reducing cardiotoxicity. But it was observed that it has skin toxicity. [*M.E. Davis et al, 2008*].
Another example of clinical application FDA approved is ABI 007-Abraxane- nanoparticle made of albumin aggregates and loaded with paclitaxel. Drug encapsulation eliminates the toxicities associated with the emulsifier Cremophor EL in the paclitaxel formulation, increasing the tolerated dose (70-80% higher than free drug). In phase III study of 454 patients with metastatic breast cancer treated with free or encapsulated taxol intravenously every 3 weeks, response rates were significantly greater in patient handled with Abraxane. It was demon-

strated a different clearence and distribution, resulting in higher Abraxan intratumoral concentration compared to Taxol. The clinical benefit fron Abraxane is probabily due to its formulations as a nanoparticle.

PEG polymers have also been conjugated with small molecule drugs to create nanoparticles, for example PG-paclitaxel conjugates is a biodegradable polymer, that have been assessed in numerous clinical trials.

Micelles, which are self-assembly closed lipid monolayers, have been successfully used as pharmaceutical carriers; an example is NK911, which consists of block copolymer of PEG and aspartic acid and doxorubicin. [*R. Singh et al, 2009*]

A variety of nanoscale particles have already been used in imaging tumor. The most advanced work in this area uses coated ultra small superparamagnetic iron oxide nanoparticles (USPIO-smaller than 50 nm) and superparamagnetic iron oxides (SPIOs- size greater than 50 nm) to image micrometastatic lymphnodes in patient with prostate cancer. Furthermore they permit a precise and prolonged marker of the brain tumor margin. Other studies have used paramagnetic, gadolinium-labeled, nanoparticulate dendrimers to image lymphatic micrometastases in a mouse breast cancer model.

Moreover the MR imaging may become an investigation tool in the study of tumoral growth kinetics in vivo. The operative principle here is that normal lymph nodes rapidly accumulate these MRI-dense particles. Tumor cells (i.e., the micrometastases) do not take up the particles and create a “signal void” against a high proximal concentration of superparamagnetic material. Normal lymphnodes appear shadowed, and those loaded with metastatic cells or portions of lymph nodes with micrometastases appear enhanced. Lumirem® and Endorem® are the commercial names of SPIOs; they are used for gastro intestinal tract imaging and for liver and spleen disease detection. [*I. Brigger et al, 2002; Q.A. Pankhurst et al, 2003; R.Singh et al, 2009*].

Another work on “in vivo” imaging with QDs has been reported for limph node mapping: a new generation called II QDs with fairly broad emission at 850 nm and a moderate quantum yield of 13%, that emit light at reduced energies. They show rapid uptake into lymphnodes, and clear imaging and delineation of sentinel lymphnodes (which are often surgically removed in patients diagnosed with breast cancer). This work shows that QD probes could be used for real-time intra- operative optical imaging. All this provides an “in situ” visual guide; so that a surgeon could locate quickly and accurately and remove sentinel lymphnodes or

even smaller lesions (e.g., metastatic tumors), which may be difficult to identify without image guidance. [*M.E. Davis et al, 2008; S. Nie et al, 2007; S.E. McNeil, 2005*]

PLGA is another good material for generating nanoparticles used in several scientific investigations, such as potential anticancer devices when loaded with cystatin and docetaxel or with a photosensitizer (*meso-tetraphenylporpholactol).* [*Y. Liu et al, 2007*]

6.2 Nanoparticles with targeting ligands

Fig 9: Applications and research targets of functionalized nanoparticles [*S.E.McNeil*, *2005*]

Nanoparticles can be used for qualitative or quantitative in vitro detection of tumor cells: Streptavidin coated fluorescent polystyrene nanosphere (Fluospheres® and TransFluospheres®) were used in flow cytometer as detecting agent. [*I. Brigger et al, 2002*].

Active targeting achieved by the inclusion of targeting ligand on nanopartilcle surface provides a most effective tharapy. PK2, a HPMA polymer Gly-Phe-Leu-Gly-doxorubicin conjugate, which also contains the sugar galactosamina, was the first ligand-targeted nanoparticle to reach the clinic. The target specificity is achieved through the galactose-based ligand that binds to asialoglycoprotein receptor expressed on hepatocytes, in the hope that its expression is greater increased in malignances liver cells than in the healthy hepatocytes.

Another example of targeted NPs applied in clinic is MBP 426. It is a liposome loaded with platinum based drug (oxaliplatin), and targeted to trasferrin receptor (knows to be upregulated in many typer of cancer). [*M.E. Davis et al, 2008*]

Another interesting work by Robert Langer (phD of MIT) team talk about second generation of nanoparticles that target prostate cancer cells in a very specific way. Localized prostate cancer is often treated using brachytherapy, although many patients respond well to this treatment, approximately 10 percent fail, so a new treatment formulation is necessary. They formed the nanoparticle's backbone using a controlled release polymer PLGA, containing docetaxel. Then they functionalized these particles with short pieces of RNA, which were

designed to bind specific proteins on the surface of prostate cancer cells. They tested this conjugate on mice bearing human prostate tumor by injecting the nanoparticles directly into tumor. The result is very positive: every treated mouse survived the study; the docetaxel-targeted nanoparticle group achieved a complete tumor regression. On the contrary, only the 57% of the animals treated with untargeted nanoparticles, survived for the duration of the study. [*D. Conrad, 2006*]

Nanoparticles with siRNA are constructed using polyethyleneimine that is PEGylated and functionalized with Arg-Gly-Asp (RGD peptide), to target the tumor neovascolature. This siRNA inhibits vascular endothelial growth factor receptor 2 (VEGF R2) expression and thereby tumor angiogenesis.

Antibody-conjugated paramagnetic liposomes (diameter 300–350 nm) are used to visualize tumor angiogenesis in vivo by magnetic resonance imaging (MRI). These nanoparticles with binding specificity for the $\alpha_v\beta_3$ integrin are synthesized conjugating biotinylated antibodies against $\alpha_v\beta_3$ to the surface of liposomes via an avidin linker. The nanoliposomes are injected intravenously into a rabbit model of squamous cell carcinoma. The tumor vessel architecture is clearly visualized by MRI. [*S. Parveen et al, 2011;Y. Liu et al, 2007*].

6.3 Gold nanoparticles and Raman spectroscopy

Multi-functional gold nanoparticles are attractive organic-inorganic hybrid materials composed of an inorganic metallic gold core surrounded by an organic and/or biomolecular mono- layer, as already said above. The particles can have a size ranging from 0,8 to 250 nm and this size can be modulated during nanoparticles preparation. Standard method provides the reduction of auric acid with sodium citrate. The biomolecules can be conjugated direcly to gold core through covalent bounds (Au-S, Au-P) or through non-covalent interaction between biomolecules and capping agents as PEG. Alternatively the conjugation can be achieved by using biotinylated molecules and streptavidin coated particles. [*S.H. Radwan et al, 2009*]

These nanoparticles have bioapplications in: diagnostic, imaging, therapeutic delivery, thermal therapy and sensitizing protocols. Their physical properties are exploited to generate contrast: for example, in trasmission electron microscopy, the strong electron absorbing properties of gold nanoparticles make them suitable as a stain for samples with poor contrast, such as tissue samples. Particle's optical properties: e.g. strong absorption, scattering and es-

pecially strong plasmon resonance, make them relevant for a large variety of light based techniques including combining scheme such as photothermal or photo acoustic imaging and heat therapy. Gold nanoparticles act as mediating objects: the absorbed light energy is dissipated into the particle's surrounding, generating an elevate temperature in their prossimity. Surface plasmon resonance (SPR) is defined as the exitation by light of surface plasmon, thus of the surface electromagnetic waves that propagate in a direction parallel to the interface. Pratically when gold NPs are exposed to light, the oscillating electric field component of light interacts with the free conduction band electrons of gold surface, causing their collective dipolar oscillation. In order to excite surface plasmon in a resonant manner, one can use an electron or a light beam. The incoming beam has to match its impulse to the plasmon surface one, in order to have surface plasmon resonance. Surface plasmons have been used to enhance the surface sensitivity of several spectroscopic measurements. For colloidal gold nanoparticles with a diameter of 20 nm SPR occurs in the visible region at 520 nm, which is responsible for their intense red color. Gold NPs have large molar extinction coefficients, which increase with particles size.

Raman spectroscopy is non-invasive, non-destructive tecniques based on radiation-material interaction. Particolarly it concerns the radiation emitted by a laser beam interacting with the roto-vibrational motions of the molecules with the consequent re-emission of light at wavelengths other than the accident one. The spectrum obtained is said Raman spectrum, it provides a fingerprint of the molecule in question, allowing its identification. The technique is based on so-called "Raman effect: when a monochromatic radiation strikes a substance can cause the following effects:

- most of the radiation passes through the sample;
- a small fraction of the radiation spreads in all directions elastically without energy loss, (Rayleigh or elastic scattering);
- a smaller fraction is diffused inelastically yielding (Stokes Raman scattering) or acquiring (anti-Stokes Raman scattering) energy in the interaction with the molecule;

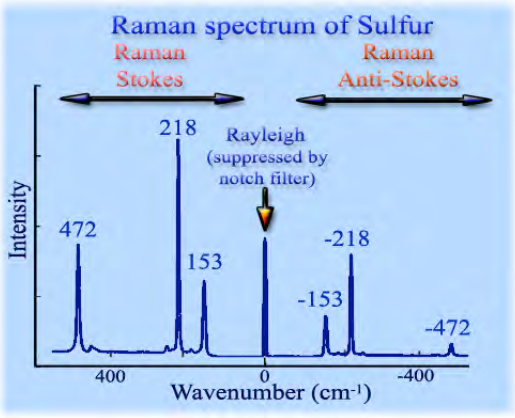

Fig 10: Raman spectrum: if the energy of the incident photon is equal to that of the scattered one, the process is called Rayleigh, in the case it is different the process is called Raman scattering.[www.fis.unipr.it/phevix/raman_tutorial.html]

All these energy transfers depend from molecule chemical structure; the pattern of shifted frequencies is determined by the rotational and vibrational states of the sample. Stokes and anti-Stokes lines are arranged symmetrically to the Rayleigh line and the difference in energy corresponds to the molecule energy purchased or sold by varying the initial vibrational level. For Raman spectrum it generally mean the end of the spectrum containing the Stokes lines (See fig 10). The Raman effect, which is a light scattering phenomenon, should not be confused with absorption (as with fluorescence) where the molecule is excited to a discrete (not virtual) energy level. Usually, Raman scattering shows weak signals compared to Rayleigh scattering or fluorescence, but when molecules are adsorbed on the surface of metallic nanostructures with plasmonic properties, a huge enhancement (until 10^8) of the differential Raman scattering cross section is observed. Most intense signals, until 10^{14}, are obtained when also the molecule is in resonance with the laser excitation, namely in the case of surface enhanced resonant Raman scattering (SERRS). SERS is one of the most sensitive diagnostic methods available. SERS labels can be a valid alternative to fluorescent tags based on organic fluorophores or semiconductor quantum dots since the spectroscopy peaks are much narrower than the band obtained in fluorescence spectroscopy and the spectral window is much broader. In particular the bandwidth of Raman peaks is in the order of few nm. This property and the distinctive Raman fingerprint of different molecules, allows the development of a wide series of SERS labels with a distinctive spectral signature.

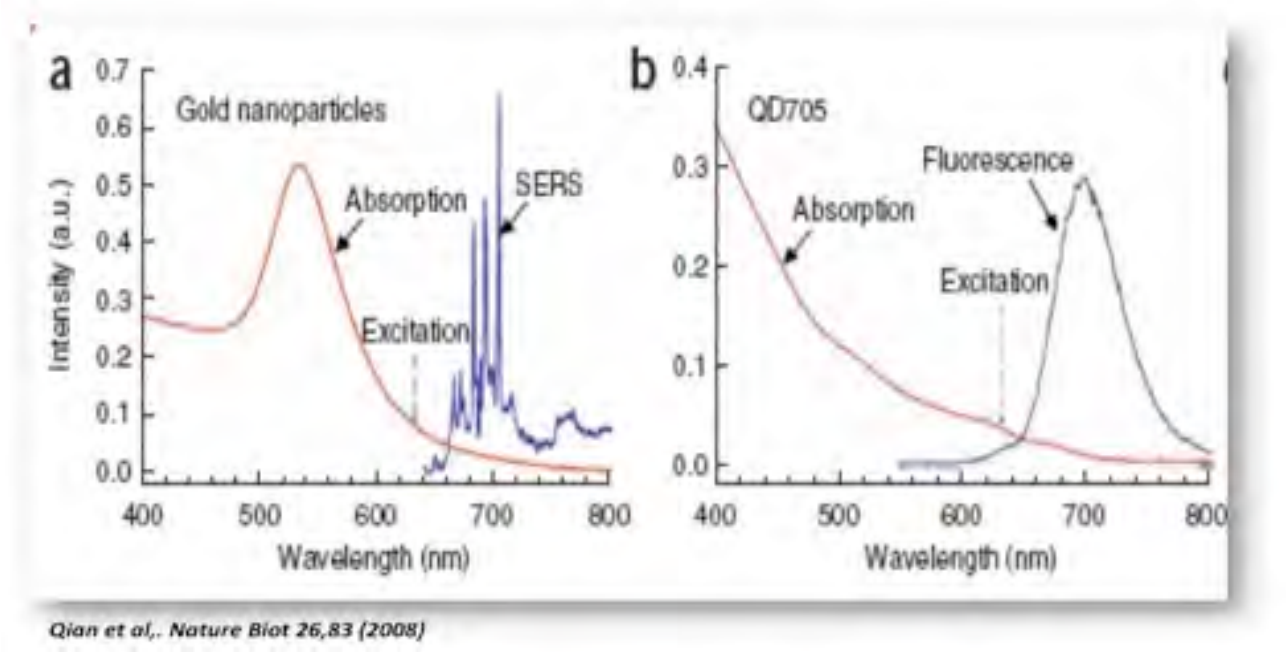

Fig 11: a) comparison between Gols NPs and QDs spectra. Optical absorption (red curves) and emission spectra (blu curves).

Multiple labels can be excited at the same time with the same laser wavelength, giving to SERS labels a great potential for multiplexed analysis. Moreover, SERS signals are suited for long time observation because they do not show photobleaching. An important difference with fluorescence is that Raman is not sensitive to the background. Therefore, higher sensitivity and lower detection limits are usually expected than ordinary fluorescent tags. It has been reported a class of non-toxic nanoparticle for in vivo tumor targeting based on pegylated colloidal gold and surface enhanced Raman scattering. These gold nanoparticles have been loaded with Raman reporters and conjugated with scFv antibody, recognizing the epidermal growth factor receptor, for in vitro and in vivo tumor targeting. These SERS gold nanoparticles were more than 200 times brighter than NIR emitting quantum dots and allowed spectroscopic detection of small tumors. [*S.H. Radwan et al, 2009; X. Qian et al, 2008*]. Moreover SERS spectra of selected reporter molecules were shown to depend on the pH value in the environment of metal nanostructure. In general the cellular SERS signature contains information on the cellular substructure. Finally, it was demonstrated that SERS enhancement signals were achieved by NPs aggregations or clusters. [*J. Kneipp et al, 2006*]

Another application of gold nanoparticles is Phothermal therapy, in which the light absorbed by surface plasmon resonance is converted into heat. This procedure can be exploited to cause a very localised temperature increase and consequent destruction of malignant cells

enviroments. After internalization of gold nanoparticles into cells, they serve as target molecules to produce increased intracellular heat when exposed to electromagnetic radiation (most in form of infrared 650-900 nm). The limitation, in these cases, is due to the use of visible light, which can be applied in case of superficial tumor (e.g. skin cancer); NIR radiation has been used successfully on other gold nanostructures. In this contest the gold particles shape is very important, in fact it is well estabilished that if the shape changes from colloidal to nanorods it is possible to change not only the absorption and scattering from visible to the NIR region, but also to increase their absorption and scattering cross section. It has also been shown that aggregated gold nanoparticles could decrease the use of laser energy and increase the efficiency of cancer cell destruction. An example of photothermal application is gold nanoparticles conjugated to antiepidermal growth factor receptor (anti-EGFR) antibodies for targeting the HSC 3 cancer cells (human oral squamous cell carcinoma). Twenty-fold lower laser power threshold has been found for the photothermal destruction of cells with the gold NPs than that required destroying the cells without nanoparticles. [*Rozanova Nadejda et al, 2009*]

Finally, gold nanoparticles can also be used as sensor, the absorption spectra of gold nanoparticles change drastically when several particles come close to each other, allowing the detection and quantification of analytes. As already said, they are not susceptible to photobleaching and their absorption and scattering cross sections are superior to those of conventional dyes of about four, five orders of magnitude. According to their size and shape, gold nanoparticles can absorb and scatter light from the visible to near infrared region. They allow the detection of zeptomolar concentration of nucleic acid. [*S.H. Radwan et al, 2009*]

Below are some recently published researches in the field of AuNP application:

- Nanoplex Biotags (Oxonica), commercial particles, composed of an Au core, a monolayer of dye and an envelope of silica, for a total average diameter of 120 nm. These nanoparticles offer the possibility to make multiplexing. [*Keren S et al, 2008*] (see fig. 12)

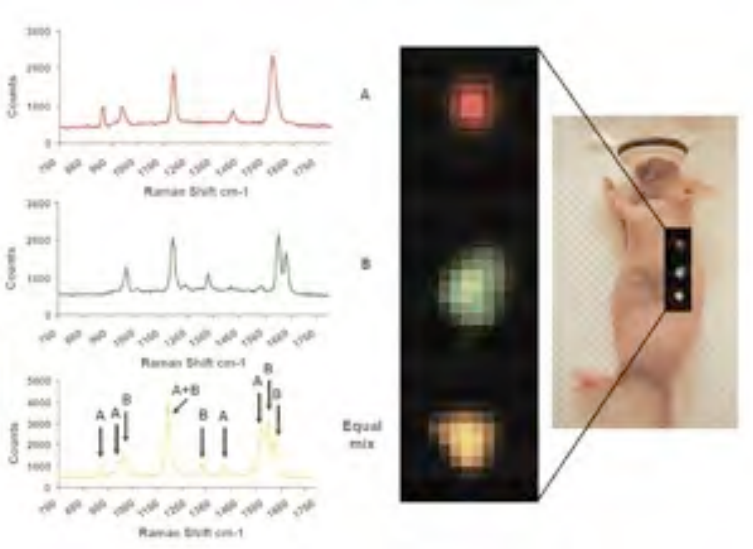

Fig 12: Evaluation of multiplexing experiment in nude mice with SERS nanoparticles. a) First SERS NPs: red color b) Second SERS NPs: green color c) equal mix of the previous ones.

- AgNPs with a dye (4-MT, 2-NT or TP), encapsulated in a shell of SiO2 and then conjugated with an antibody (CD10 or HER2) have shown good signals and high specificity for their target cells. [*Y.S. Lee et al, 2006*].
- AuNPs conjugated with anti-EGFR antibodies have been used for diagnosis of carcinoma of the oral mucosa, using the scattering properties of these particles. [*I.H. El-Sayed et al, 2005*].
- AuNPs conjugated with the monoclonal Ab, Herceptin, which recognizes antigens present on breast cancer cells, have proved to be effective and stable for in vitro and in vivo targeting.[*M. Eghtedari et al,2009*].

6.4 Photodynamic therapy

Photodynamic therapy (Photodynamic Therapy - PDT) is a non-invasive therapy applicable to many tumors and diseases including macular degeneration and certain microbial infections. In photodynamic therapy, a particle is placed within the body and illuminated with light from outside; the light could come from a laser or from a light bulb. The light is absorbed by particles causing different results. If the particle is a simply metal nanodot, the energy from the light will heat the particle and any tissue within its neighborhood. With some particular mo-

lecular dots, light can also be used to produce highly energetic oxygen molecules. These agents are called photosensitizing agents. The photosensitizing agent activated by light energy generates highly reactive oxygen species (ROS) in a process that depends on intracellular interactions between photosensitizing agent and light and oxygen. These species, especially singlet oxygen (O_2•), trigger a cascade of reactions leading to oxidative damage and cell death. This therapeutic idea is referred to as photodynamic therapy because they not only are promoted by light but also depend on the excited state dynamics of involved moleculas. This type of therapy is an attractive alternative to surgery or radiation therapy with less morbidity and can preserve the anatomic and functional integrity of many organs. In addition to directly killing cancer cells, PDT appears to reduce or destroy tumors in two other ways. The photosensitizer can damage blood vessels in the tumor, thus preventing the cancer to receive nutrients. In addition, PDT may activate the immune system to attack cancer cells [*Dolmans et al. 2003; Juarranz et al., 2008*].

However these agents show a low selectivity and the risk of severe burns over the entire body when exposed to light for 1-30 days, after the treatment, depending on the used agent. [*I.H. El Sayed et al, 2006*]. A limitation of PDT application is due to the hydrophobic nature of many photosensitizer agent; they can aggregate in aqueous medium, decreasesing the biodistribution and thus therapeutic efficacy. To overcome this problem and to improve the PDT efficiency and selectivity, we can build nanotools exploiting the opportunities provided by emerging nanotechnologies.

It is important to know the subcellular localization of the photosensitizer in order to deduce what will be the photodamage to the cell caused by PDT. We must also take into account that the response of a tissue to phototherapy depends on the type of photosensitizer and light used, the type of treated cells and state of tissue oxygenation.

The photosensitizers are molecules that have accessible triplet excited states that can promote the generation of O_2•. A photosensitizer for PDT must have an optimized set of well-defined properties:

- a narrow and intense absorption band located mainly in the window of transparency of biological tissues (700-900 nm), in order to ensure a high light penetration in neoplastic tissues,
- the possibility of developing a suitable formulation for its intravenous administration,
- a very low cytotoxicity in the absence of light
- a high quantum yield of O_2• generation.

The first generation of photosensitizers, such as Photofrin®, are ematoporphyrin derivatives. Photodynamic therapy based on Photofrin® is being proved effective in the treatment of a broad type of cancer, but some limitations and side effects have been documented. The first treatment involves the use of a laser irradiation at 630 nm. At this wavelength the penetration of the laser beam inside the tissue is limited to a maximum depth of 3-10 mm, limiting their application only to superficial disease. All of these limiting features of first-generation photosensitizers have pushed the research towards the identification of new photosensitizers agents: 5-aminolevulinic acid and other porphyrins derivates. Since in this case, the porphyrin photosensitization of origin (the excitation of PpIX also takes place at 630 nm), there are substantial advantages compared to treatment with HPD regarding the depth of tissue penetration. This new generation of photosensitizing action ensures greater tumor selectivity, due to their absorption wavelengths close to the spectral range of red and far red, allowing to intervene against the deepest tumors. They also have a faster elimination time, resulting in fewer side effects on skin photosensitivity, allowing to the patient to be exposed to direct sunlight a few days after treatment.

Among all the photosensitizer agent approved in clinic, one of the most used is Foscan ®. It is a termoporfirin belonging to the class of clorine and its chemical name is meta-tetra (hydroxyphenyl) chlorine (mTHPC). In 2001, Foscan® was approved in the EU, Norway and Iceland for the palliative treatment of patients with advanced states of cervical and brain cancer for whom traditional therapies have not led to improvements and it is impossible to treat with radiotherapy, surgery and chemotherapy. The absorption spectrum of mTHPC shows absorption maximum at 430 nm, the wavelength used for fluorescence diagnostic purposes, and one at 652 nm, the wavelength used to trigger the effects useful in photodynamic clinical applications. The Foscan® is one of the most commonly used photosensitizing substances and requires an excitation at 652 nm, the penetration depth in tissue is about 8-10 mm. Treatment requires low doses of the drug (up to 0.1 mg kg-1) and low light (up to 10 J cm-2), making it 100 times more active than Photofrin®.

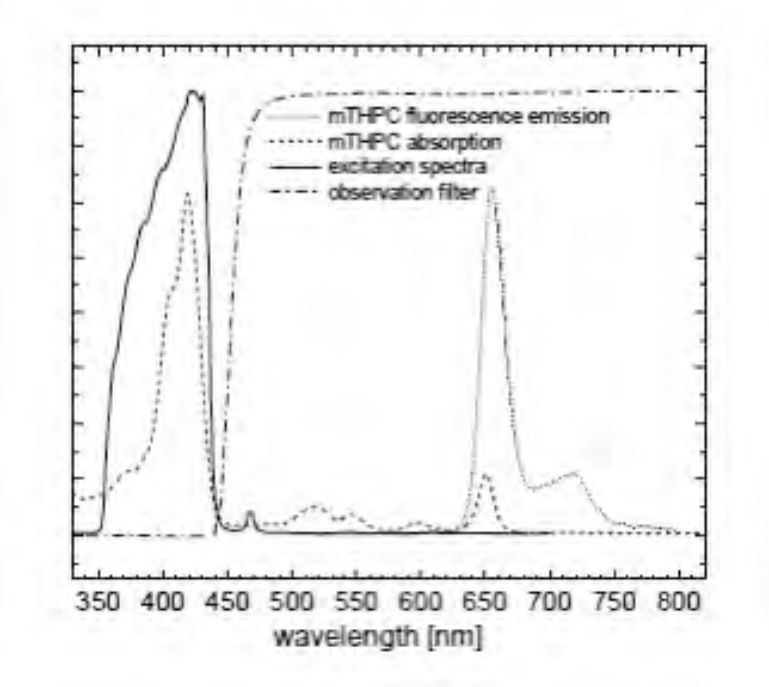

Fig 13: meta-tetra (hydroxyphenyl) chlorine (mTHPC) spectra

Porphyrin	Photofrin®	HpD	Axcan Pharma Inc.	www.photofrin.com
Porphyrin	Photogem®	HpD	Moscow Research Oncological Institute	www.times.net/photogem/index.htm
Porphyrin	Levulan®	ALA	DUSA Pharmaceuticals, Inc.	www.dusapharma.com
Porphyrin	Metvix®	M-ALA	PhotoCure ASA	www.metvix.com
	Hexvix®	H-ALA	PhotoCure ASA	www.photocure.com
Porphyrin	Visudyne®	Verteporfin	Novartis Pharmaceuticals	www.visudyne.com
Texaphyrin	Antrin®, Lu-Tex	Lutexaphyrin	Pharmacyclics	ir.pharmacyclics.com
Chlorine	Foscan®	Temoporfin	Biolitec Pharma Ltd	www.biolitecpharma.com
Chlorine	LS11, Photolon®, Litx™, Apoptosis™, Laserphyrin	Talaporfin	Light Sciences	www.lightsciences.com
Chlorine	Photochlor	HPPH	RPCI	www.roswellpark.org
Phthalocianines	Photosens®	Phthalocyanine	General Physics Institute	www.gpi.ru
	Pc4	Phthalocyanine	CWRU	www.cwru.edu
Padoporfin	Tookad	Bacteriochlorophyll	The Weisman Institute of Science	www.weizmann.ac.il

Fig 14: Clinically available photosensitizer. [*R.R. Allison MD et al, 2010*]

Despite the major achievements of the porphyrins and their partially reduced derivatives, some problems persist today in modern techniques of PDT, including: (i) the aggregation in situ during irradiation, (ii) optimization of irradiation protocols according to the pharmacokinetics of the photosensitizer, (iii) a decreased absorption in the NIR spectral region, (iv) high chemical stability that causes photosensitivity of the skin following the treatment. Finally, a

high number of porphirins and no porphirins derivatives have been proposed in order to further expand the PDT opportunities.
As described above, injectable nano-carriers are excellent systems for drugs delivery to tumor cells and as agents for imaging and diagnosis of cancer. For the above reasons, development of new photosensiting agents is more and more required. They are currently studying the agents of the third generation. This generation includes the conjugates of molecular vectors like antibodies or nanoparticles, an example of that is the SiO_2-NPs. A big advantage in the production of transport systems for photosensitizing agents is the non-necessity of the drug release from the carrier. It is enough a good oxygen permeability so as to allow the production and the diffusion of O_2• [*A.P.Kumar et al, 2009*].
NPs have many other advantages such as: transparency to light, hydrophilicity, biocompatibility thanks to PEG coating, ease preparation and a large porosity which, as mentioned, make them permeable to oxygen.

6.5 Magnetic nanoparticles

Magnetic nanoparticles offer some interesting applications in biomedicine. They have controllable sizes ranging from a few nanometers up to dozen of nanometers, this means that they can 'get close' to the biological entity of interest. Moreover, they can be coated with biological molecules allowing interactions with or bind to a biological entity, thus providing a tool to control targeting. Secondly, the nanoparticles are magnetic, which means that they obey Coulomb's law, and can be manipulated by an external magnetic field. This 'action at a distance', combined with the intrinsic penetrability of magnetic fields into human tissues, opens up many applications involving the transport and/or immobilization of magnetic nanoparticles, or of magnetically tagged biological entities. Finally, the magnetic nanoparticles can answer to a time varying magnetic resonance, with advantageous results related to the transfer of energy from the exciting field to the nanoparticle. For example, these particles can be heated when subjected to an alternating magnetic field, and then they can be used as hyperthermia agents, delivering toxic thermal energy as a targeted therapy against cancer cells. This one, and many other applications are possible, due to the particular physical properties of magnetic nanoparticles. Through multilayered functionalization, MNPs can simultaneously act as imaging agents and drug carriers.

Mainly two types of iron oxide (magnetite, Fe_3O_4 and maghemite, Fe_2O_3) were used for various biomedical applications. Magnetite is a very promising candidate for its biocompatibility. Furthermore, if these materials are prepared in the form of nanoparticles, they have a superparamagnetic behavior at room temperature and they are also strongly magnetized by external magnetic field but retain no permanent magnetism once the field is removed. This quality leads to easy dispersion, as the particles are unlikely to clump together.

Thus, we here refer to iron oxide MNPs as "MNPs". Typically, the magnetic nanoparticles are synthesized and dispersed in a homogeneous suspension, called ferrofluid. Each MNP consists of a magnetic core and a non-magnetic coating with different surface chemistry. The superparamagnetic phenomenon is due to a set of properties: thermal energy, quantum effects, size and large surface area for MNPs. Based on the biokinetics of particles, the size of 10-100 nm are optimal for delivery in vivo, as a quick escape renal clearance (<10 nm) and sequestration by the reticuloendothelial system (RES) of the spleen and liver (>200 nm). [*V.I. Shubayev et al, 2009*]

Numerous engineering approaches aimed at achieving uniformity of MNP size, shape and composition. Surface chemistry is another factor that regulates the physical-chemical properties of MNPs, and therefore strongly influences the fate of MNP in the biological systems, including the mechanisms of cell recognition, biodistribution and immune response. It presents a specific focus for advancing engineering strategies to minimize potential nanotoxicity.

Several coating groups are used to modify MNP surface chemistry:

- organic polymers, such as dextran, chitosan, polyethylene glycol, polysorbate, polyaniline
- organic surfactants, such as sodium oleate and dodecylamine
- inorganic metals, such as gold
- inorganic oxides, such as silica and carbon
- bioactive molecules and structures, such as liposomes, peptides and ligands/receptors.

Antibodies are conjugated to magnetic beads in cell sorting and imaging applications, but due to their large size as MNP cores, they often suffer from steric hindrance, poor internalization into the cells and display low affinity.

MNPs represent a particularly appropriate tool based on their ability to be simultaneously antibody functionalized and guided by an external magnetic field.

A new term was created to talk about of MNPs applications: Theragnostics: the fusion of therapeutic and diagnostic approaches.

The main fields of application of MNPs are:

a) *Cell labelling and Magnetic separation*: In biomedicine it is useful to separate specific biological entities from their original environment, in this way concentrated samples can be prepared for subsequent analysis or for other uses. A way to achieve this goal is the magnetic separation using biocompatible nanoparticles.

   It is a highly sensitive technique useful for the selection of cancer cells present in low concentration in blood, and it is particularly suitable for the separation of a low number of target cells.

b) *Drug delivery*: The most promising application of these magnetic NPs is the site-specific drug delivery. These NPs may carry therapeutic agents on their surface or inside, as it is formulated with polymers, which could be guided to the target organ by an external magnetic field and then released there. For these applications, the chemical size, charge and surface of the magnetic particles are particularly important because these properties strongly influence both their blood circulation time and the bioavailability of the particles within the body. Furthermore, the magnetic properties and the internalization of particles in the target tissues depend strongly on the size of magnetic particles.

   The principles of magnetic orientation of MNP-conjugated drugs were applied experimentally, and have reached clinical trials in cancer therapy. Nanoparticle-based drug and gene delivery systems could solve the insurmountable obstacle to treat neurological diseases: the delivery through the blood-brain barrier. But the potential problems of embolization due to the formation of MNP aggregates in capillaries and the need of large distances between the malignant tissue and external magnetic field still represent a challenge. For this type of use, the nanoparticles must maintain a sufficient hydrophilic surface and not to exceed 100 nm to avoid rapid clearance by the RES. Moreover, the smaller, the more neutral and the more hydrophilic surface, make nanoparticles plasma half-life much longer. Since 1970, a series of magnetic nanoparticles and microparticles vectors have been developed to deliver drugs in vivo to specific sites. The optimization of these vectors continues today. In general, the magnetic core is coated with a biocompatible polymer such as PVA or dextran, although recently inorganic coatings such as silica have been developed. The coating acts to protect the magnetic particle from the surrounding environment and can also be functionalized with carboxyl groups, biotin, avidin, carbodi-imide and other molecules.

c) *Hypertermia:* Hyperthermia is based on the localized heating of malignant tissues above 43° C for 30 min. Different degrees of heat depends on the magnetization properties of MNP formulations and specific parameters of the magnetic field. Heat generated by nanoparticles is spread in the immediately surrounding tissue, so if the temperature can be maintained above the therapeutic threshold of 42°C for 30 minutes or more, it can destroy the cancer. Most of the hyperthermia devices are limited in their usefulness because of an unacceptable random healthy tissue heating. Magnetic particle hyperthermia is attractive because it offers a way to ensure that only the target tissue is heated. [*Q. A. Pankhurst et al, 2003*]

   The specificity against the tumor sites has been greatly improved through functionalization approaches. For example, MNPs-conjugated to antibodies specific for tumor antigens improved selectivity of MNP uptaken by tumors during hyperthermia therapy. Experimental investigation of magnetic material application for hyperthermia date back to 1957 when *Gilchrist et al* using nanoparticles of γ-Fe_2O_3 exposed to a magnetic field of 1.2 MHz are able to heat tissue samples. Since then a lot of publications have been edited, describing a variety of experiments using different types of magnetic materials, field strengths, different frequencies, and different methods of encapsulation and particle delivery. [*Q. A. Pankhurst et al, 2003*]

d) *Mri contrast agent:* MNP-MRI is based on the quality of superparamagnetic iron oxide MNPs. Several dextran coated MNP formulations have been approved for clinical use as contrast agents for magnetic resonance imaging, including ferumoxides, ferumoxtran and ferucarbotran. The nanoparticles are used for the detection of primary tumors, metastasis, angiogenesis and vascular imaging. In addition, the ability to specifically label macrophage cells allows using them in inflammatory image, including atherosclerosis, multiple sclerosis and rheumatoid arthritis. FITC-conjugated MNPs were used by surgeons to delineate gliomas, both pre-operatively, by means of magnetic resonance imaging, and during the intervention, based on fluorescent tags. This is particularly important since some cancers, such as gliomas, may change position during surgery [*V.I. Shubayev et al, 2009*]. A number of studies demonstrate the high potential of MNP-based molecular MRI as a combination imaging and drug/gene delivery strategy. For example, monocrystalline iron oxide MNPs (3 nm core) sterically protected by a layer of low-molecular weight dextran and covalently conjugated to holo-transferrin are used to visualize transgene expression directly in vivo, exploiting overexpression

of engineered transferrin receptor (ETR). Increasing the receptor level causes a considerable enhancement of MR signals. Thanks to the upregulation of certain surface proteins in different tumors, these receptor target MNPs can be used specifically to enhance in vivo tumor detection. [*R. Weissleder et al, 2000; V.I. Shubayev etal, 2009*]

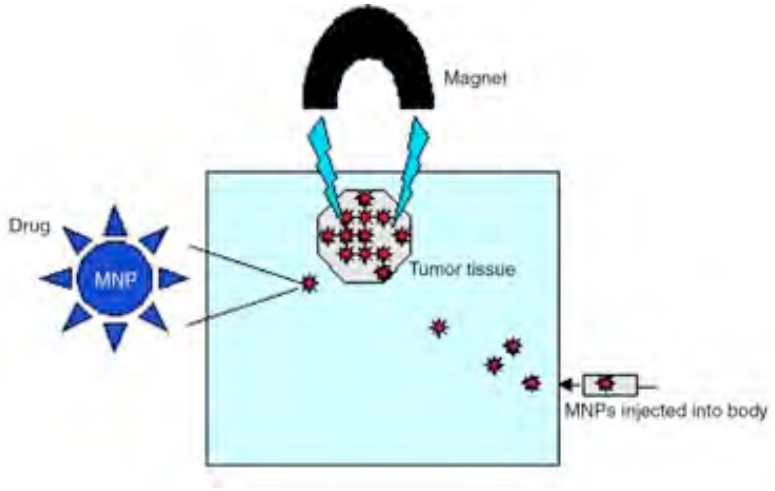

Fig 15: MNPs specifically targeted to malignalt tissues by an external magnetic field. [S. Parveen et al,2011]

7. NANOTOXICOLOGY

In recent years a rapid development of nanotechnology has become aware of the importance of studying the possible immunological and toxicological effects caused by nanomaterials. Nanotoxicology has emerged as the discipline that aims to investigate the safety of nanotechnologies. Nanotoxicology aims are: to assess the risks associated with exposure to nanomaterials; to explore the routes of entry of nanoparticles into the body and to study the molecular mechanisms of nanoparticles toxicity [*Oberdorster G. et al, 2005; Fischer H.C. et al, 2007*]. There are up to now no usual standard methodologies to assess the toxicity of nanoparticles, as nanomedicine is a relatively new field. To assess the potential toxic and immunogenic nanoeffects, a close collaboration between medical scientists and biological material scientists is required. Nanomaterial needs to be thoroughly characterized before being applied to the cells, thus allowing a better understanding of how the different properties of nanoparticles can influence the biological response. The small size of nanoparticles is useful in medicine, but at the same time it is a factor that can make them potentially hazardous to hu-

man health. Something smaller than 200 nm is not absorbed by phagocytes, so nanoparticles can travel in blood and move randomly throughout the body. Thanks to their small size nanoparticles are able to escape the detection by the body's immune system as well as they have the ability to pass through the blood brain barrier (if nanoparticle diameter is < of 100 nm [*S.V. Vinogradov et al, 2004*]). So nanoparticles have almost unrestricted access to the human body. Normally, specialized phagocytes that are responsible to protect the body from "foreign substances" absorb exogenous particles that enter in the bloodstream.

Since the immune system is our first defense, it is important to study the immune responses caused by these nanoscale formulations. To understand how nanoparticles, of different materials, shapes and sizes, interact with the immune cells will also allow to optimize the design of nanoparticles for future biomedical applications. It is seen that the surface characteristics of the particles affect the way they interact with the various constituents of blood. Cationic NPs, including gold and polystyrene have been shown to cause hemolysis and blood clotting, while anionic particles are usually quite non-toxic. Depending on the type of coating, the surface reactivity of nanoparticles can cause chemical damage to surrounding tissues. Nanoparticles whose surfaces are not modified to prevent absorption of opsonins (proteins that give an eat- me-signal to cells) are readily removed from the blood stream by macrophages. If it is requested, surface hydrophobicity or charge can be changed, e.g. by coating the particles with polyethylene glycol (PEG). It is still unknown the fate of nanoparticles within the cells: the nanoparticles can remain structurally unaltered, altered or metabolized. It is developing studies about how nanoparticles interact with the cells. Ideally, the nanoparticles should be secreted or degraded, without toxic side effects.

The exact biodistribution of nanoparticles in the body is still difficult to predict. Biodegradable substances are normally broken down and their waste products excreted by the kidneys and intestine. However, non-biodegradable nanoparticles have been studied and seem to accumulate in specific organs, especially the liver. It is not known how long the deposits stay, the potential damage that can trigger, or the dosage that hurts. Some organs like the brain are more vulnerable and need special attention. We must ensure that the nanoparticles do not affect any physiological process, disrupting normal function of the body [*N.Sanvicens et al, 2008*].

In the literature there are several studies on different types of nanoparticles. They report that there is an inverse relationship between size and concentration and their adverse effects:

quantum dot with smaller sizes and higher concentrations being more cytotoxic. In this context, *Lovric* and his co-workers found that the quantum dot induced cell death was more pronounced in small green-emitting quan- tum dots than in the large red-emitting quantum dots [*Lovrić J. et al, 2005*].

As for nanoparticle dose-dependent cytotoxicity, we can notice that higher concentrations (even at levels used for studies) of nano-60 fullerene, gold and iron oxide nanoparticles induce higher levels of cell death [*Pisanic T.R. II et al, 2007; Sayes C.M. et al, 2005; Pernodet N. et al, 2006*].

Some studies prove the influence of geometry on the toxicity of nanoparticles: carbon nanomaterials with different geometry, such as single-walled or multi-walled nanotubes and nano-60 fullerenes, exhibit in vitro differential cytotoxicities [*Jia G. et al, 2005*]. Some nanoparticles, such as Qdots, which contain toxic elements, such as cadmium and selenium, without a protective coating that prevents premature breakown, could lead to unpredictable collateral damage. [*Nel A. et al, 2006*].

Gold is an inert material, and then it is a good candidate for biological applications. In fact, the gold salts have been used for years in rheumatic patients although some minor side effects occurred in about half of all patients. However, gold nanoparticles can interact with cells due to their small size. It is therefore important to study the potential toxic effects of gold in the form of nanoparticles. The first toxicological studies have been performed mainly on cell lines. Toxic effects have been identified as size dependent: the larger particles of gold from 4 to 18 nm appear to be harmless. The particles from 1 to 4 nm size cause an indistinct toxicity versus healthy and tumor cell lines because of their ability to bind to DNA [*Tsoli M. et al, 2005; Pan Y. et al, 2007; Connor E. E. et al, 2005*]. In other studies, it did not detect any toxicity, thus leading to the conclusion that the toxicity was due to salt presursor solution and not to the same gold nanoparticles. It should also be noted that the nanoparticle toxicity depends on the characteristics of the coating. These results show that to study the toxicity of these particles, it must be taken into account the purity of the preparation due to different methods of synthesis and the experimental set-up, otherwise these experiments are exposed to conflicting results. [*Connor E.E. et al, 2005*]

Another example of conflicting results is described for the quantum dot. In fact, some authors indicate Qdots as activators of caspase mediated apoptosis. According to other authors Qdots activate caspase independent apoptosis. Therefore we can conclude that the cellular toxicity,

due to a contact with a material may differ significantly from exposure to the same material but in the "nanoparticolate form". [*Chan W.H. et al, 2006; Lovric J. et al. 2005*].

Conflicting results were observed even for silica nanoparticles. In this case, the toxicity does not seem to depend on the size, but rather on the concentration and exposure time. The damage generated is an oxidative damage due to the increasing ROS levels and decreasing glutathione [*Lin et al, 2006*]. Even *Chang et al* demonstrated a reduction in cell viability upon exposure to high doses of SiO_2, cells that proliferate more slowly are more susceptible to this material [*Chang et al, 2007*].

Cell death was probably not caused by apoptosis [*Jin et al 2007*]. On the contrary, for cationic silica nanoparticles it was observed low or no cell toxicity, using amino-hexyl-amino- propyl-trimethoxysilane as a surface modifier. [*Ravi Kumar et al 2004*].

Only a few studies, assessing the risks associated with exposure to nanoparticles, have indicated silica NPs as a biologically inert material and thus suitable for application in vivo. In support of this hypothesis, several studies have demonstrated that nanoparticles injected into live animals produce no detectable toxicity [*Voura E.B. et al, 2004; McAteer M.A. et al, 2007;Akerman M.E. et al, 2002*].

Other animal studies show on the contrary inflammatory reaction in the lungs, and accumulation in the liver, spleen, lymph nodes and bone marrow. [*Akerman M.E. et al, 2002; Ballou B. et al, 2004; Gopee N.V. et al, 2007*]

Examples of these contradictory results are shown in Table 7, which highlight the influence of the experimental conditions and the nanoparticle physicochemical characteristics on the results. [*Sanvincens et al, 2008*]

It is not yet clear the intracorporeal pathway of nanoparticles, the nonspecific uptake, and the residence time in the body. So further pharmacokinetic and pharmacodynamic studies are needed before the promise of nanoparticle technologies can be translated into the clinic.

Nanoparticle	Cell or animal	Toxicity
Pegylated dendrimers	Male CH3 mice	No toxicity was observed at doses up to 2.56 g/kg i.p. injection
Cationic dendrimers	Male CH3 mice	100% mortality at 160 mg/kg i.p. injection
Carbon nanotubes	Male Dunkin Hartley guinea pigs	Do not induce any abnormalities of pulmonary function or measurable inflammation
Single-wall carbon nanotubes	Male Crl:CD(so)IGS BR rats	High-dose induced mortality within 24 h post-instillation Pulmonary inflammation (granuloma formation)
CdSe quantum dots	B16F10 melanoma cells	No detectable toxicity
	C57BL/6 mice	No detectable toxicity
CdTe quantum dots	Human hepatoma HepG2 cells	Cytotoxicity in a concentration- and size-dependent manner
		Few signs of functional toxicity
	Sprague-Dawley rats	Transient reduction in motor activity
Fe_3O_4 nanoparticles	COS-7 cells	Excellent biocompatibility
		No toxicity observed
Fe_2O_3 nanoparticles	Rat pheochromocytoma cell line PC12M	Dose-dependent diminishing viability
		Reduced ability to respond to nerve growth factors
Pegylated gold nanoparticles	Nude mouse	No toxicity or physiological complications
Gold nanoshells	BALBc mice	Dose-dependent toxic effect

Table 7 : Cytotoxicity studies in nanoparticles. [*Sanvincens et al, 2008*]

AIM of the research:

The PhD thesis here presented is the result of a collaboration work with Padua University.
The first part (in collaboration with Prof. Meneghetti Nanophotonics Laboratory, Physical Chemistry Departmenthas) has been focused on the synthesis and characterization of metallic nanoparticles (gold and FeOX) nude or armed with mAbs and loaded with chemoterapeutic drugs. These nanodevices can act in cancer targeting, imaging and therapy.
The second part (in collaboration with the research group of Prof. Mancin, in European project Nanophoto) aims to developing of silica nanoparticles loaded with Foscan® and functionalized with specific ligands, such as mAbs against TAAs.
The main objectives of this project are:

- generation with a new synthesis method (LASiS) of mAb conjugated metallic nanoparticles;
- generation of mAb conjugated silica nanoparticles;
- characterization of their binding and internalization properties on antigen positive and negative cells;
- evaluation of SERS signal (gold nanoparticles) for imaging potential in vivo and ex vivo;
- evaluation of cell sorting and manipulation by external magnetic field (MNPs),
- evaluation in vitro of the selective toxicity of Foscan® loaded silica nanoparticles in PDT, evaluation of toxicity of gold nanoparticles loaded with doxorubicin.

MATERIALS AND METHODS

1. Gold nanoparticles

- gold nanoparticles (AuNPs) aggregates;
- SERS dye;
- Monoclonal antibody (anti PSMA, anti PSCA) derived from a hybridoma clone developed in our lab;
- SW780: human cell line of urinary bladder carcinoma;
- PC-3: human cell line of prostate carcinoma established from the bone marrow metastasis;
- LNCaP: human cell line of prostate carcinoma established from lymph node metastasis;
- B16: mouse melanoma cell line;
- HeLa: human epithelial cell line;
- DU145 cells: human prostate cancer cell line;
- U937 cells: human leukemic monocyte lymphoma cell line;
- PC3 PIP: transfected human cell line expressing hPSMA;
- PC3 PSCA: transfected human cell line expressing hPSCA;
- LNCaP PSCA: transfected human cell line expressing hPSCA;

All the above cell lines derive from ATCC collection and they are grown in flasks at 37 °C, 5% CO_2, using the following medium: RPMI 1640 medium (with 40 mg/l folic acid, 2 g/l $NaHCO_3$) (Biochromag) and DMEM (with 1,000 or 4,500 mg/l glucose) (Sigma) supplemented with 10% Fetal Calf Serum (FCS), 2 mM L-Glutamine, 10 mM Hepes and penicillin-streptomycin 100 U/ml. All supplements are added into the medium after sterilization through 0.22 µm filters. Hybridoma clone are grown in Hybridomed DIF 1000 Serum free medium (Biochrom AG).

hPSCA – hPSMA transfected cell lines were obtained by transfection with the linearized plasmid codifying for the two proteins, according to the following protocol: cells were plated in a 6 well plate and grown until 50% confluent. Five ml of lipids and 2.5 mg of DNA were added to

250 ml of OPTIMEM. The two solutions were combined to form DNA complex and incubated for 30 minutes at room temperature. Cell medium was replaced with 500 ml of fresh medium plus 500 ml of DNA complex. The following day, new fresh medium was added to the cells. To select the transfected cells, two days later the transfection, it was added the antibiotic to the medium in different concentrations, for each cell line.

Monoclonal antibodies against PSCA and PSMA were obtained by immunization of Balb/c mice with recombinant PSCA protein purified from bacteria. Polyclonal hybridomas were created following the Khöler-Milstein protocol and antigen-reactive polyclonal hybridomas were identified by ELISA and flow cytometry. Positive polyclonal hybridomas were adapted to growth in complete RPMI cell medium and then cloned by limiting dilution protocol. Monoclonal hybridomas were re-analyzed for the ability to recognize the antigen protein. mAbs were purified from hybridoma supernatants using the affinity chromatography on sepharose-protein G column.

1.1 Synthesis and conjugation of Gold nanoparticles

Gold nanoparticles were synthetized by laser ablation in solution (LASiS) in collaboration with Prof. Meneghetti, Nanophotonics Laboratory, Physical Chemistry Department, University of Padova. This technique is a green technique that requires no reagents, only a metal plate and a solvent such as water.

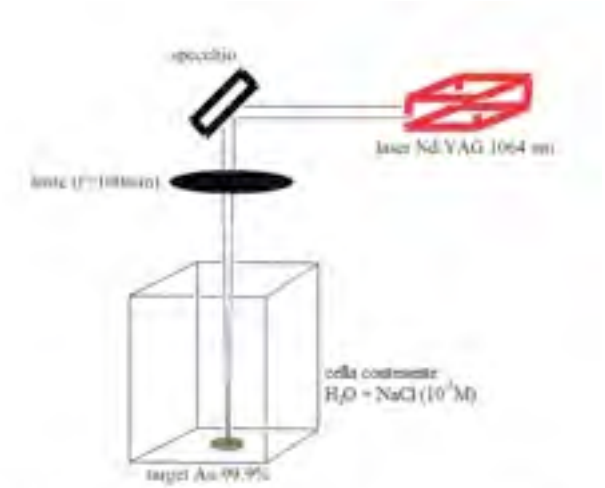

Fig 16: Sperimental set up of laser ablation

The experimental set-up is quite simple: it consists of a pulse mode laser, whose radiation is directed by a system of mirrors and lenses to the metal target immersed in an appropriate solvent: H_2O added with various organic solvents (DMSO, THF, acetonitrile, various aliphatic alkanes and alcohols). The reaction mechanism by which nanoparticles are formed is complex and not yet entirely clear. In short, the incident photons are absorbed and cause heating and photoionization of the irradiated material in the form of vapor issuing, liquid droplets, solid or plasma fragments. With this method gold nanoparticles have an average diameter of about 20 nm. They are mixed with a freshly prepared reporter solution (Texas Red or Malachite green) and than treated with a mixed thiol-PEG solution (PEG-COOH and PEG-OCH3). Derivatization of PEG-COOH groups with EDC/Sulfo NHS were used to covalently link via amino groups the mAb to the NPs. mAb-NPs were washed 4 times from unbound mAb by centrifugation and used for the analysis. Another reagent used for the conjugation by Meneghetti group was 2-iminothiolane for the antibody derivatization in order to add a SH group and to allow the binding with the SH group that was on NP surface. It was also added on the NP surface the hemi-monoclonal antibody, reduced with DTT (Dithiothreitol).

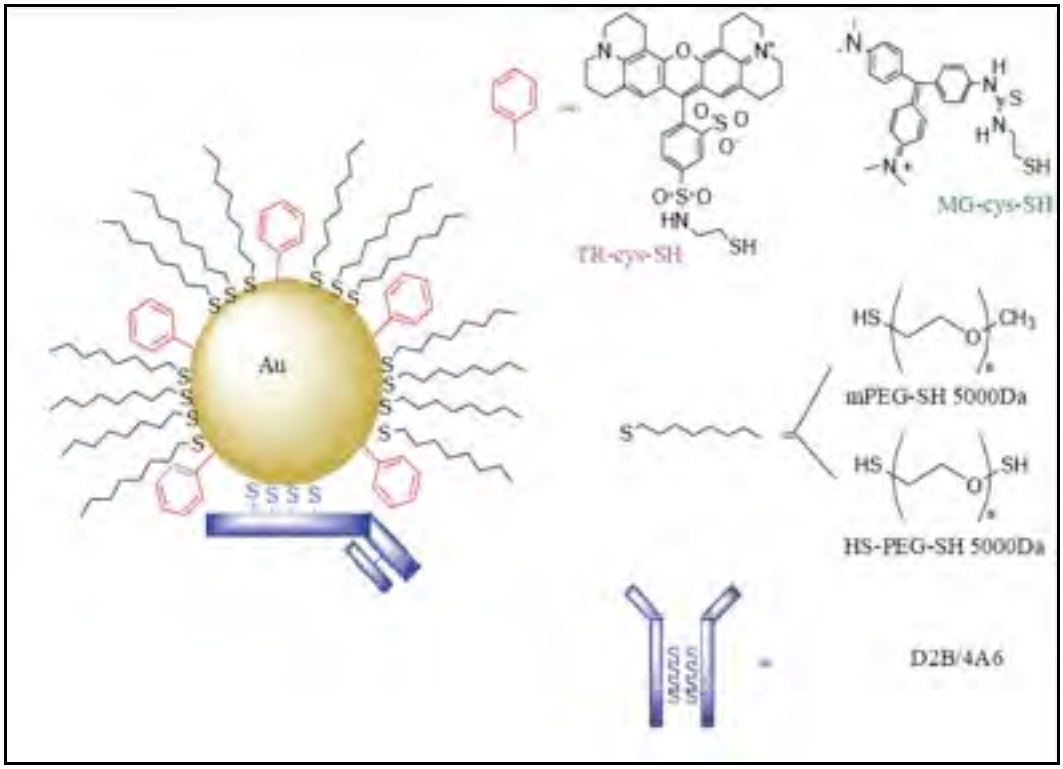

Fig 17: Scheme of mAb conjugation method.

In regard to doxorubicine loaded gold nanoparticles, the synthesis protocol for nanoparticles preparation is the same reported previously. We focused our attention on different binding methods, which not affect drug activity. The drug was firstly covalently bound to the particles via thiol linker (attached by ammino group of the carbohydrate), then dororubicine was simply adsorbed to gold nanoparticles by means of elettrostatic interactions. Finally, it was used a peptide of 18 residues, that acts as bridge between particles and drug. This type of peptide is hydrolysed by intracellular enzymes, in this way doxorubicine is free within the cell.

1.2 Sers labels for quantification assay

AuNPs with average size of 19 nm, loaded with two different Raman dyes: Texas Red and Malachite Green are used to correlate the SERS signals to the concentration of the SERS labels (based on AuNP amount) for *in vitro* quantitative biological applications. The quantitative evaluation of the concentration was based on the fitting of the surface plasmon resonance signals with a calibration curve and correlation with the amount of AuNP taken up by cells measured by ICP MS (inductively coupled plasma mass spectrometry).

The human non-adherent monocyte-like U937 cells were differentiated into macrophages by a 48 hours exposure to PMA (phorbol 12-myristate 13-acetate, Sigma-Aldrich) at a concentration of 40 nm. On day 0 cells were plated 0.5 10^6 cells/well in a 6 well plate and treated with PMA; after 48 hours the medium was changed and the cells resuspended in complete medium without PMA. On day 3 the uptake experiments were performed. Briefly, cells were incubated in complete medium at 37°C for two different time lengths (5 and 10 hours) with 2nM final concentration of three different NP preparations (NP-MG, NP-CV and a 1:1 mix of NP-MG+NP-CV). A mock treated control was also prepared. At the end of the incubation procedure, each well was washed four times with PBS to eliminate the non internalized NP and adherent cells were detached in PBS solution with a cell scraper. The cells obtained from each experimental point were subsequently counted in a Neubauer chamber, centrifuged for 5 minutes at 1,000 rpm and resuspended in a specific concentration ($1.25x10^5$ cells/ml) with lysis buffer solution (Tris 50mM pH=8.0, NaCl 100 mM, EDTA 2 mM, Triton X-100 1%). Samples were stirred by vortex, incubated for 30 minutes at 0° C and centrifuged (13,000 rpm, 20 minutes); then the

protein concentration of each supernatants was estimated by the BCA methods (Pierce). It was observed only slight differences in protein concentration among each sample; all this confirms that the cell lysates were obtained working with the same cells/volume ratio.

1.3 Guided gold nanoparticle characterization

Multiple assays were performed to assess the yield of conjugation and the functionality of the nanocomposites.

ELISA:

The ELISA assay was performed on fixed cells or on recombinant antigen (PSMA-PSCA). Cells grown on a 96 wells plate were fixed with 2% paraformaldehyde, 2% sucrose in PBS for 5 min at RT. After five washings with 0.001% phenol red in PBS buffer the neutralization was performed by incubation with 0.1 M glycine in PBS phenol red buffer for 10 min at RT. After five washings with PBS phenol red, fixed cells were stored with 1% BSA, 0.02% NaN3, 0.001% phenol red in PBS at 4°C. The recombinant antigen was diluted at 2 µg/ml in PBS buffer and 50 µl/well were used to sensitize a 96-well plate (Maxisorp, Nunc). After o/n incubation at 4°C, one wash was made with PBS and wells were quenched by addition of 200 µl/well blocking solution (3% w/v BSA in PBS) and incubation for 1 hour at 37°C. After a wash with PBS, the primary antibody was diluted at 5 µg/ml in blocking solution and 100 µl/well were dispensed. After 2 hours incubation at 4°C, wells were rinsed twice with 0.05% Tween-20 in PBS and twice with PBS.
Secondary antibody-HRP, diluted in blocking solution, following manufacturer's instructions, was dispensed at 100 µl/well and incubated for 1 hour at 4°C. After two washings with 0.05% Tween-20 in PBS and two washings with PBS the assay was developed by addition of 100 µl/well TMB substrate (Sigma) and the reaction stopped with 100 µl/well 1M HCl. The plate was analyzed using the VERSAmax microplate reader with a 450 nm beam and subtracting the background absorbance at 650 nm. To calculate approximately the number of antibodies on NPs surface, the absorbance value was compared with a calibration curve made with known concentrations of monoclonal antibodies.

IMMUNOENZIMATIC ASSAY

The nanoparticles were first washed twice with PBS 1% BSA to remove any traces of free mAb still present. Thus, the NPs were added with anti mouse HRP (Sigma) at suitable dilution for 1 hour at room temperature. After incubation, the nanoparticles were washed by centrifugation in PBS, and then it was added the substrate for peroxidase, TMB (Sigma), until color development. Then the reaction was stopped with HCl 1M. After two washes with PBS, the supernatant was analyzed at 450 nm.

WESTERN BLOT

This method allows us to visualize the antibody on the nanoparticles surface, and even free antibody contamination. It was also applied to analyze the products of papain enzymatic digestion performed on nanoparticle that allowed us to confirm further the antibody presence on nanoparticles surface.

Proteins and nanoparticles separated by SDS-PAGE were blotted on nitrocellulose membranes (Trans-Blot transfer Medium, BioRad) following the manufacturer's indications. The polyacrilamide gel and nitrocellulose membrane were assembled as a sandwich in a Mini Trans-Blot Electrophoretic Transfer Cell (BioRad) according to the manufacturer's instructions, and a tension of 100 V was applied for 1 hour. Nanoparticles, due to their high molecular weight, stop in the stacking, so the entire gel was transferred.

Subsequently nitrocellulose membrane was incubated in blocking solution (5% w/v powder milk in deionized H_2O) under stirring at room temperature for 1 hour. After blocking, the membrane was incubated with a horseradish peroxidase (HRP)-conjugated secondary antibody that interacts with the Fc portion of the mAb. The antibodies were diluted in blocking solution and the membrane was rinsed twice for 5 minutes in 0.05 % Tween-20, PBS and twice for 5 minutes in PBS after each incubation. Bands corresponding to nanoparticles or free mAb were finally detected by a chemiluminescent reaction using the ECL Western Blotting Substrate (Pierce), according to the manufacturer's instructions, and visualized by development of a photographic plate (Hyperfilm MP High performance autoradiography film).

FLOW CYTOMETRY

The flow cytometry is a technique that allows to perform statistical analysis of samples in liquid suspension of microscopic particles, mainly through optical measures and exploiting phenomena of light scattering and fluorescence.

This assay exploits the analytical capacity of flow cytometry on nanoparticles alone to detect the fluorescence emitted by the mAbs-NPs recognized by a FITC- conjugated Ab specific for mAbs present on NPs surface. In this way we can analyse the mean fluorescence intensity (Mean Fluorescence Intensity, MFI) of the samples recorded in 120 seconds compared to a negative control performed with PBS. In this protocol 12 μg of nanoparticles were incubated with FITC conjugated mAb, diluited in PBS BSA 2% for 30 minutes at room temperature. At the end of incubation, to remove free Ab three washes were carried out and NPs were precipitated at 13,000 rpm for 25 minutes, resuspended in 500 μl of PBS. The samples were then analyzed by flow cytometry (FACS Canto, and Beckton Dickinson). It was analyzed the number of events recorded in 120 seconds and the value of MFI of FITC.

Flow cytometry is normally performed on cells in order to assess some parameters of nanoconjugates such as: specificity of binding antigen positive cells, internalization and accumulation only in positive cells.

To evaluate binding specificity: antigen positive/negative cells were detached with Trypsin-EDTA 0.02%, harvested, washed two times with PBS-BSA 0.2% and re-suspended in cold PBS-BSA 0.2% containing mAbs-NPs under study or the control ones. After 180 minutes incubation on ice, cells were washed two times with ice-cold PBS-BSA 0.2% and then incubated with saturating concentrations of a goat $F(ab')_2$ anti-mouse immunoglobulin (goat anti-mouse, GAM) fluorescein isothyocianate (FITC-labeled).

Cell associated fluorescence was analyzed by a flow cytometer (FacsCanto, BDBiosciences) in the FITC channel. The background fluorescence, not due to the specific cell binding of conjugate was determined using cells prepared as a negative control added only with secondary antibody.

In order to test the nanoconjugate stability in human serum, mAb-NPs were pre incubated o/n at 37°C in presence of human serum and then tested in flow cytometr assay.

IMMUNOFLUORESCENCE

Immunofluorescence is a technique used for light microscopy with a fluorescence microscope. This technique allows visualisation of the distribution of the target molecule through the use of antibodies that bind specifically their antigen.
Cells were grown on polylysin coated coverslips o/n in cell incubator. Before NPs incubation, cells were quenced in PBS BSA 1% to avoid the aspecific absorption of NPs on the glass cover. Then after two washings with cold PBS, cells were incubated at 4°C for 1 hour and 30 minutes with mAb-NPs diluted in PBS-BSA 0.2%. After 3 washings with cold PBS, goat anti-mouse fluorescein isothyocianate diluted in PBS BSA 0.2% was added for 1 hour at 4°C. At the end the cells were fixed with 4% paraformaldehyde for 20 minutes at room temperature and after 4 washings with PBS the coverslips were mounted on objective glass with moviol. Samples were kept in the dark and observed by fluorescence microscopy.

CONFOCAL SPECTROSCOPY

This technique allows us to obtain images of the distribution of target substances within cells, in a non-invasively way and with appropriate marking fluorophores. Unlike an ordinary optical microscope, the source is a focused laser beam, which makes a point-to-point scan and then it permits the reconstruction of an image with high resolution. Also the use of a diaphragm (or pinhole) to prevent light from reaching the areas out of focus photomultiplier increases depth resolution, thus only the light signal is recorded on the focal plane.
Using confocal fluorescence microscopy images of internalization and selective adhesion of nanoconjugates in antigen positive cells were recorded. Resonant scattering, collecting the scattered radiation at the same frequency of the incident radiation, at a wavelength of 633 nm where it is known that the particles have a good cross section of scattering, revealed the gold particles.

Cells were grown on polylysin coated coverslips in complete medium o/n at 37°C, then after 30 minutes quenching in PBS BSA 1% (to avoid non specific binding of nanoconjugate to the glass), the cells were incubated with nanoconjugate for at least 2 hrs at 37°C. After the first incubation, cells were washed and incubated with secondary antibody to stain cell walls or nucleus. Cells were then fixed with 4% paraformaldehyde for 30 minutes at room temperature and

after 4 washings with PBS, the coverslips were mounted on objective glass with moviol. Samples were kept in the dark and observed by confocal microscopy

CYTOTOXICITY ASSESSMENT BY THYMIDINE INCORPORATION

The effect on uptake of tritiated thymidine (^{3}H-TdR) by cells was taken as a measure of the growth inhibition caused by treatment with nanoparticles preparation. Cells were resuspended in complete medium and seeded in a volume of 90 µl in each well of 96-well plates (Greiner Bio-one) at 60% confluence. The molecules to be tested were dialysed in PBS, and diluted in sterile PBS containing 0.2% BSA and Penicillin/streptomicin. 10 µl of differently diluted nanoparticle preparation were finally added in each well. The plate was incubated at 37 °C, 5% CO_2 with nanoparticles. After the incubation the medium was taken and replaced with new one. Finally 10 µl of ^{3}H-TdR, from a 1-1.2x10^{5} cpm/ml stock, diluited in RPMI, were added for 8 hours before the end time of experiment, after which the plate was kept at -20 °C and thawed at RT the day after. Using a cell-harvester (Wesbart), the content of each well was transferred to filter paper and radioactivity measured using a beta counter (Wallac 1409, Pharmacia)

1.4 In vitro Raman spectroscopy

The RAMAN-SERS measurements were performed at Padua University by Meneghetti's group using an InVia instrument (Renishaw ®) connected to a confocal microscope Leika DM-LM and interfaced to a computer. This instrumentation has two lasers (Argon anf He-Ne). The one used for this work (Helium-Noen) emits in red at 632 nm, with an intensity of about 17 mW. Briefly, the laser beam within the instrument is conveyed through some filters and is thus attenuated. Finally, it reaches a lens system that act as a beam expander, so the incoming radiation becomes a laser bundle. Between the two blocks, there is a diaphragm, called pinhole, used to perform confocal microscopy if necessary. The beam is reflected by a notch filter (a filter that selectively reflects the lasr radiation) to the microscope and then to the sample. The radiation scattered by the sample is directed back towards the notch filter, in which the Raman radiation passes. Raman radiation is scattered on a reticulum (1,800 lines/mm) and then sent towards the detector CCD (Charge-Coupled Device). This instrumental apparatus is

provided with high stability and optical efficiency; capabilities of continuously scan for large windows and high spectral resolutions space.

Incubation procedure of nanosystem is similar to that performed for confocal microscopy assay. Cells were grown on polylysin coated coverslips in complete medium o/n at 37°C. After 30 minutes quenching in PBS BSA 1% (to avoid non specific binding of nanoconjugate to the glass) cells were incubated with appropriate dilution of nanoconjugate for at least 2 hrs at 37°C. After incubation, the cells were washed and then fixed with 4% paraformaldehyde for 30 minutes at room temperature and the coverslips were sent to Padua after 4 washings with PBS.

1.5 Ex vivo Raman spectroscopy

In view of future application of SERS analysis in vivo, we tested a preparation of conjugated NPs in mice C57/B16 males. It were injected subcutaneously 1 x 10^6 murine melanoma cells (the B16 hSMALu8) expressing hPSMA, which generally result in metastases into the lung. These cells were injected subcutaneously since the tumor was very aggressive and grows rapidly. Once developed the tumor, 100 µl of nanoparticles preparation were injected directly into the tumor. After 3-6-24 hours, the mouse was sacrificed; the tumor was taken and stored in Tissue TEK ® O.C.T. compound (SAKURA). The tumor was dissected by Kryostat 1720 digital (Leitz) and thin layers were deposited on glass slides for the following analysis at Raman spectroscopy.

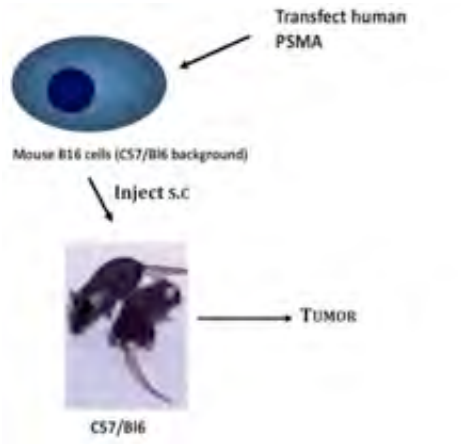

Fig 18: Scheme of ex vivo assay with gold NPs conjugated with an anti PSMA antibody.

2. Magnetic nanoparticles

- FeOx MNPs (magnetic nanoparticles);
- DU145 cells: human prostate cancer cell line, derived from ATCC collection, manteined in RPMI plus 10% Fetal);
- U937 cells: Human leukemic monocyte lymphoma cell line, were obtained from the American Type Culture Collection (ATCC).

All cell lines are grown in flasks at 37 °C, 5% CO_2, using the following medium: RPMI 1640 medium (with 40 mg/l folic acid, 2 g/l $NaHCO_3$) (Biochromag) supplemented with 10% Fetal Calf Serum (FCS), 2 mM L-Glutamine, 10 mM Hepes and penicillin-streptomycin 100 U/ml. All supplements are added into the medium after sterilization through 0.22 μm filters.

2.1 Synthesis and functionalization

FeOx–MNPs were obtained by Laser Ablation Synthesis in Solution (LASiS), in collaboration with Prof. Meneghetti (Padua University). Briefly, laser ablation was obtained with laser pulses at 1064nm (9 ns) focused with a 10 cm focus lens on a 99.99% pure iron plate placed at the bottom of a cell containing bidistilled water. Pulses of 10 J cm^{-2} at a 10 Hz repetition rate for 90 min were employed. Disodium ethylenediaminetetraacetate (>98%, Sigma Aldrich) was added with a 5mM final concentration to the so obtained FeOx–MNPs solution and heated at 55 °C for 60 minutes. Particles were washed a lot of times with bi-distilled water by centrifugation at 5000 rpm. Functionalization was made adding the ligands by means of a synthetic procedure. This procedure consisted in the addition of a 0.01% in weight aqueous solution of BSA or F-BSA (Fatty Acid Free BovineSerum Albumin or Albumin–fluorescein isothiocyanate conjugate from Sigma Aldrich) and 0.005% aqueous solutions of F–PEG–NH2 (Fluorescein–PEG–Amine, Mw 5000, from LysanBio), FITC (fluorescein isothiocyanate mixed isomers from Sigma Aldrich), to an equal volume of FeOx–MNPs in water (0.5 mg per ml iron). They tested various pH conditions by incubating the FeOx–MNPs with the ligands at acidic (pH 4) or basic (pH 9) conditions and they found that the best conjugation efficiency was obtained in acidic pH. This was likely due to a good stability of FeOx–MNPs observed at acidic pH, as also it was proved by DLS measurements. In order to prevent the adsorption of carboxylic or phosphate

molecules on particles surface, the pH was set by adding controlled amounts of very diluted HCl or NaOH solutions. After 24 hours of incubation at room temperature, the solutions were washed at least twice by centrifugation at 5,000 rpm with bidistilled water and twice with 5 mM PBS solution.

2.2 Cell labelling and manipulation

First nanoparticles characterization was made on DU145. Nanoparticles, after 30'' sonication, were incubated with cells (previously seeded in a 6 well plate) for 24 hrs at 37°C and then analyzed in FITC channel by flow cytometer (BD FACS Canto).

The uptake was tested on U937 cells. The human non-adherent monocyte-like U937 cells were differentiated into macrophages by a 48 hours exposure to PMA (phorbol 12-myristate 13-acetate, Sigma-Aldrich) at a concentration of 40 nM. On day 0, cells were seeded at $0.5x10^6$ cells per well in a 6 well plate and treated with PMA; after 48 hours the medium has been replaced and the cells resuspended in complete medium without PMA. On day 3 the uptake experiments were performed. The uptaken efficacy of NPs was evaluated by flow cytometry analysis of this cells incubated in complete medium with FITC-FeOXMNPs equivalent to a final concentration of 0.36 mg per ml of iron for 4h at 37°C. A mock-treated control well was also prepared. A sample of cells treated with MNPs and a sample of non-treated cells were incubated with APC-labelled (allophycocyanin) anti-human CD13 (BD Biosciences Pharmingen, NY, US, macrophage membrane marker) to select the macrophage population. For cell sorting experiments we used an aliquot of cells treated as above. Magnetic separation was performed at 4°C for 10' with a magnetic trap based on NdFeB magnet. After a 10 minutes exposure to a magnetic field, non-attracted cells were washed out. Magnetic sorted and non-attracted cells were re-analyzed by flow cytometry.

Another characterization assay was done at confocal microscopy. U937 cells, seeded in a 24 well plate on polylysine coated glass slides, were differentiated into macrophages and they were treated with FeOx–MNPs as previously described. Cells were washed in order to remove the non-internalized FeOx–MNPs, and then they were fixed in 2% paraformaldehyde. After four washings with PBS, the cells were stained with APC anti-human CD13. Glass slides were

washed in PBS and mounted for confocal microscopy analysis (Zeiss LSM 510 confocal microscope).

CYTOTOXICITY ASSESSMENT

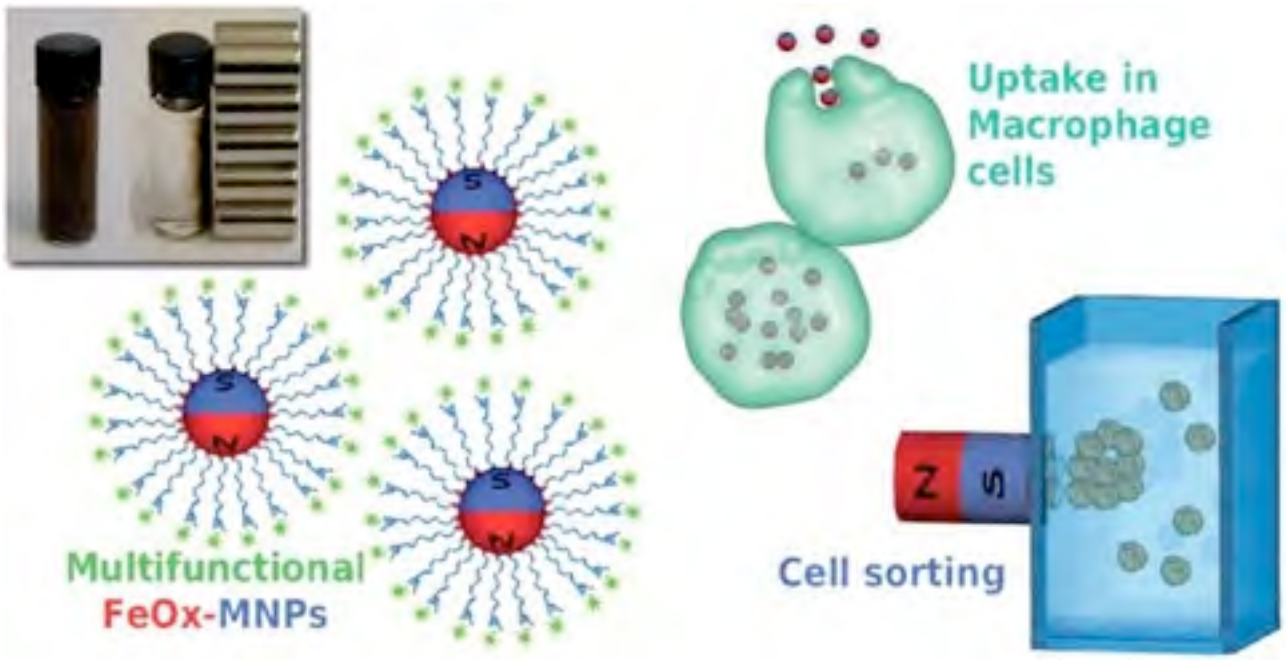

Fig 19: Magnetic Iron Oxide nanoparticles used for magnetic sorting of macrophages. [Amendola et al, 2011]

In order to evaluate the cell toxicity of this type of material it was done a XTT assay after FeOx-MNPs incorporation. Briefly, U937 differentiated cells were obtained according to the above described protocol and treated with FeOx–MNPs at 37 °C for 4 hours at a final iron concentration of 0.18, 0.36 and 0.72 mg ml-1. Then, the cells were washed to remove FeOx–MNPs and the medium was replaced. After 20 hours, the cell viability was measured with an XTT assay: cells were resuspended in medium with no red phenol and added with XTT reagent 50μg/100μl. Then the plate was analyzed using the VERSAmax microplate reader with a 450 nm beam. On the contrary, cell apoptosis was assessed by the human Annexin V-FITC Kit (Bender MedSystems, Wien, Austria). Cells were incubated with FeOx–MNPs at 37 °C for 4 hours (iron concentration of 0.36 mg ml-1), then washed to remove excess FeOx–MNPs and the medium was replaced. After 2 hrs and 20 hrs, cells were treated with the human Annexin V-FITC Kit and analysed with flow cytometry.

3. Silica nanoparticles

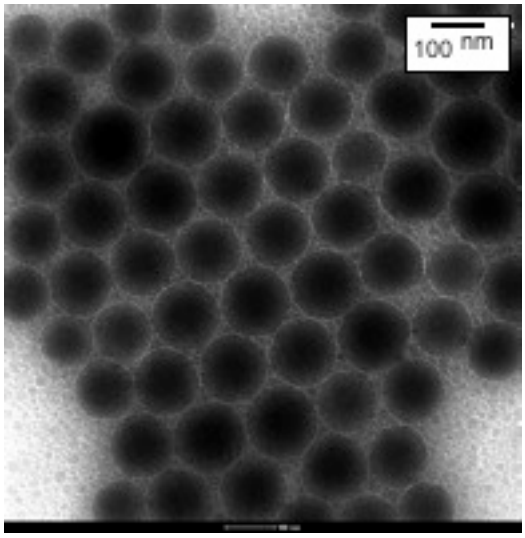

Fig 20: Silica nanoparticles

- Silica nanoparticles loaded with mTHPC;
- Monoclonal antibody (anti PSMA) derived from a hybridoma clone developed in our lab;
- Commercial monoclonal antibody anti EGFR (Erbitux®- Merck);
- BSA (*Bovine Serum Albumin*) (Sigma);
- SW780: human cell line of urinary bladder carcinoma;
- PC-3: human cell line of prostate carcinoma established from the bone marrow metastasis;
- LNCaP: human cell line of prostate carcinoma established from lymph node metastasis;
- B16: mouse melanoma cell line;
- Hela: human epithelial cell line;
- Hela EGFR: human epithelial cell line transfected to increase EGFR expression (provided from Padua University);
- DU145 cells: human prostate cancer cell line;
- U937 cells: human leukemic monocyte lymphoma cell line;
- PC3 PIP: transfected human cell line expressing hPSMA;
- A431: human epidermoid carcinoma, expressing high level of EGFR.

All cell line derived from ATCC collection and are grown in flasks at 37 °C, 5% CO2, using the following medium: RPMI 1640 medium (with 40 mg/l folic acid, 2 g/l NaHCO3) (Biochromag) and DMEM (with 1,000 or 4,500 mg/l glucose) (Sigma) supplemented with 10% Fetal Calf Serum (FCS), 2 mM L-Glutamine, 10 mM Hepes and penicillin-streptomycin 100 U/ml. All supplements are added into the medium after sterilization through 0.22 µm filters. Hybridoma clone are grown in Hybridomed DIF 1000 Serum free medium (Biochrom AG).

hPSMA transfected cell lines were obtained by transfection with the linearized plasmid codifying for the two proteins according to the following protocol: cells were plated in a 6 wells plate and grown until 50% confluent. Five ml of lipids were added to 250 ml of OPTIMEM and 2.5 mg of DNA to 250 ml of OPTIMEM. The two solutions were combined to form DNA complex and incubated for 30 minutes at roomtemperature. Cell medium was replaced with 500 ml of fresh medium plus 500 ml of DNA complex. The following day new fresh medium was added to the cells. To select transfected cells the antibiotic was added to the medium two days after transfection at different concentrations for each cell line.

Monoclonal antibody against PSMA was obtained by immunization of Balb/c mice with recombinant PSCA protein purified from bacteria. Polyclonal hybridomas were created following Khöler-Milstein protocol and antigen-reactive polyclonal hybridomas were identified by ELISA and flow cytometry. Positive polyclonal hybridomas were adapted to growth in complete RPMI cell medium and then cloned by limiting dilution protocol. Monoclonal hybridomas were re-analyzed for the ability to recognize the antigen protein. mAbs were purified from hybridoma supernatants using the affinity chromatography on sepharose-protein G column.

3.1 Synthesis and conjugation

Silica nanopartilces were synthetized in collaboration with Prof. F.Mancin (University of Padova, Italy) with a new one-pot procedure and doped with a second-generation photosensitizer, meta-tetra hydroxyphenil chlorine (mTHPC). The nanoparticle synthesis procedure consists in the polymerization of vinyl-triethoxysilane (VTES) in Brij35 micelles in

water, using a PEG-trimethoxysilyl derivative as a cosurfactant. During the synthesis, hydrophobic molecules, like mTHPC, were spontaneously trapped in the silica matrixs. The conjugation was based on the formation of a highly stable thio-ether binding among the previously functionalized NPs and biomolecules. Different methods were investigated for the derivatization of nanoparticles and antibodies, changing reagents, incubation time and ratio.

Finally the proteins were functionalized by 2-iminothiolane (Traut reagent-Sigma) reaction that modified the NH2 of lysin animoacid with sulfhydryl SH groups, while the NPs were functionalized with maleimide groups by reaction with 3-Maleimidobenzoic acid N-hydroxysuccinimide ester (MBS-Sigma) for 2 hrs at 30°C. The SH group of NPs, reacting directly with the same group of proteins, developed the thio ether binding.

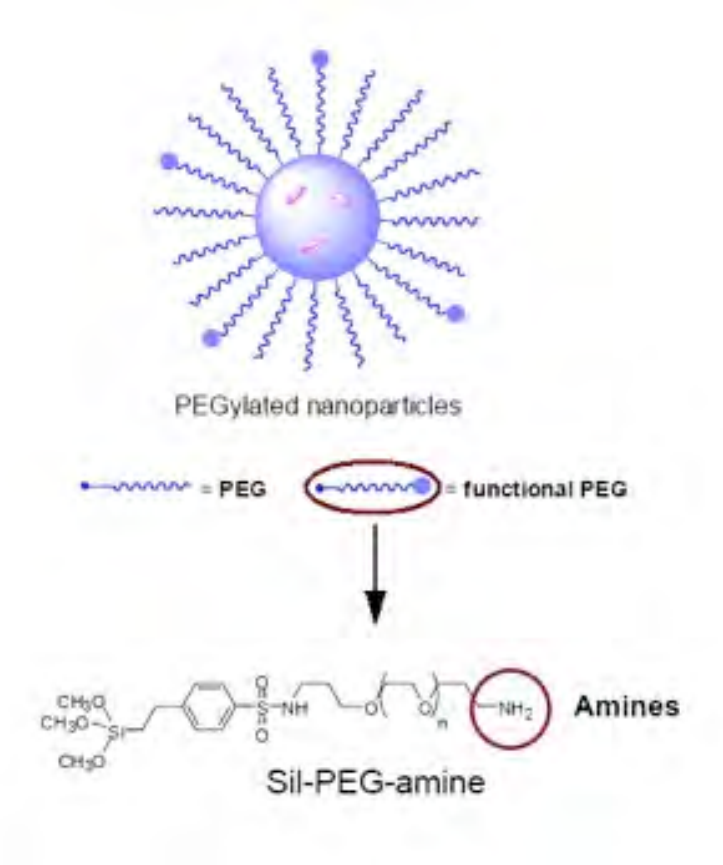

Fig 21: PEG coating of Silica NPs.

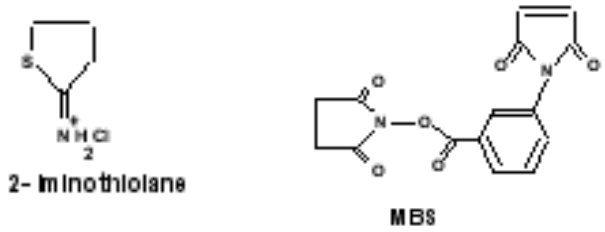

Fig 22: 2-iminothilane and 3-Maleimidobenzoic acid N-hydroxysuccinimide ester used for chemical conjugation.

The antibody functionalization reaction was performed at 30°c for 2 hrs and o/n at 4°C. Then the reaction was blocked with Glycin 0.2 M for 20 minutes at room temperature and finally the compound was purified by gel filtration in PD10 column Sephadex G-25M (GE Healthcare) in order to remove the excess of reagent. Once purified derivatized ligand, the number of SH groups was determinated using the Ellman assay, in which 5, 5'ditiobis-2-nitrobenzoic acid (DTNB) (Sigma) reacts selectively with thiol residues to form the chromophore 2-nitro, 5-tiobenzoato (Habeeb, 1972). The concentration of SH groups was calculated by reading the absorbance at 412 nm. The protein concentration (mg/ml) was determined by spectrophotometric reading (Perkin Elmar Lambda 35 UV/VIS) at 280 nm and confirmed experimentally by the bicinchoninic acid (BCA) (Sigma) using bovine serum albumin (Sigma) as standards for the construction of the calibration line.

The nanoparticles offshoot was purified by centrifugation at 35,000 rpm for 45 minutes for two times and then quantified by reading absorbance at 225 nm for mg/ml, at 654 nm for Foscan® concentration. The conjugation was performed o/n at 30°C and for 24 hrs in dyalisis (in PBS EDTA 10 mM) at room temperature.

Nanoconjugate was seperated from the unreacted reagent by centrifugation at 35,000 rpm for 45 minutes. Finally we obtained a suspension of nanoparticles in PBS. We also tried to purify by molecular exclusion chromatography (HiLoad 16/60 Superdex 75 prep grade, GE Healthcare) FPLC (Fast Performance Liquid Chromatography-BIORAD Biologic Workstation), but the use of this technique led to loss a large amount of the nanoparticle starting batch.

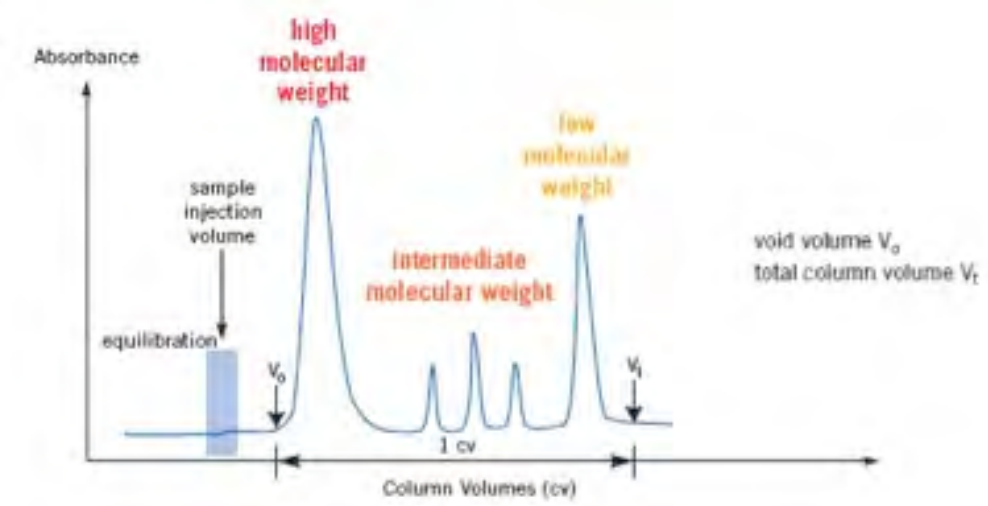

Fig 23: Molecular exclusion chromatography

3.2 Guided silica nanoparticles characterization

In order to estimate the NP concentration we performed an absorbance reading with the spectrophotometer at 225 nm for mg/ml and at 654 nm for Foscan® concentration. After that, silica nanoconjugate batch was characterized in the same way as gold nanoparticles. It was performed western blot assay to verify the presence of protein on NPs surface, and the absence of free reagents in nanoparticle solution.

A further characterization was performed at flow cytometry, both on nanoparticles alone and on cells. The same protocol, as described above, was followed. In the case of silica nanoparticles, however, since they are loading with mTHPC that emits at 660 nm, we considered also the APC (allophycocyanin) channel. In this way, we could further verify the link between the NPs, which emit in the window of the APC, and the ligand. We analyzed the FITC MFI of the samples recorded in 120 seconds compared to a negative control performed with PBS.
In addition, flow cytometry was used to assess the binding specificity, also to evaluate cell uptake and accumulation. Cells were plated in 24 well and grown in complete medium, o/n at 37°C. The cells were plated in order to reach 70-80% confluence at the experiment time. Then cells were incubated in presence of nanoconjugates in several concentration and for different times at 37°C. The NPs were diluted in complete medium. At the end of incubation cells were detached with trypsin EDTA, washed and resuspended in 500 µl of PBS and the samples were ready to be analyzed by flow cytometry. The background fluorescence was determined using

cells prepared as “negative control”. The parameters considered for the analysis of the data were MFI values of the APC.
In order to test the nanoconjugate stability in human serum, mAb-NPs were pre incubated o/n at 37°C in presence of human serum and then tested in flow cytometer assay.

For CONFOCAL MICROSCOPY ASSAY it was followed the same protocol described above. Cells were grown on polylysin coated coverslips in complete medium o/n at 37°C, then after nanoparticle cells incubation and washing cells were fixed with 4% paraformaldehyde. The coverslips were mounted on objective glass with moviol. Samples were kept in the dark and observed by confocal microscopy. NPs are APC (allophycocyanin) labelled; cell membrane was detected with a fluorescein dye.

The CYTOTOXICITY was assessed by XTT assay and by Thymidine incorporation. The plate was incubated for 1 hr and 30 minutes or for 24 hrs at 37 °C, 5% CO_2 with nanoparticles.

3.3 Phodynamic therapy

The phototoxic activity of mTHPC was evaluated assaying cell viability with the MTS assay at university of Padova in collaboration with the research group of Prof. Papini. For these experiments, the cells were seeded in 35 mm diameter plastic tissue culture dishes in complete medium. It was used a cell concetration for well, depending on different cell type. After 24 hrs, the medium was replaced with fresh RPMI containing 3% FBS and various concentration of guided silica nanoparticles. Different incubation time at 37°C was tested. After incubation with mTHPC, the cell monolayers were washed, and irradiated in PBS with 0.12 J cm^{-2} of red light (600-700 nm) emitted from a PTL penta quartz halogen lamp (model STL-B-049, Desys SA, S. Antonio, Switzerland). Immediately after irradiation the cells were brought back to the incubator after replacement of the PBS with complete medium. Cell vialibilty was determinated 24 hrs later with MTS assay. The samples were incubated in 100µl of serum free medium plus plus 20 µl of Cell Titer 96® Reagent, for 1.5 hr at 37°C. After that, the absorbance at 490 nm was measured by Spectramax 190 (Molecular Devices) plate reader. The cell viability was expressed as a percentage of the absorbance on the control cells.

RESULTS

1. Nanoparticles without targeting ligands

1.1 Gold Nanoparticles

The gold nanoparticles in the range of 1-120 nm size have characteristics distinct from the massive material, as it has already been mentioned in the introduction, and this made them a source of growing interest in the last century. The AuNPs have interesting physical, chemical and biological properties: strong absorption in the visible, stability and biocompatibility. They are resistant to photoirradiation and to attack by most acids. The synthesis of metal nanoparticles can be performed through many different physical and chemical methods. Depending on the procedure we obtain nanoparticles of different shape and size. The LASiS technique is a physical method, which consists of a laser ablation in solution of a metal plate. The nanoparticles are formed by condensation of a plasma cloud that is formed as a result of ablation. This method does not require the use of hazardous chemicals reagents, and through modulation of the power and pulse duration of the laser light it is obteined particles of different size. TEM images as shown in Fig 24 demonstrate that the nanoparticles obtained with LASiS technique have size ranging from 3 to 300 nm and are mostly spherical. The Meneghetti's group using this technique, obteined AuNPs with an average size of 20 nm.

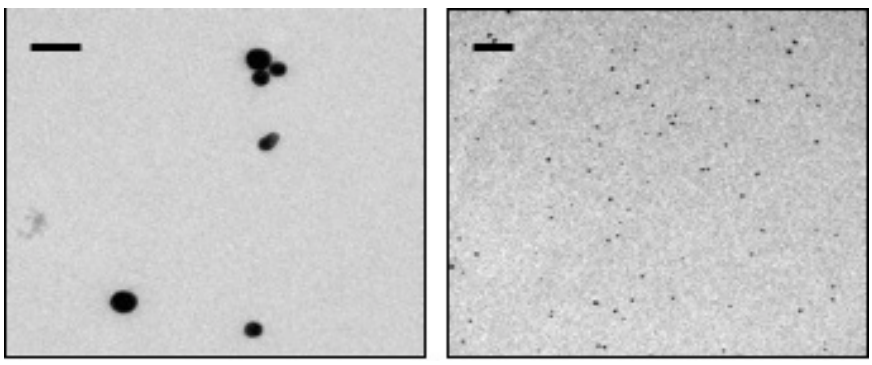

Fig. 24 : Representative TEM images of pegylated AuNP loaded with MG dyes: Left: scale bar 100 nm. Right: scale bar 1 μm. [Amemdola V. et al 2011]

Furthermore they add freshly prepared Raman active dye solution, such as malachite green, cresyl violet or texas red. The dyes are linked to the particle surface by electrostatic interactions. Finally, these nanoparticles are functionalized with targeting moieties, such as monoclonal antibodies and PEG capping.

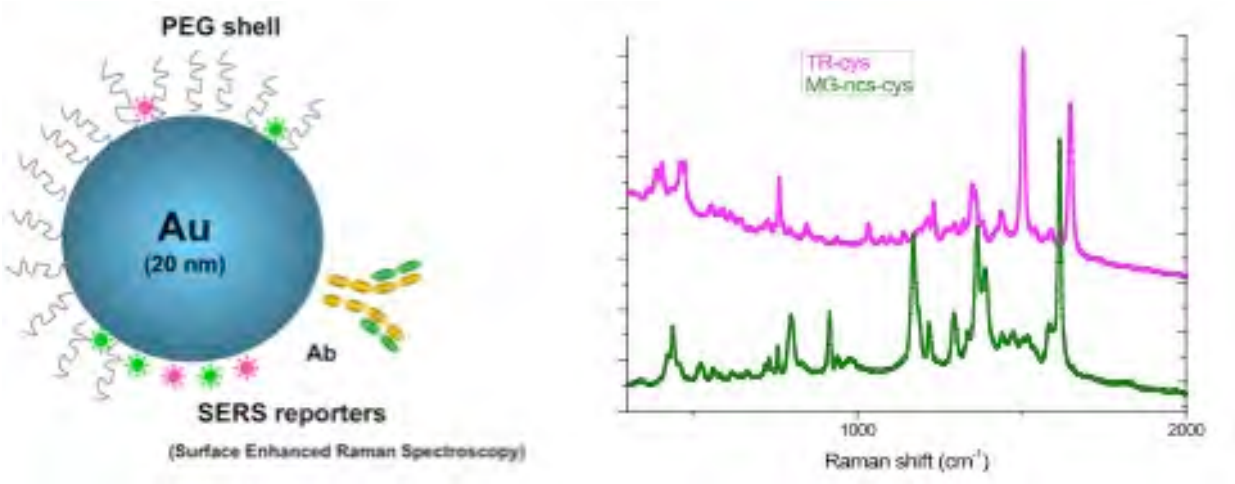

Fig. 25: (left)Representation of guided AuNP SERS loaded. (right) Raman spectra of two SERS labels. [Meneghetti 2011]

First we characterized Raman activity of SERS label gold nanoparticles in collaboration with Padua University. The concentration of AuNP after functionalization process (with SERS labels) was measured by fitting the UV-visible spectra with the Mie-Gans model (fig 25). The accuracy of this method was evaluated also by means of direct comparison with inductively coupled plasma mass spectrometry (ICP-MS) assay.

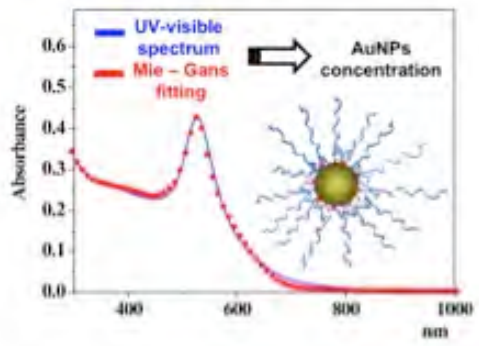

Fig. 26: Fitting dots of the UV visible spectrum of SERS labels solution (line) with a model based on the Mie and Gans midels allowed the determination of AuNP concentration. [Amendola et al 2011]

It was demonstrated a linear dependence between signal intensity and label concentration (fig 27). Furthermore, in the same figure, we can appreciate that the brighter SERS labels can be detected at a concentration as low as few picomoles per litre. The accurate determination of the AuNP concentration is a prerequisite for obtainig calibration curve between the Raman signal and the concentration of SERS labels.

Finally in this work we want to demonstrate the reliability of this method for a medical analytical application. So we considered in vitro cell uptake in macrophage differentiated U937 human cells. The uptake of nanoparticles by cells and the detection of Raman signals from inside cells are topics of interest for several medical applications.

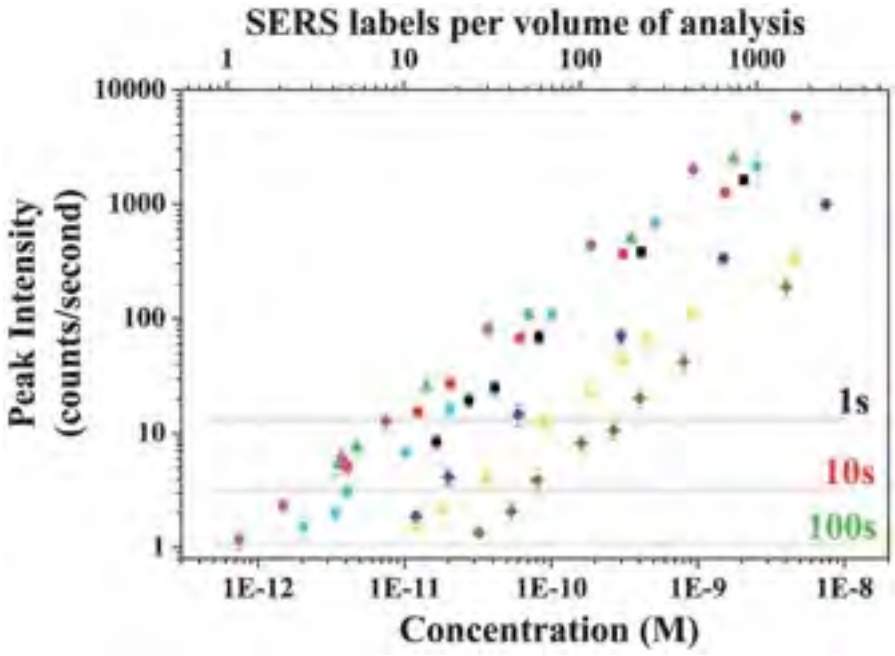

Fig 27: The correlation between the insity of the most intense Raman peaks and the concentration of 8 SERS labels. [Amendola et al 2011]

The uptake of particles by macrophages is interesting for using these cells as Trojan horse for delivering functional nanomaterials into malignant tissues. Briefly, we assessed the quantitative uptake of two different SERS labelled (e.g. malachite green and cresyl violet) nanoparticle preparations. Fig 28 shows a picture of U937 cells and their Raman spectra after 5 hrs of incubation with SERS labelled nanoparticles.

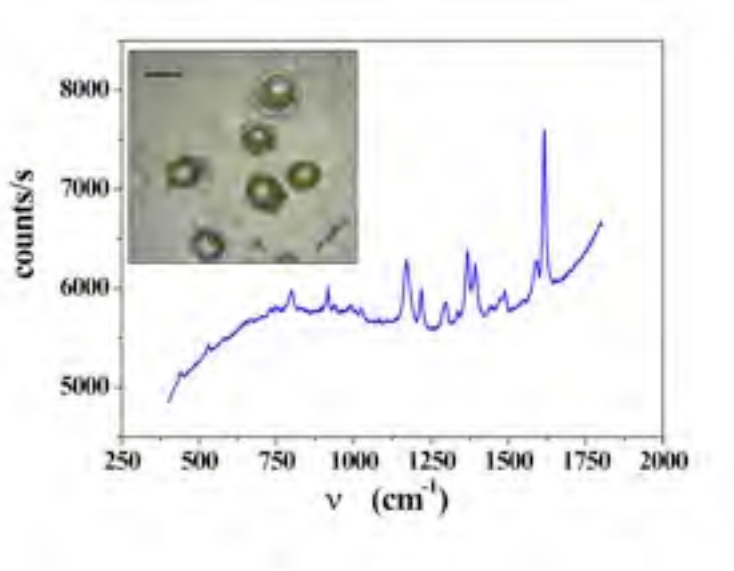

Fig. 28: Raman spectra collected on a single U937 macrophage cells incubated with MG SERS labels.

The lysis procedure was exploited for transforming the macrophage cells into a solution containing the AuNP based SERS labels, in order to correlate the Raman signal to the amount of uptaken nanoparticles. In this way we were sure to work with the same number of cells. Cell lysates were performed with Triton X-100, the only lysing agent that does not cause decreasing of Raman signal. All samples were normalized to contain the same amounts of cells and the Raman analysis was repeated multiple times on each samples.

In all cases we detected a sharp signal that was correlated to SERS label concentrations by a calibration curve obtained for each SERS labels in the same experimental conditions and diluted in the same matrix (Fig 29).

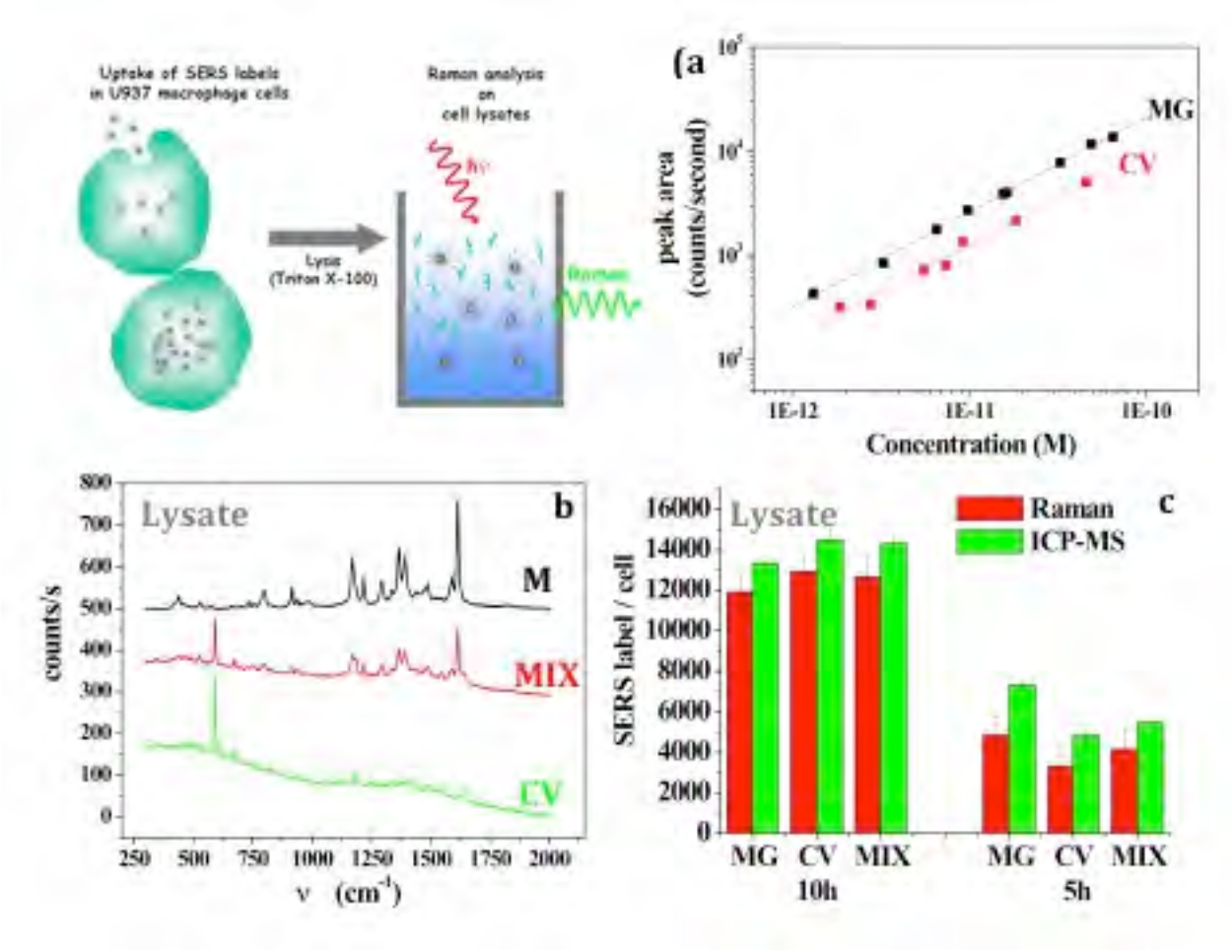

Fig 29 : Sketch of the procedure follow for the Raman analysis on SERS labels uptaken by macrophages and calibration curve of the two SERS labels. Measurements were performer by diluting SERS labels solution at a ratio of 1:4 with cell lysate solution. B) Raman spectra collected on lysates of cell incubated with SERS loaded nanoparticles. c) The average number of SERS labels uptaken by macrophage differentiated U937 cell evaluate by Raman spectroscopy and ICP-MS. [Amendola et al 2011]

These experiments demonstrated that both labelled nanoparticles were uptaken by macrophages in a similar amount, in the order of thousands of nanoparticles per cell per hour. To confirm these data we also carried out an independent measurement on nanoparticle uptaken by ICP-MS (e.g. standard practice to quantify the uptake of metal nanosystems). The results (Fig 29c) show an underestimation of about 20% by Raman analysis with respect to ICP-MS analysis that can be due to the slow release of Raman reporters in physiological medium. We can conclude that this new analytical approach can be used in multiplexed quantification of SERS labels in biological application. This new analytical approach required both small volumes (less than 20µl) and small amounts of tissue per cell (about 25,000). These features can

open the way to an ultrasensitive quantitative analytical assay, which is able to detect picomolar concentration of biomarkers for better cancer diagnosis.

1.2 Magnetic nanoparticles

Multifunctional iron oxide magnetic nanoparticles are a promising tool in theranonistic field. In this work, we used FeOx-MNPs obteined by Laser Ablation Syntesis in Solution (LASiS) of a bulk iron target.

The synthesis procedure was performed at Padua University by Meneghetti's group. These NPs were characterized by transmission electron microscope (TEM) analysis; they have sizes in the 5-30 nm range and a well-defined spherical shape. After verifying the magnetic nature of these nanoparticles, they were functionalized by inserting the ligands (like fluorescent alkylamines, fluorescent isothiocyanates). The functionalization procedure consisted in the incubation of the FeOX MNPs at room temperature for 24 hours with the ligand solution (F-PEG-NH_2). After incubation, excess of ligands is washed out with PBS.

When incubated with macrophage cells, the MNPs are readly uptaken due to their size in the range of nm; after NPs internalization macrophage cells become sensitive to an external magnetic field. Therefore it is possible to manipulate and to drive these cells by means of a magnetic field. So we moved to characterize the nanoparticle internalization and effects also on other cell lines. After 24 hours of incubation, cells (e.g. DU145, prostate carcinoma cells) were analysed by flow cytometry (e.g. nanoparticles are FITC labelled) and FITC channel was considered to evaluate the uptake. Treated cells showed an MFI value of 1,368 higher than the MFI value (73) measures on untreated cells; so we have demonstrated that these magnetic NPs could be applied for managing both macrophage and non macrophage cells.

Due to the higher ability of macrophage differentiated U937 cells to internalize these NPs we had to investigate the labelling and manipulation of these cells alone. The macrophage cells were labelled with anti-human CD13 APC marker (selective for the membrane of macrophage cells) to track them in flow cytometry.

In Fig 30, we can see all macrophage cells, stained with membrane marker, APC positive. The same APC positive population show also a clear FITC fluorescence signal (due to the fluorescein adsorbed on FeOx MNPs). Flow cytometry indicated that more than 95% of macrophage cells had a magnetic fluorescent payload.

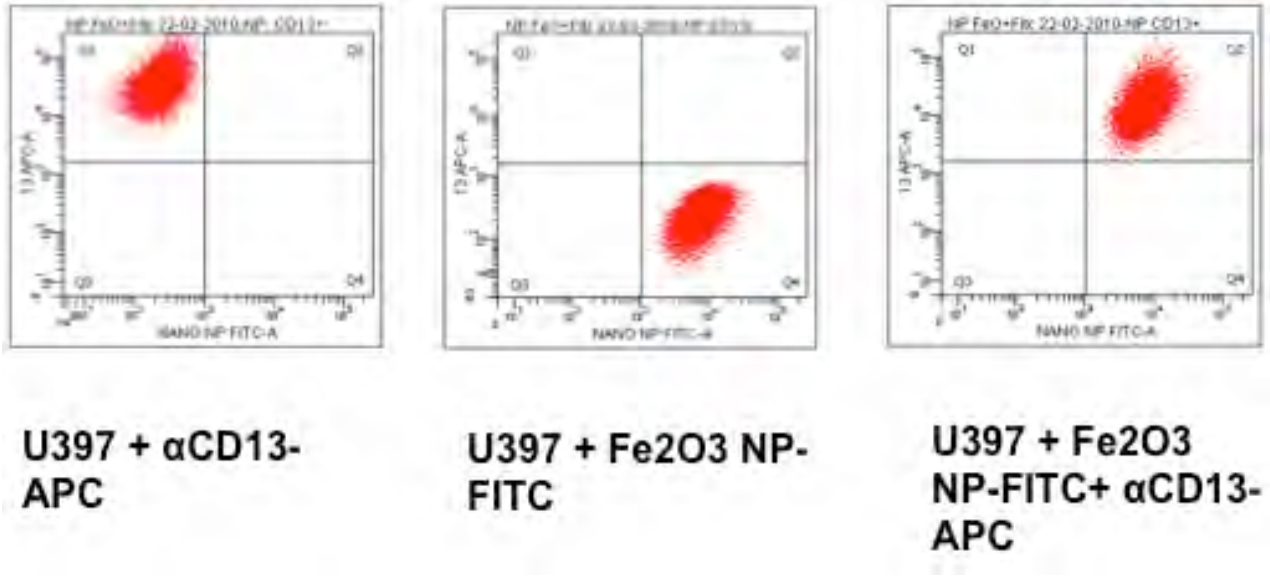

Fig 30: Flow cytometry assay of treated U937 cells with FeOxMNPs and APC anti human CD13. On X-axis: FITC channel, on Y-axis APC channel.

After the application of a magnetic external trap, the cells separated have been assessed by flow cytometry. Then it has been quantitatively analyzed the double fluorescence signal associated to MNPs and to CD13 staining (Tab 8).

	Events	**FITC MFI**	**APC MFI**	**(positive events/total events) %**
Cells+NP+CD13 Sorted	34,958	7,843	14,393	88.9%
Cells+NP+CD13 Not Sorted	4,363	6,725	13,536	11.1%
Cells+NP Sorted	40,623	8,220	276	96.7%
Cells+NP Not Sorted	1,379	6,214	173	3.3%

Tab 8: MFI value of cell sorting evaluated by FACS assay.

It was found that the magnetic trap effectively captured the 90% of the macrophages after 10 minutes of exposure. The flow cytometry shows that lower fluorescence intensity in the FITC channel is measured for non sorted cells, in agreement with a lower payload of FeOX-MNPs in these cells (fig 31). Magnetic field cannot manipulate only the 3,3% of cells payloaded with MNPs.

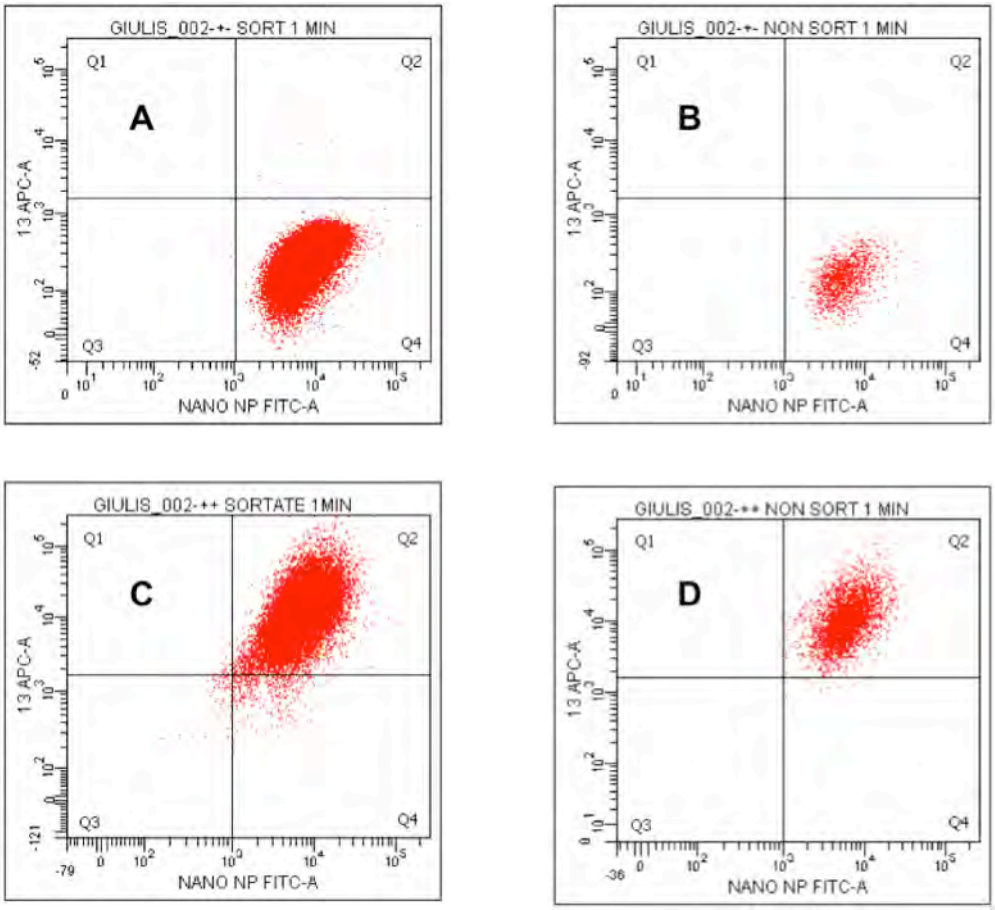

Fig 31: Flow cytometry assay a) cells + MNPs sorted. b) cells + MNPs not sorted. c) cells + MNPs+ ∝CD13 sorted. d) cells + MNPs + ∝CD13 not sorted.

Confocal microscopy images show that the fluorescence is present in the central part of the cells, as expected after phagocytosis of particles, while anti CD13 staining cell wall, provided a good contrast for the visualization of cell membrane (fig 32).

Finally, we studied the effects on cell viability and apoptosis triggering after the nanoparticles uptake. We performed the XTT assay, which measures cell viability by monitoring the activity of intracellular reductase enzymes and the Annexin assay which shows primary apoptosis events. As shown in fig 33 no influence of MNPs on the cell viability has been brought out by the XTT assay.

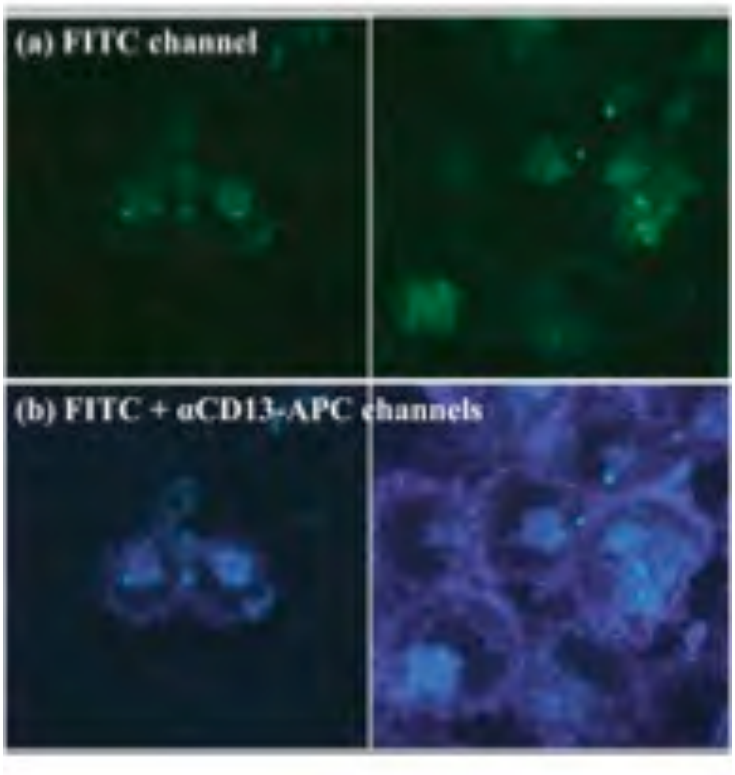

Fig 32: Confocal microscope images of macrophages after incubation with FeOx MNPs and staining with anti human CD13. a) FITC fluorescence only. b) merged images of CD13-APC and FITC fluorescence channel.

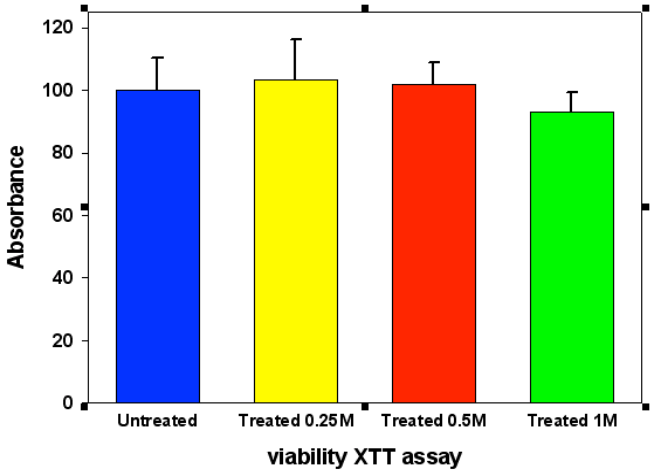

Fig 33: XTT assay of cell viability: U937 differentiated cells were incubated with FeOx MNPs at an iron concentration of 0.18,0.36 and 0.72 mg ml $^{-1}$ and cell viability was detected after 20 hr.

Moreover apoptosis assays assessed after 2 hrs and 20 hrs of cell incubation with MNPs, demonstrated (Fig 34) that cells treated with the nanoparticles showed no apoptosis signal in contrast with those treated with the drug taxol (apoptosis positive control).

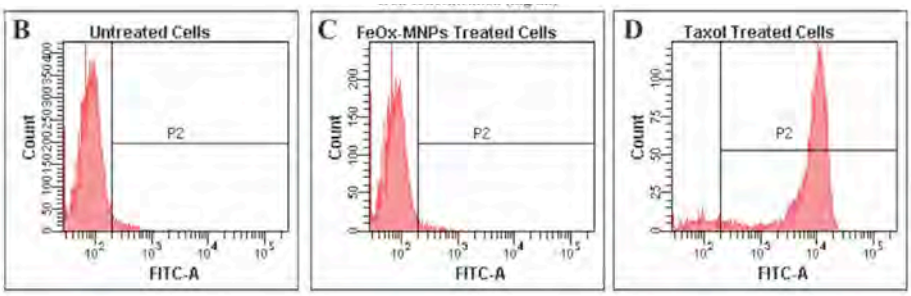

Fig 34: Evaluation of cell apoptosis using human Annexin V FITC protocol.

Investigation of macrophage uptake of magnetic nanoparticles is important in terms of future application. Macrophages have the ability of infiltrating and accumulating in a variety of lesions, and can act as efficient and selective carrier to targeted sites not reachable by EPR effect (deep cancerous tissues). Likewise fluorescent magnetic nanoparticles can be used for multimodal images by magnetic resonance and finally they are efficient heaters for magnetic hyperthermia. Furthermore these magnetic NPs could be used to increase the drug delivey or in magnetic transfection (MF, magnetofections). In gene delivery, MNPs are used as carriers of DNAs encoding for anti-tumor therapeutic molecules (e.g. Interferones, cytokines) in order to increase transfection efficiency. By holding the magneto carrier at the target site via external magnetic fields, the therapeutic gene is in contact with the tissue for a longer period of time, increasing the efficiency of gene transfection and expression.

2. Nanoparticles with targeting ligands

2.1 mAb functionalized Gold nanoparticles characterization

Once analyzed the features of SERS loaded gold nanoparticles without targeting moieties, we decided to study the possibility to improve the accumulation in the tumor sites by conjugation of the same gold nanoparticles with monoclonal antibody. Gold nanoparticles conjugated with monoclonal antibodies or their fragments (e.g. scFv) due to their greater specificity can be used to carry tracer molecules or therapeutic substances to target tissues. Through LASiS technique we produced armed gold nanoparticles in collaboration with Prof. Meneghetti (Padua University). Gold nanoparticles of about 20 nm (see fig. 35) in diameter were mixed with a freshly prepared reporter solution (Texas Red or Malachite Green) and treated with thiol PEG solution. Derivatization of PEG-COOH groups with EDC/sulfo NHS was used to link covalently via amino groups the mAb (D2B: anti PSMA and 4C4: anti PSCA). The nanoparticle diameter was evaluated in TEM microscopy, recording size distribution.

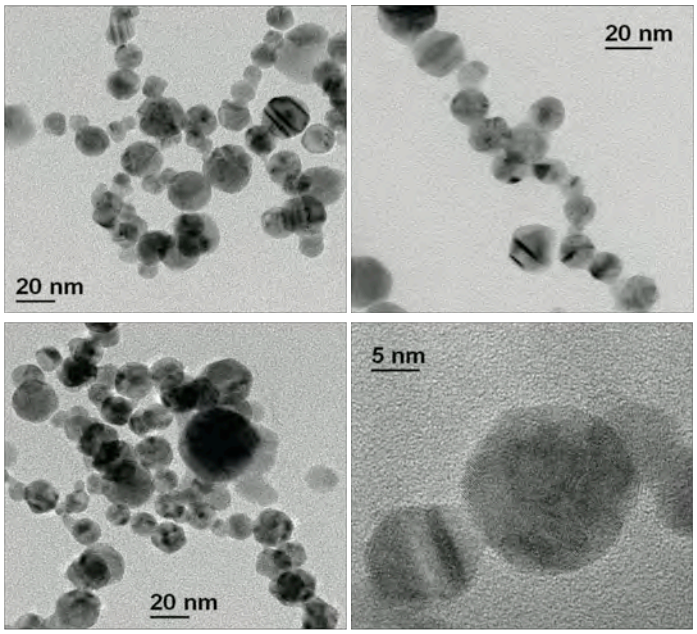

Fig 35: TEM images of gold nanoparticles**.**

Before starting with chemical linking, it was evaluated the antibody stability in DMSO solution, the buffer used for the synthesis. The antibody has been incubated o/n at 4°C in different DMSO concentration 30%-50%-70%; at the end of the incubation time, it was assessed the antibody functionality by flow cytometry on antigen positive cells. It has been used a FITC labelled goat anti mouse (SIGMA) to detect the antibody (D2B or 4C4) binding, and we considered FITC channel for the analysis. As you can see in the table 9 the antibody is still active until 70% of DMSO concentration.

	MFI	**% positive cells**
Cnt –	1,311	4
Cnt +	7,257	99.2
PBS	6,607	99.6
30%	7,556	99.8
50%	7,667	99.4
70%	2,195	52.1

Tab 9: FITC MFI value of antibody stability assay

After the conjugation reaction we had to verify the absence of free antibody, which could decrease the quantitative analysis of the NP binding characteristics. As you can see in picture 36, nanoparticle preparation doesn't have free antibody.

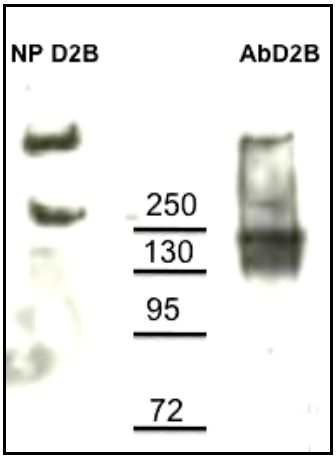

Fig 36. Western blot of conjugated nanoparticle: D2B was used as positive control. To detect the bands corresponding to mAb it was used an anti mouse HRP. The NP bands are much higher than the control mAb, so all the mAb is binding to NPs.

The bands corresponding to free antibody are not present in NP line. Afterwards we investigated the antibody presence on NP surface by papain Kit. Nanoparticle preparations have been incubated in presence of papain enzyme for different times. In SDS PAGE gel, the Fc band confirmed the antibody presence on the nanoparticle surface. (See fig 37)

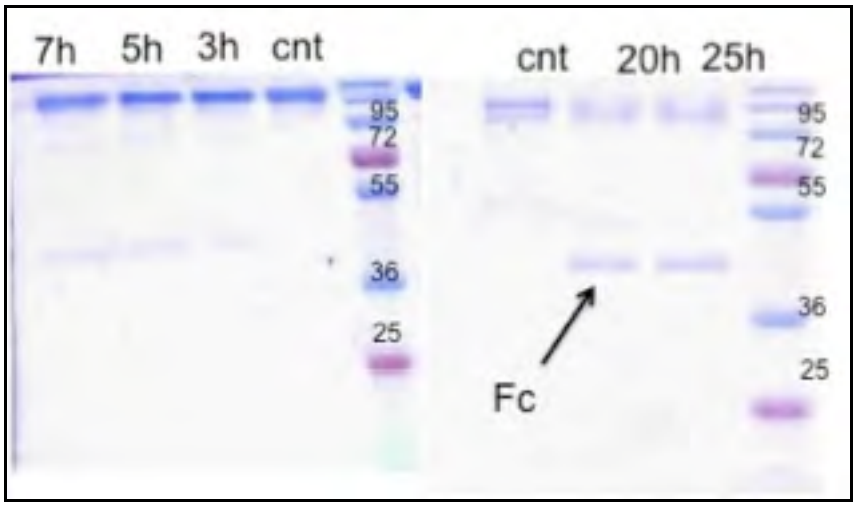

Fig 37: SDS PAGE of functionalized nanoparticles digestion with papain for different times (3-5-7-20-25 hr). The higher bands correspond to undigested antibody, the lower bands are Fc fragment of digested antibody.

We also verified the functionalization by pre-treating driven-NPs with reducing buffer in order to separate heavy and light antibody chains. In western blot we confirmed the presence of a lighter band at about 20 KDa. Flow cytometry is an alternative method we applied to inspect the presence of antibody on the nanoparticles surface. Working with only nanoparticles (without cells) we investigated the presence of antibody by incubation with goat anti mouse FITC labelled.

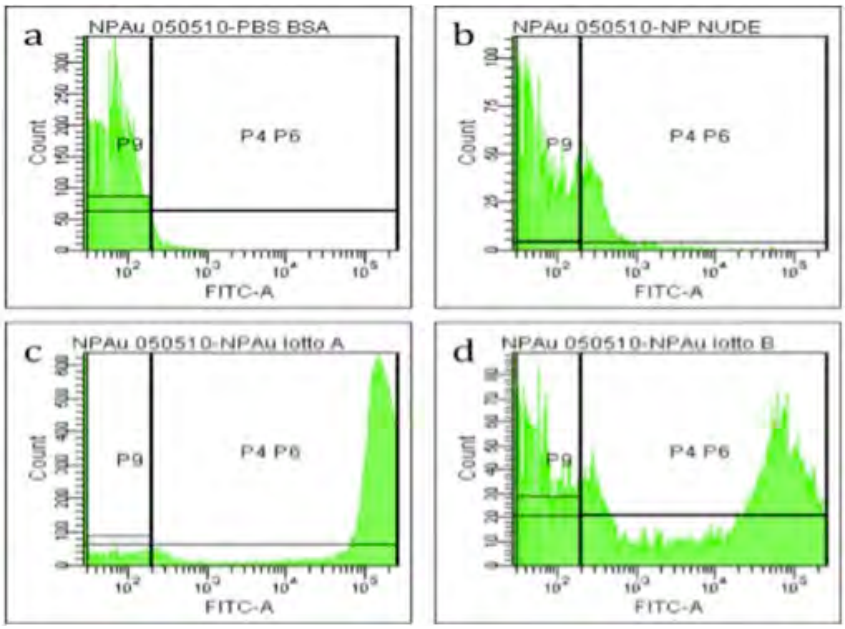

Fig 38: Flow cytometry analysis: a) PBS BSA sample used to detect the instrument back ground (e.g. noise) b) NPs without mAb functionalization c) and d) two different batches of mAb linked NPs. All samples have been stained with goat anti mouse Ig FITC labeled.

Fig 38 shows that the functionalized nanoparticles stained with the goat anti-mouse Ig-FITC have an MFI value > 10^5, whereas non conjugated nanoparticles did not show staining (e.g. MFI of about 10^2).

We applied several assays, such as ELISA and flow cytometry protocol based on a calibration curve (see fig 39) to assess the Ab/NP ratio.

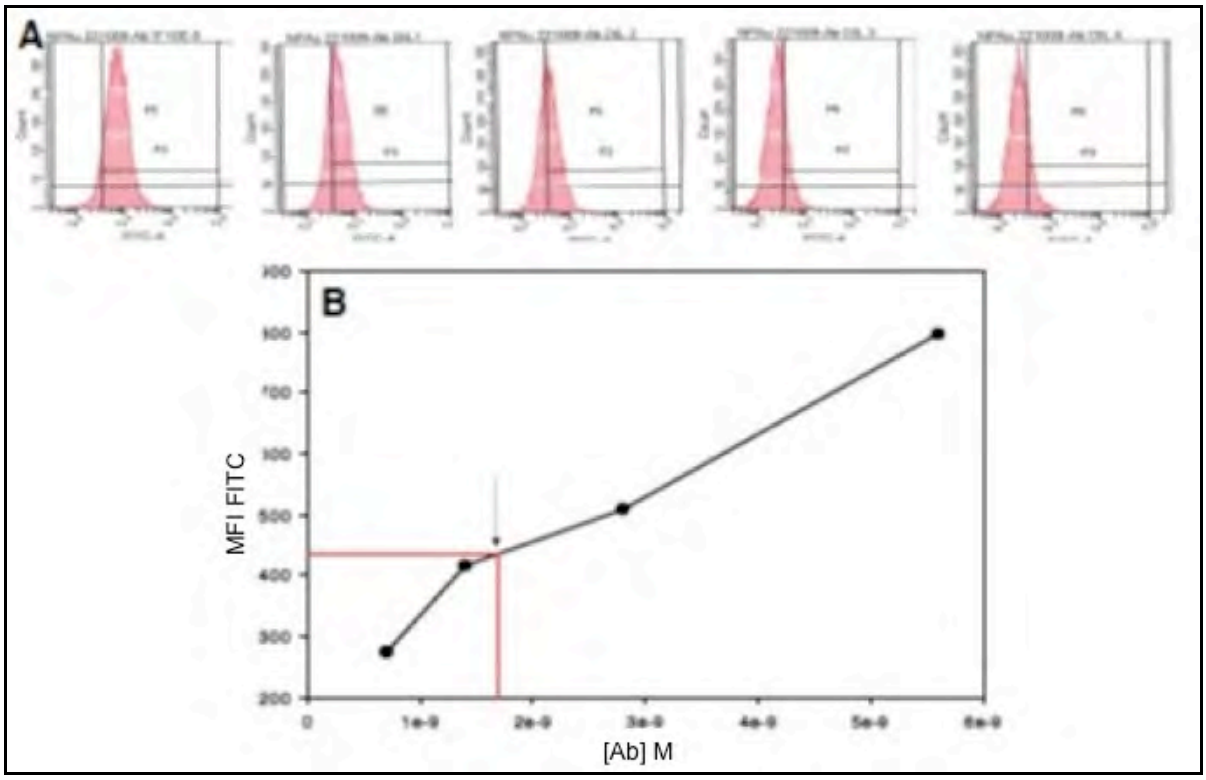

Fig 39:A) FACS analysis of LNCaP cells incubated with decreasing amount of Ab. B) Calibration curve created plotting MFI value and Ab concentration. The Ab/NP ratio was estimated using this curve.

The calibration curve was created incubating LNCaP cells with decreasing mAb concentration and plotting the MFI value measured by FACS analysis vs the mAb concentration. The best batch of armed NPs showed about 2-3 antibodies for NP.

In these first series of experiments we characterized the chemical conjugation of nanoparticles with the ligand moieties; after that we moved to analyze their binding characteristics (e.g. functionality).

mAb-gold NPs binding to antigen positive cells (such as LNCaP for PSMA, PC3 hPSCA for PSCA) was assessed by flow cytometry staining mAbs bound NPs with a policlonal goat anti mouse Ig FITC labeled. Below it is depicted (see Fig 40) an example of this analysis, we measured a MFI value of 1,383 for D2B NPs, working on LNCaP cells with anti-PSMA mAb-NPs: whereas the MFI of the negative control was 68, the MFI value of the positive control (free mAb D2B) was 3,970.

No aspecific staining was observed when D2B NPs were assessed on Jurkat or DU145 (both PSMA- cells). MFI value of 101 and 81 were obtained for the negative control on Jurkat and DU145 cells, respectively.

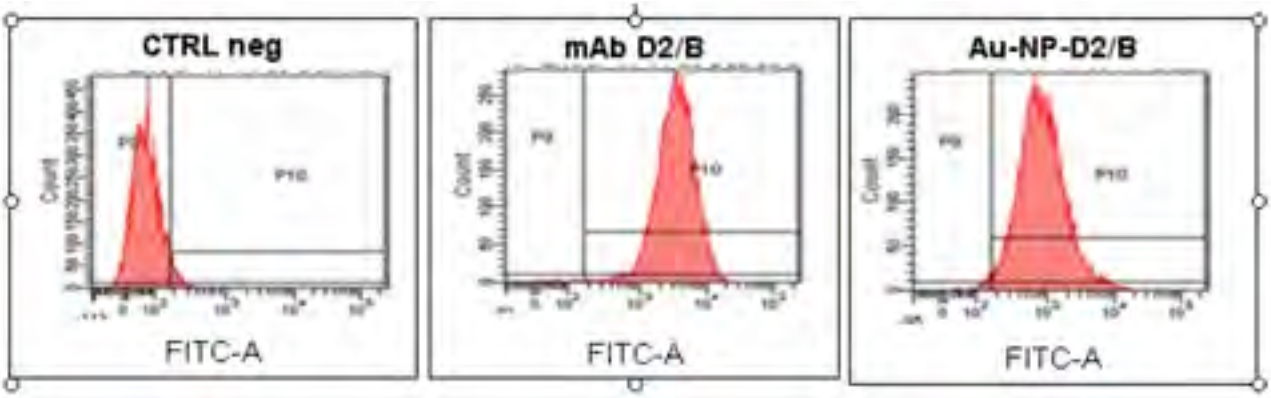

Fig 40: D2B NPs binding experiments perfomed on LNCaP PSMA+ cells and analyzed by flow cytometry.

As negative cell lines, we also used U937, PC3 WT and SW780. All these lines are negative for PSMA expression, and therefore no staining has been detected (fig 41). To increase the panel of antigen positive cells we assessed PC3 hPSMA and B16 hPSMA transfected cells.

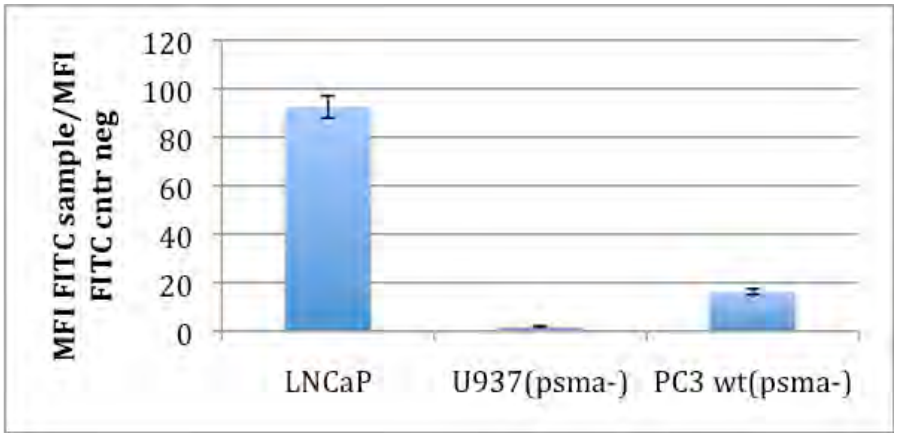

Fig 41: D2B NPs binding experiments performed by flow cytometry. It was plotted the ratio between FITC MFI of D2B NPs and the negative control (cell not incubated with nanoparticles).

Moreover the binding specificity was confirmed by a binding competition experiments performed on LNCaP cells coincubating mAb D2B biotin labeled and D2B-NPs; the signal was obtained by incubating with FITC-labeled Avidin and measuring the fluorescence by flow cytometry. By coincubating D2B-biotin with D2B-NPs or "nude" mAb D2B, we observed a similar decreasing of the MFI value (MFI of 139 and 120, respectively) in comparison with the MFI value measured with D2B-biotin alone (MFI=303). All these analysis, competition experiments and assays on Ag- cells, confirmed that the mAb linked on the NP surface drives specifically our nanosystems to the target cells.

	MFI	% of positive cells
FITC Avidin	54	3.2
D2B biotin + FITC Avidin	303	71.3
D2B biotin+D2B+ FITC Avidin	120	18.9
D2B biotin+ NP D2B+ FITC Avidin	139	22.8

Tab 10: MFi value of competition experiment performed on LNCaP cells.

The same binding experiments were performed with anti PSCA mAb-NPs, on SW780 cells but with not satisfactory due to the low and variable PSCA antigen expression on SW780 cell line (the only one cell line, available nowadays, that constitutively expresses PSCA). For these reasons we then transfected different cell lines to increase and stabilize the expression of PSCA antigen; we transfected LNCaP (human prostate adenocarcinoma cell line) PC3 (human prostate cancer cell line) and T3M4 (human pancreatic carcinoma) cell lines with a PSCA–pcDNA 3.1 vector.

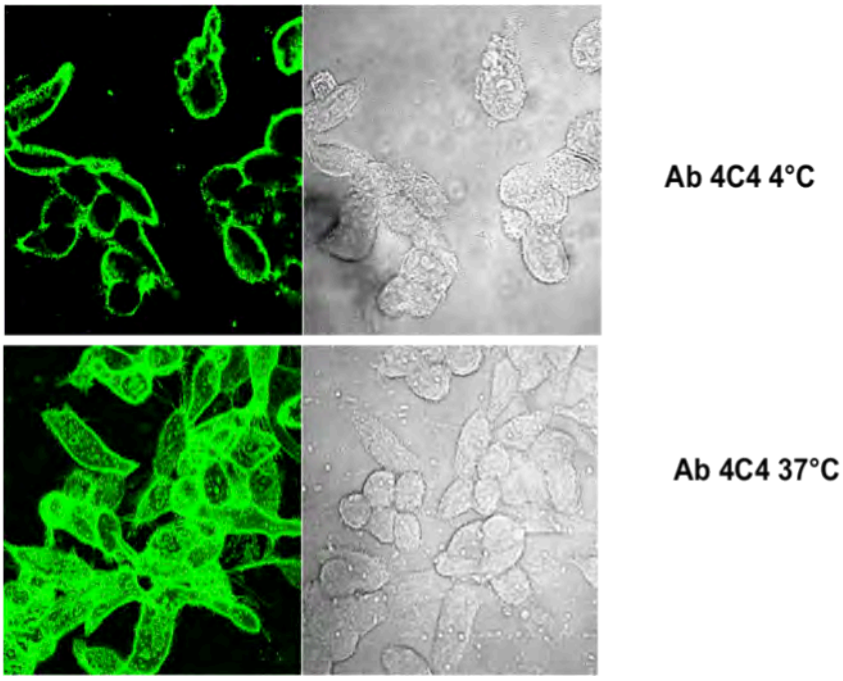

Fig 42: Confocal images of LNCaP hPSCA transfected cells incubated with anti PSCA mAb and stained with goat anti mouse Ig FITC.

The transfections were confirmed by checking the PSCA expression applying confocal microscopy (see fig 42). Working with these PSCA transfected cells we observed that the anti PSCA guided NPs showed the same high specific targeting, as the D2B-NPs.

After that we performed saturation experiments in order to evaluate the sensitivity of these nanosystems in detecting the target cells with low aspecific staining.
Positive and negative cells were incubated with scalar concentration of NP D2B. After incubation with policlonal goat anti mouse Ig FITC labeled, samples were analyzed by flow cytometry.

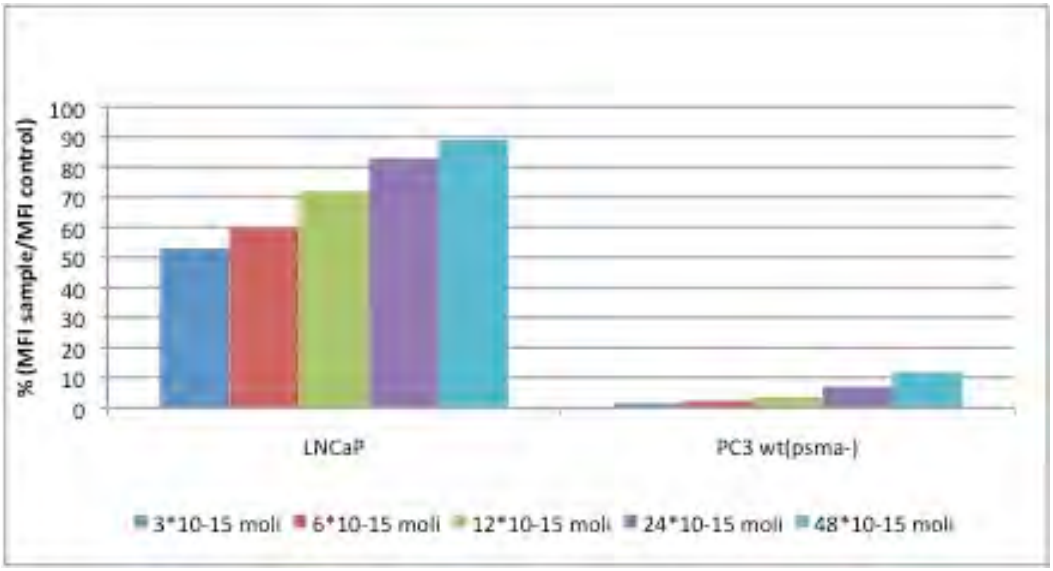

Fig 43: Saturation experiment performed on LNCaP cells with NP D2B. The binding was detected with policlonal goat anti mouse FITC. The results are plotted as ratio between MFI of sample and of negative control (cells without nanoparticles).

Fig 43 shows that when we used a higher amount of D2B-NPs, we observed a better staining of Ag+ cells, but it was appreciated a decreasing of the binding specificity. The best specific/aspecific signal ratio was obtained using D2B-NPs at a molar concentration ranging from $3*10^{-15}$ to $48*10^{-15}$.
Moreover mAb-NP binding at +4°C and internalisation at +37°C were studied by confocal microscopy on LNCaP and DU145 cells. The fluorescence signals confirmed the specific binding of functionalized NPs on antigen positive cells (LNCaP), on the contrary the absence of fluorescence staining on tumor antigen negative cells (DU145) underlines that the mAb also maintains an elevated antigen specificity when it was conjugated on the nanoparticles surface.

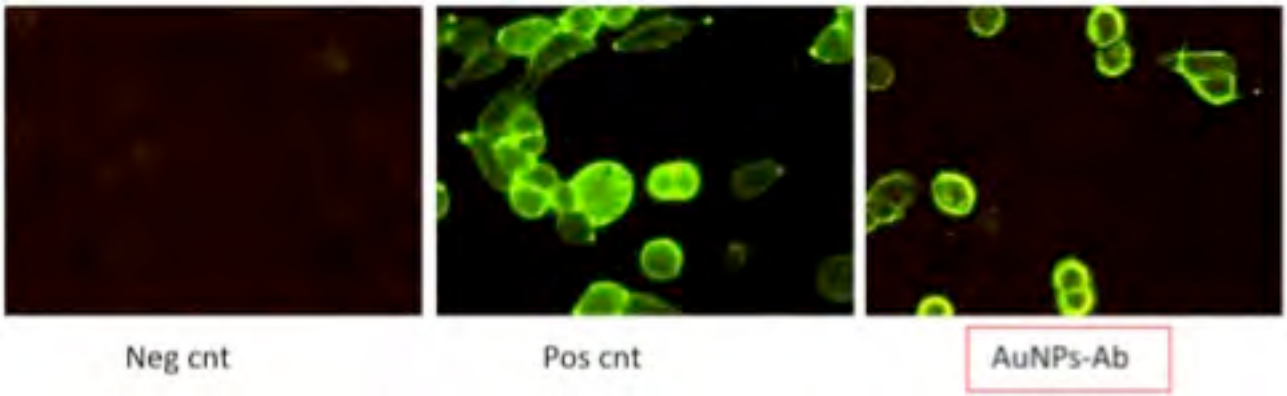

Fig 44 : Confocal images of D2B AuNPs internalized into antigen positive cells (LNCaP). The signal was detect using policlonal goat anti mouse FITC. In the positive control cells were incubated with D2B mAb. Cells were incubated with the nanoparticle preparation for about 1h 30' min.

So far we focused our attention only on the presence and the activity of mAb linked on the NP surface. In order to demonstrate that NPs are linked to mAb and that these gold NPs loaded with SERS dye are functional for cell imaging, we performed experiments to detect the signal due to the NPs accumulation in cells (e.g. LNCaP, PSMA+, and DU145, PSMA- cells).
Using Raman spectroscopy we were able to measure amplified Raman signals (see NPs loaded with SERS molecules) and therefore we could detect the cells in which the NPs were accumulated. This very sensitive technique could be applied to identify antigen positive tumor cells (immunodiagnostic approach); we demonstrated that Raman Spectroscopy is able to discriminate between LNCaP (PSMA+cells) and DU145 (PSMA- cells) as shown in Fig. 45 where it is depicted the Raman peaks of the Texas Red SERS molecules loaded in the NPs

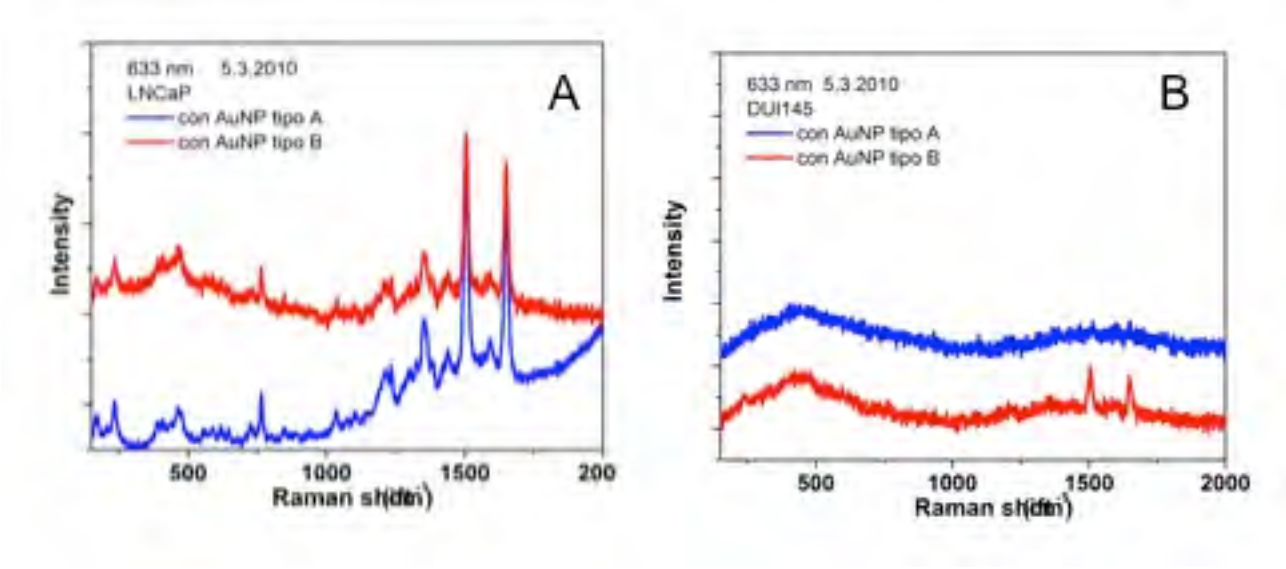

Fig 45: Raman spectra of cells incubated with D2B NPs. A) On antigen positive cells LNCaP. The two peaks correspond to Texas Red SERS molecule loaded on the nanoparticles. The red line corresponds to NPs incubated with cells, the blu line corresponds to NPs alone. B) Same experiment on Ag negative cells (DU145).

All the Raman measures were conduced by Meneghetti staff at Padua University. Further some images of Raman mapping are reported. This assay was performed on LNCaP cells grown on glass slides and incubated with nanoparticles. In this way we have a more detailed description of nanoparticle cell accumulation. The instrument used for Raman measures works also in confocal mode, thanks to a lens with higher enlargement (50x). This modality localizing with good resolution the nanotag within the individual cells. The parameter under investigation is the height of the Texax Red Raman peak at 1505 cm $^{-1}$. Each focused point was been associated with colours that reflect the recorded counts. (Fig 46-47-48)

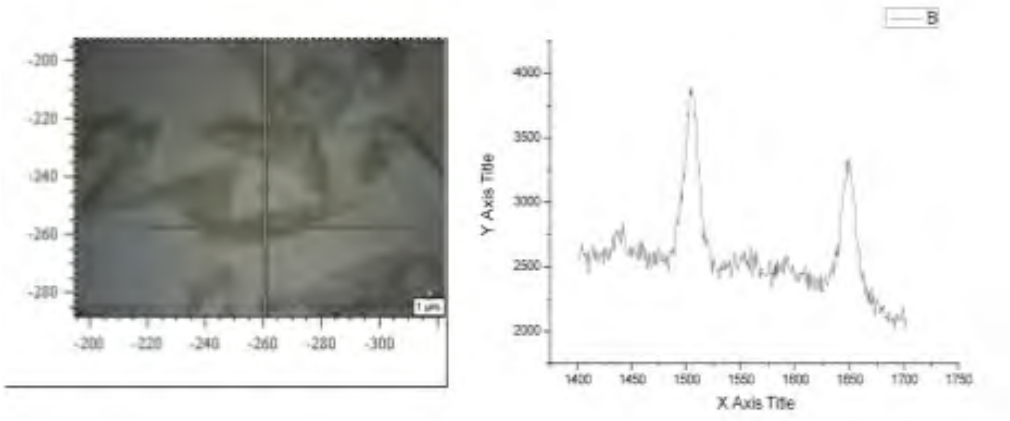

Fig 46: Pictures of LNCaP cells acquired in confocal mode at Raman instrument and Raman spectrum of a point focused by laser.

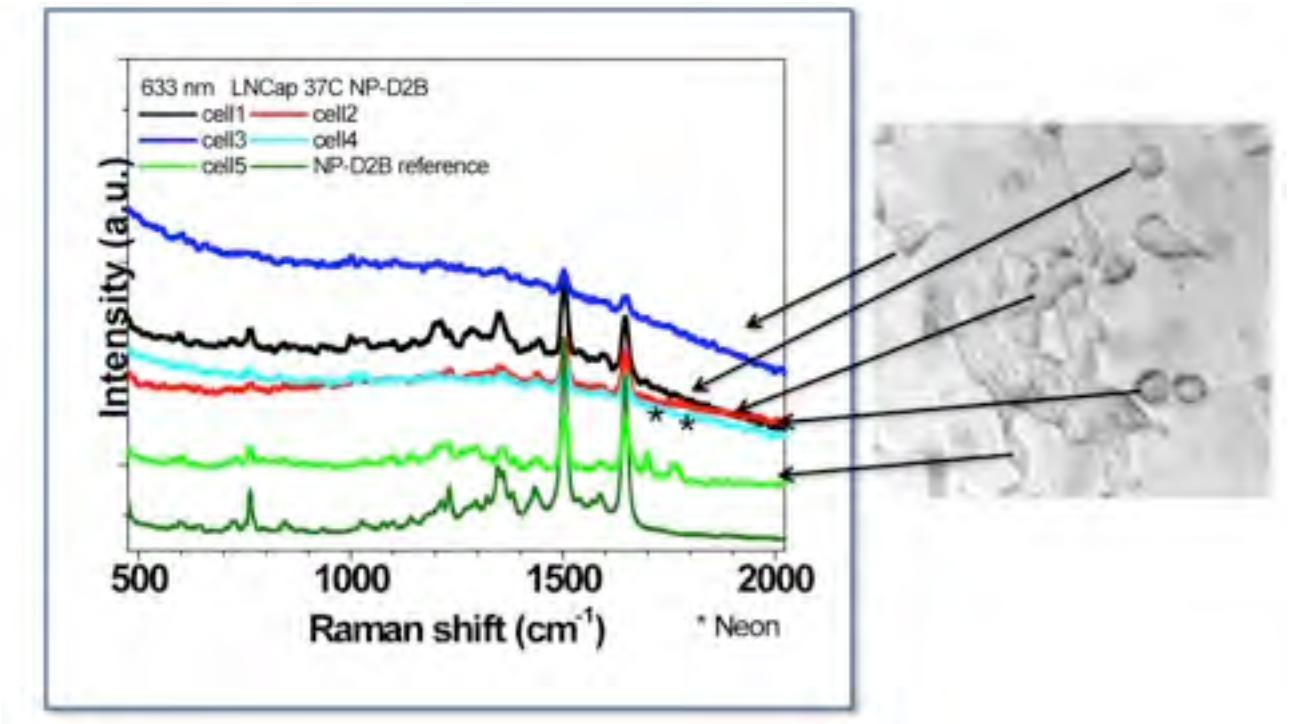

Fig 47: LNCaP Raman spectrum**.**

Fig 48: Raman signal map acquired on LNCaP cells.

The same experiments were performed on T3M4 hPSCA with 4C4 NP.

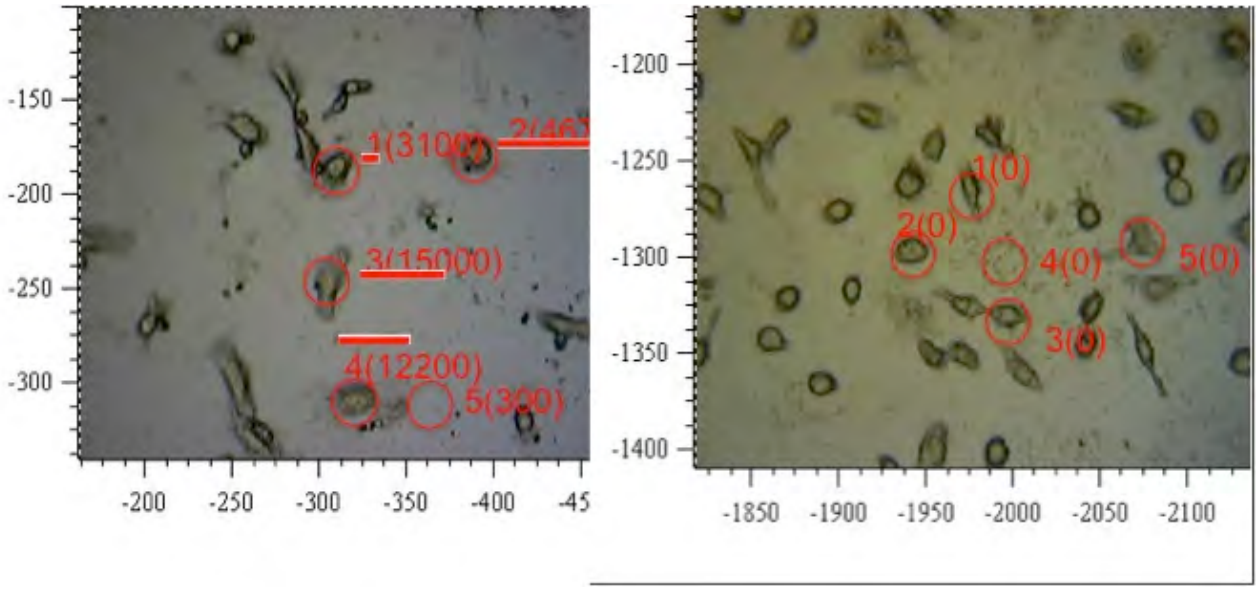

Fig 49: Pictures of T3M4 cells obtained by a Raman microscopy apparatus (left) with 4C4 NPs (right) with nude NPs.

As shown in the picture 49, the nanoparticles functionalized with 4C4 antibody demonstrate the same recognizing capability of the D2B ones. Furthermore, in the picture it is shown that the incubation with not functionalized nanoparticles does not give Raman signal.
We also recorded profiles along z-axis, using a micrometer vertical translator. (Fig 50)

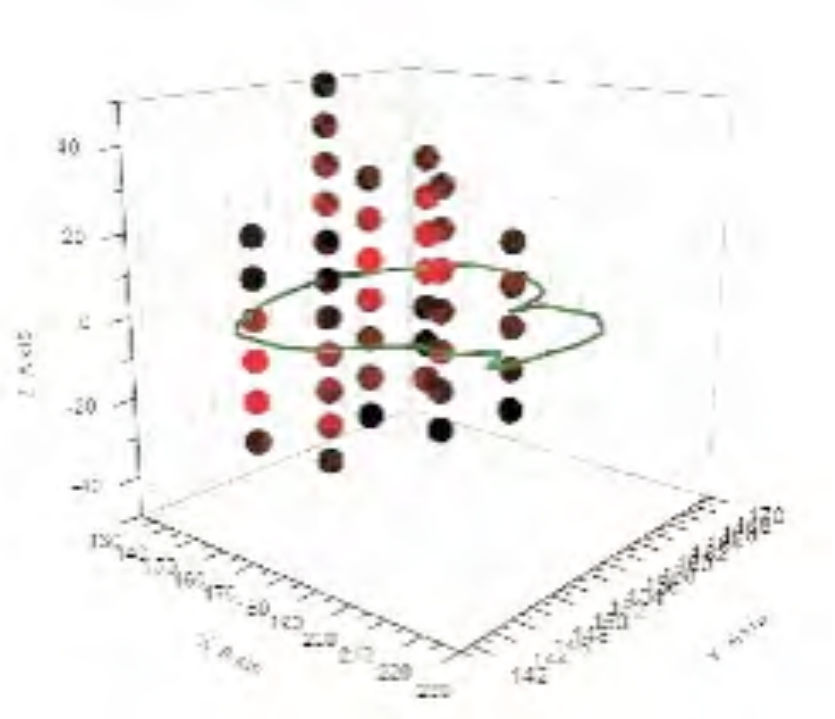

Fig 50: Three-dimensional reconstruction of LNCaP Raman signal. In green it is the cell perimeter.

Moreover, we collected 20 Raman spectra from as many cells, using the lens 5x (larger diameter of the laser) that allows the acquisition of an average of the signals present in the cell. In this way we obtained a statistics of the nanotag efficacy. We plotted the results by setting a threshold at 500 cps (fig 51).

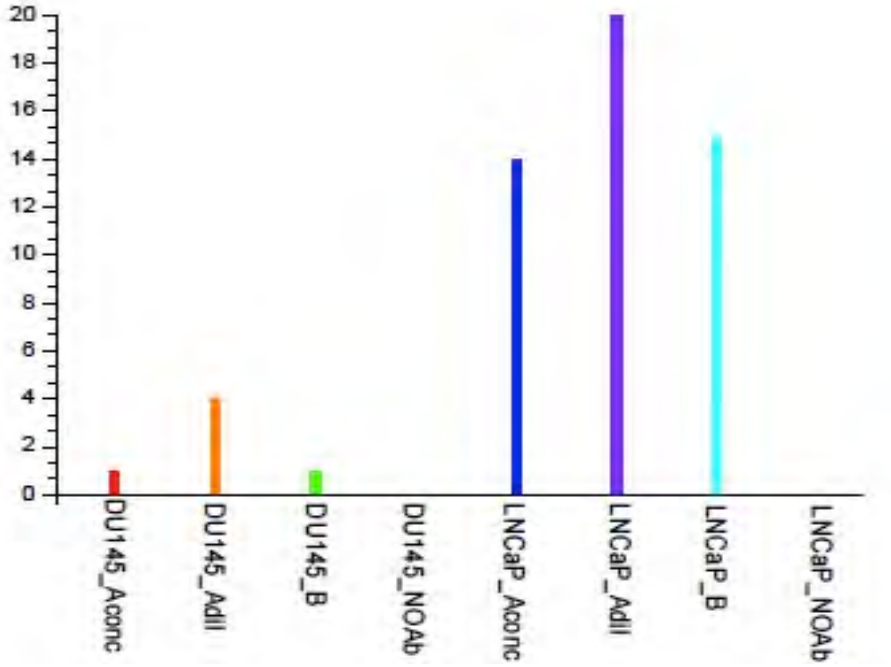

Fig 51. Graph of Raman signals collect on 20 LNCaP and 20 DU145 cells analyzed by Raman microscopy apparatus. In graph there are the cells that have a signal above the 500 cps threshold.

The presence of low Raman signals in DU145 cells (PSMA negative) is probably due to an aspecific bound of antibody on cell surface and also to aspecific cell phagocitosis. Positive antigen cells show Raman signal much higher than the negative ones. These results support us to look on the SERS targeting nanoparticles as promising tool in the diagnostic procedures allowing the discrimination between target and unrelated cells.

Another methods that allows us to confirm the goldNP accumulation into the cells, even in the case of SERS dye is absent, is the resonant scattering. Resonant scattering revealed the gold particles, collecting the scattered radiation at the same frequency of the incident radiation at a wavelength of 633 nm, where it is known that the particles have a good cross section of scattering. To better appreciate the distribution of the NPs inside the cells by resonant scaterring, the cells were counterstained with two fluorophores: concanavalin A (FITC) for dyeing cell wall and propidium ioduro (APC) to highlight the nuclei. Nanoparticles light scattering is depicted in blue. (Fig 52)

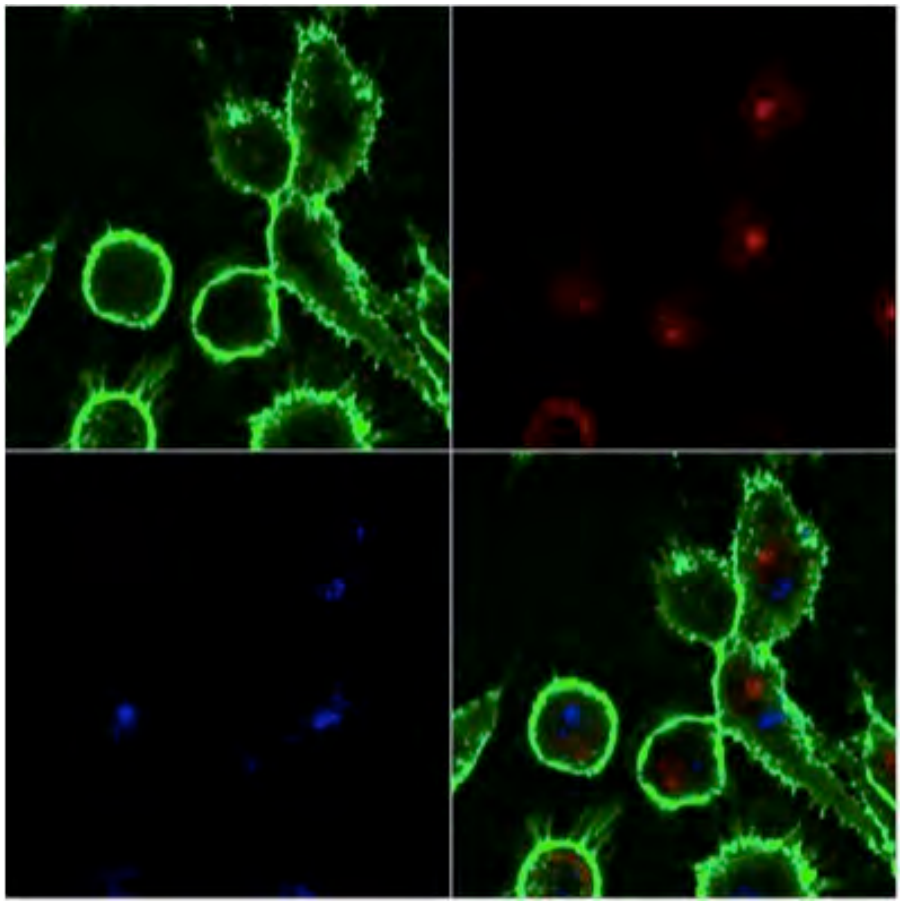

Fig 52: Scattering confocal image: LNCaP cells stained with ConA (FITC) for membrane stainig and PI (APC) for nucleus. Resonant scattering in blue highlights Nanoparticles.

Conjugated nanoparticles are clearly visible inside LNCaP cells as cluster and also at the cell membrane level (fig 53).

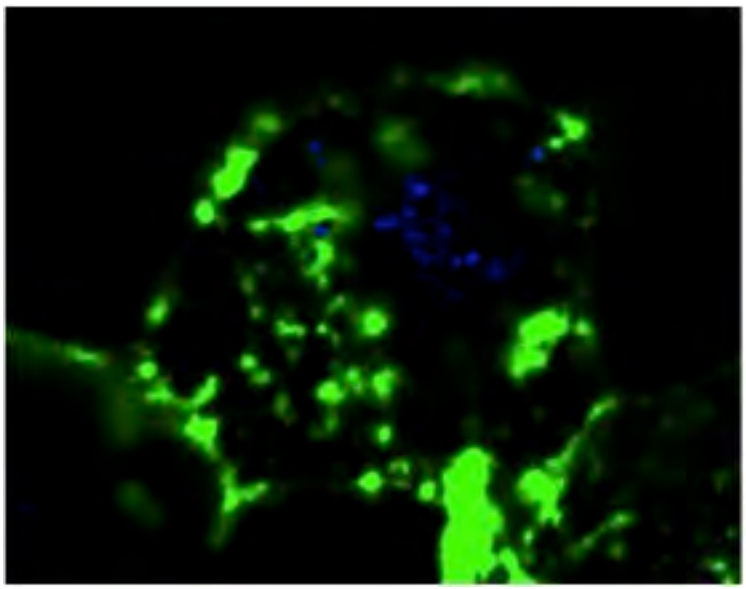

Fig 53: Confocal picture of LNCaP cell. Green ConA staining of the cell membrane, Blue staining of the nanoparticles.

PC3 WT, PSMA negative cell line, was incubated with the same nanoparticle preparation; confocal microscopy analysis shows a low scattering signal in some areas on the bottom of the slide, and not inside the cells, probably due to an inadequate cleaning. The nanotag does not bind the cells not expressing the antigen. All these results are in agreement with the previous ones confirming the good specificity of our nanoconjugate targeting.

2.2 Ex vivo assays with armed nanoparticles.

Living organisms are very complex systems and can change substantially the properties of a nanomaterial. So it is important to check the stability of nanomaterials in a real environment to see if they maintain their targeting and imaging properties. To evaluate the nanoparticles fate once injected in a animal model, we have been initiated some studies by injecting nanoconjugates in healthy mice. Then we analyzed, ex vivo, the SERS response of the tissues. These experiments were made in *ex vivo* mode because nowadays there isn't any laser yet for *in vivo* detection. We injected intravenously a solution of 500 µl of D2B conjugated nanoparticles. After 6 and 24 hours mice were sacrificed and some organs were explanted, and we performed SERS measures on the lysates derived from these explants. After 24 hours the results of the liver, lungs and blood show that the particles have been completely cleared away and accumulated probably within the spleen and kidneys. After 6 hours, on the contrary, Raman signals are recorded both in the liver and in the lungs, as can be see from Figure 54. This is the first demonstration that the nanoconjugate are stable within living organisms, and Raman signal can be detected within a few hours of their entry into circulatory system with low background.

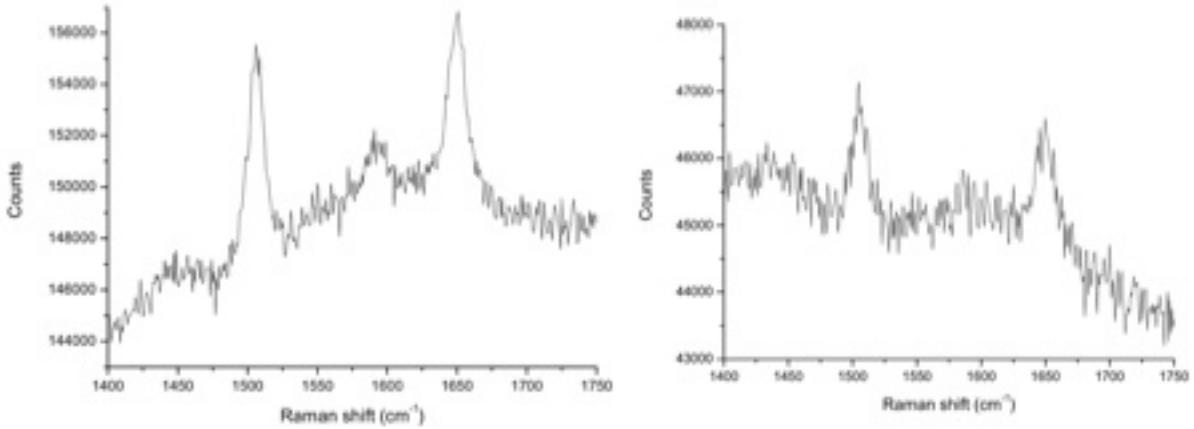

Fig 54: Raman spectra of tissue lysates. Liver (left) and lung (right) after 6 hrs from nanotag injection.

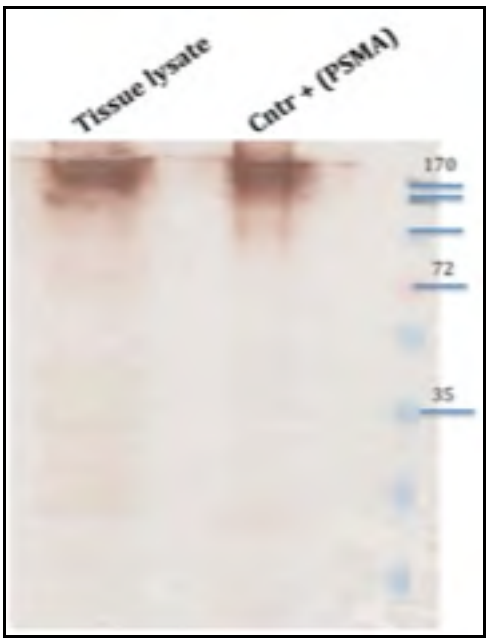

Fig 55: Western Blot on tissue lysate to check PSMA presence. The membrane was stained with diaminobenzidine. The lysate band is at the same height as tha PSMA control, confirming the PSMA presence in tissue lysates.

In another preliminary study we used a syngenic tumor model C57/BL6 mice, injected subcutaneously with B16 murine melanoma cells, hPSMA-transfected, treated with 100 µl of D2B NPs. In Fig 55 we demonstrated that the transfected tumor cells express hPSMA antigen. After 3 hours, mice were sacrificed, the tumor removed and sectioned in order to analyze the presence of the SERS signal of the Texas Red dye. The images of tumor sections were recorded using the 5x and 20x objectives.

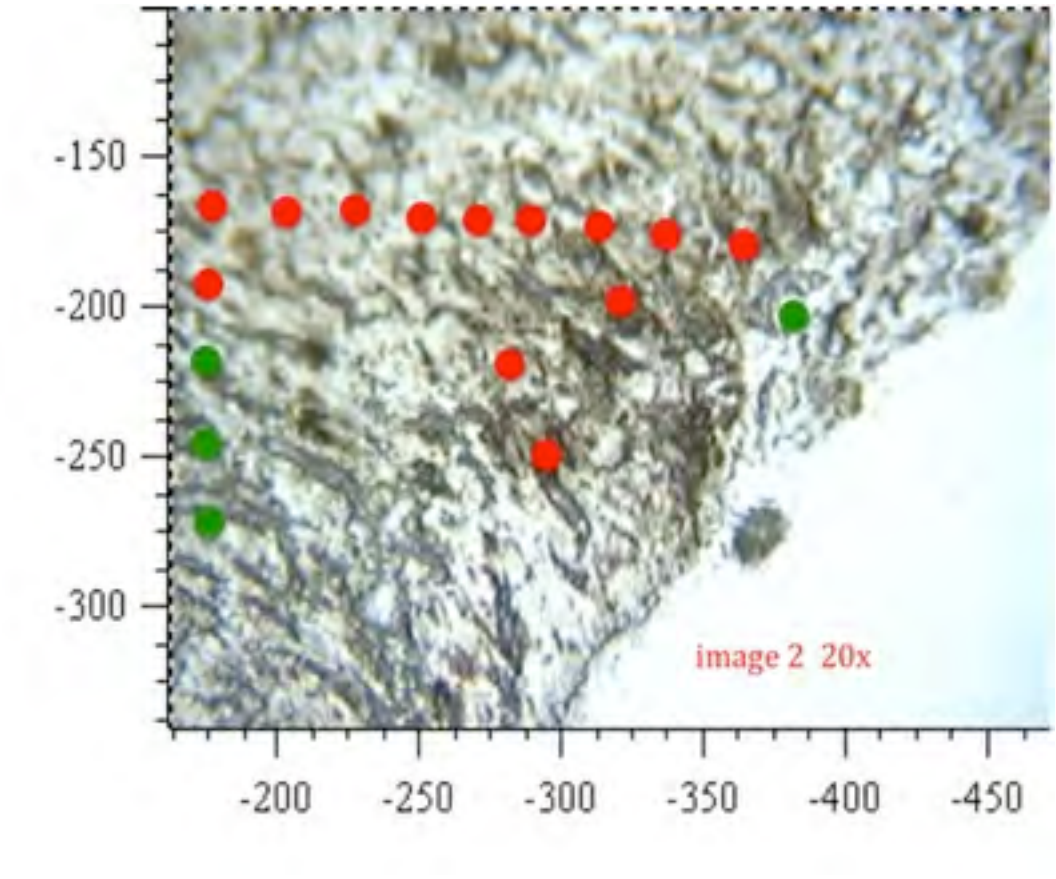

Fig 56: Picture of tissue section analyzed by Raman microscopy. Red dots correspond to points where it was detected SERS signal of Texas Red.

From the picture above we can observe that the SERS signal of Texas Red was detected on many locus of the explanted tumor. This proves that the nanoconjugates created are indeed stable within living organisms and therefore their targeting and imaging properties are preserved. This opens up interesting prospects for in vivo imaging that can be investigated in the future.

2.3 Multiplexing assay with functionalized Gold Nanoparticles

Another interesting application of the functionalized gold nanoparticles, guided with different antibodies and loaded with a variety of SERS molecules, is the ability to detect simultaneously two or more biological markers. This type of image cannot be obtained with optical imaging techniques. Therefore, in another section of my study I investigated the ability of make multiplexing with Raman spectroscopy. In collaboration with Padua University we synthesized two different batches of gold nanoparticles:

- AS 1: AuNPs + Texas Red+ D2B mAb (anti PSMA)+ mPEG SH
- AS 2: AuNPs + Malachite Green + 4C4 mAb (anti PSCA) + mPEG SH

Firstly we evaluated the binding and targeting specificy of each batch on specific cell lines. The experiments were carried out on cells grown on glass slides. Below we can see some pictures of these cells obtained with the optical microscope by illuminating the sample with the visible light using the 20x objective. To record the Raman spectra and thereby gaining the imaging, the laser at 632.8 nm was focused on each cell and on some external points, called points of "empty". The examined points have been labelled with a number in order to allow their recognition. The measurements were performed with a laser power of 10% of maximum power and an acquisition time of 10 seconds.

For an easier representation, the cells were stained in red when the characteristic spectrum of the dye TR-cys-SH was revealed, on the contrary, the cells which revealed the MG-cys-SH spectrum were stained in green. The color gradation corresponds to the intensity of the detected signal.

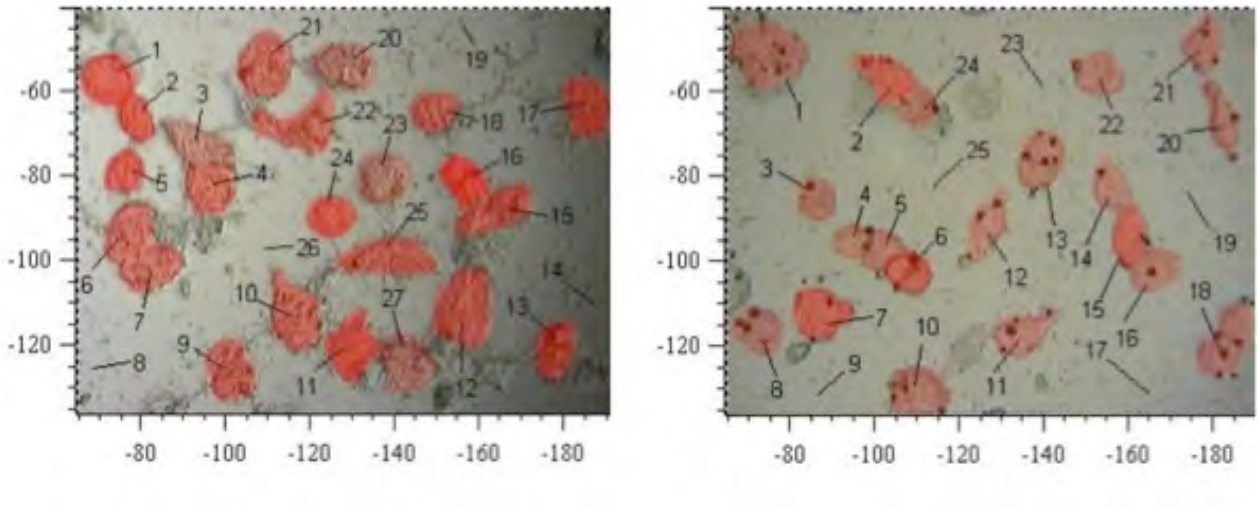

Fig 57: LNCaP cells incubated with AS1 (D2B-TR) nanoconjugate. (left): incubation with 20 µl of NP. (right) incubation with 10 µl.

The image 57 shows LNCaP cells incubated for 1 hour and 30’ with the preparation AS1, as you can see each cell shows SERS signal. The bottom of the analyzed slides was almost always devoid of signals. In addition, the colour gradation indicates a concentration-dependent cellular uptake. The cells incubated with 20 µl showed higher signal intensity. The same results occurred with other PSMA positive cells (PC3 PIP) and PSCA positive cells (such as PC3 hPSCA and LNCaP hPSCA) incubated with AS2 batch. On the contrary incubating the antigen negative

cells with nanoparticles, rare and low-intensity signals have been recorded, probably due to the wrong quenching of the slide surface. In addition, we wanted to incubate the cells with a mixture of the two preparations to ensure that each nanoparticle batch maintains its binding specificity to antigen positive cells, even in the presence of the other batch. Overall we can say that the selectivity of the antibodies used for the targeting and their functionalization with the particles did not alter their activity.

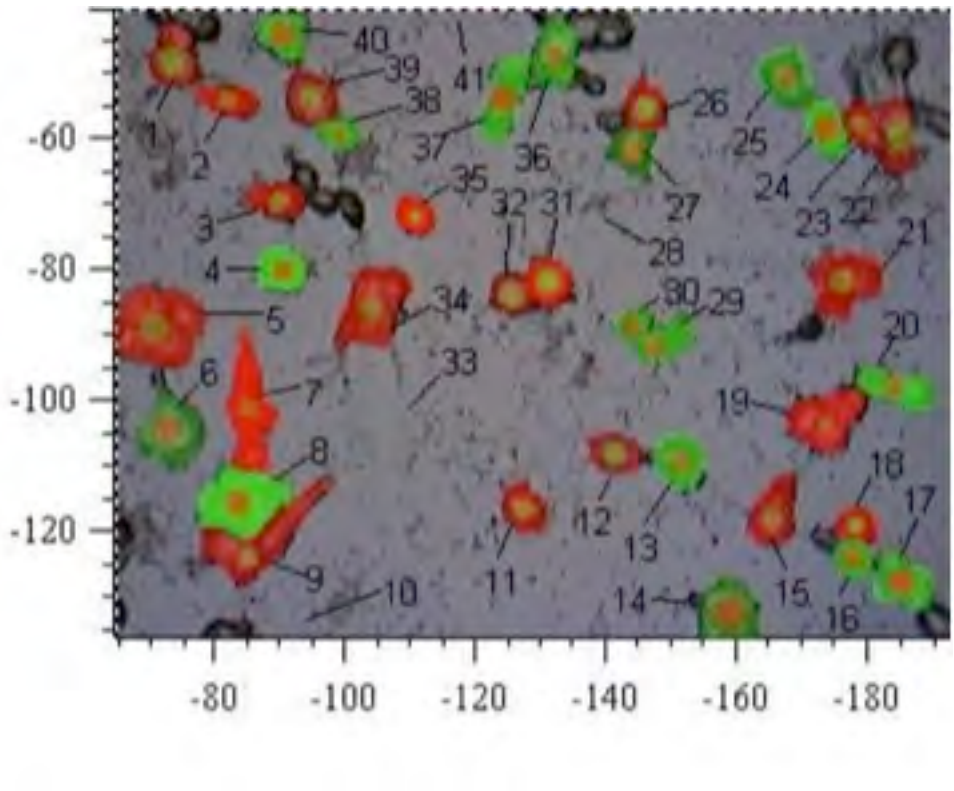

Fig 58: LNCaP hPSCA cells (PSMA+ and PSCA +) incubated with As1 and As2 mix.

In Figure 58 it can be observed that if double positive cells were incubated with a mixture of the two nanoparticle preparations, it was possible to record both SERS signals. We can see almost a regular distribution of the two SERS reporters. These same results were also confirmed by confocal microscopy analysis using the scattering properties of gold nanoparticles.
In this way we demonstrated the good targeting and the good signal strength suitable to realize new tumor imaging technique. In order to further inquire the possibility to make multiplexing, we analyzed the binding specificity of these two preparations on a mixture of cells, each expressing a different antigen. The procedure for the analysis of the slides is similar to the one above. The graphics show the images of the cells observed under the microscope

(on X-axis there are the points analyzed in the glass slide, on Y axis there is the SERS signal intensity of the main peak).

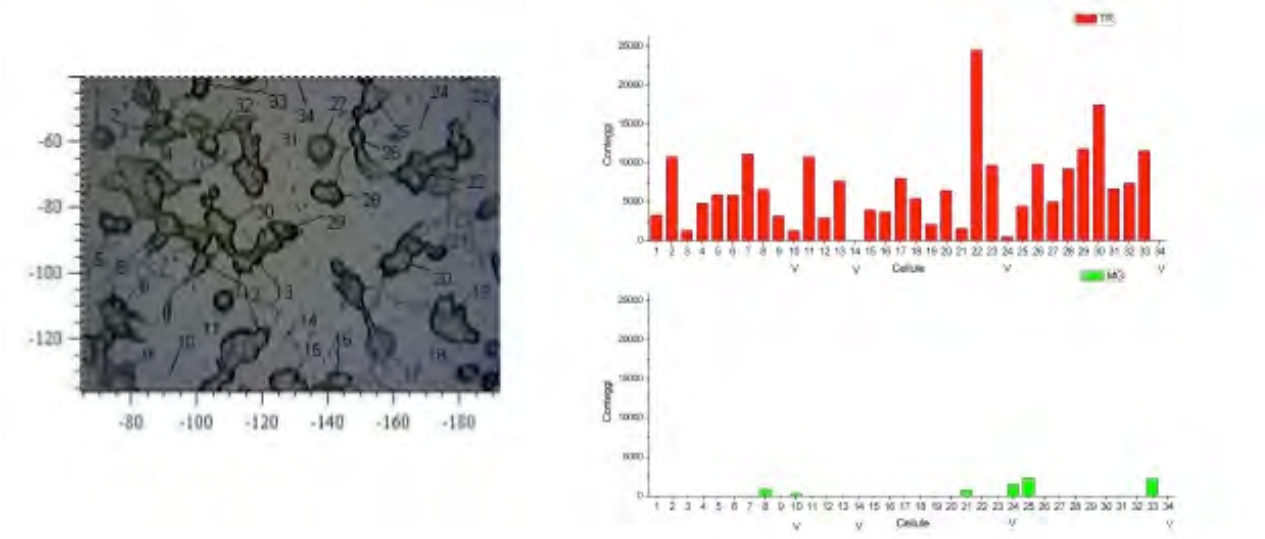

Fig 59: LNCaP e PC3 hPSCA at ratio of 50 to 1 and incubated with preparation mix. (left) picture of cells captured by confocal microscopy (right) graphics of SERS signals detected.

On the slide seen in fig 59 PSMA positive cells (LNCaP) and PSCA positive cells (PC3 PSCA) are deposited in relation 50 to 1. The cells were incubated with a mixture of equal amounts of the two nanoconjugates. As it can be seen from the graphs, the SERS signal of Texas Red SERS is dominant and present in almost every cell, as expected.

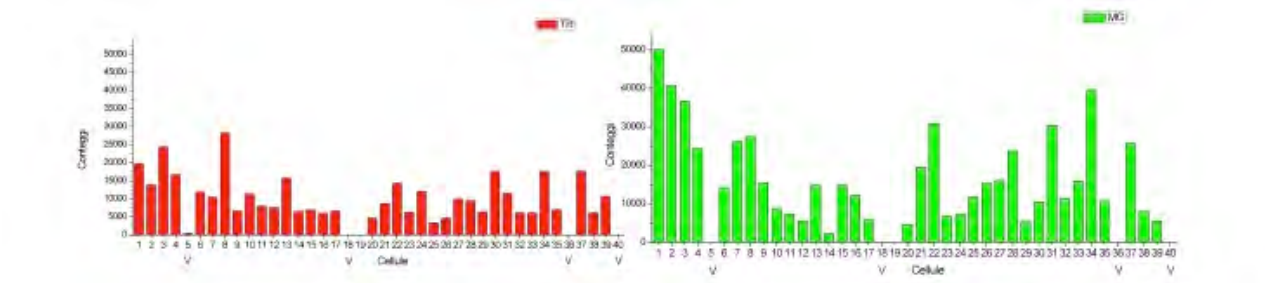

Fig 60: LNCaP hPSCA e PC3 wt at ratio of 50 to 1 and incubated with preparation mix. (left): Texas Red measurements. (right): Malachite green measurements.

In Figure 60 there are double positive cells mixed (PSMA + and PSCA+) and incubated with the mix of the two preparations. From the graphs above it is clear that in almost all the cells both SERS spectra were recorded. If PSCA positive cells were seeded in relation 50 to 50 with negative cells, the spectrum of malachite green was detected in about half of the cells (fig 61). On the contrary, when the incubation is carried out on PSMA positive and PSCA positive cells in equal ratio, the SERS signals recorded reflect this ratio (fig 62).

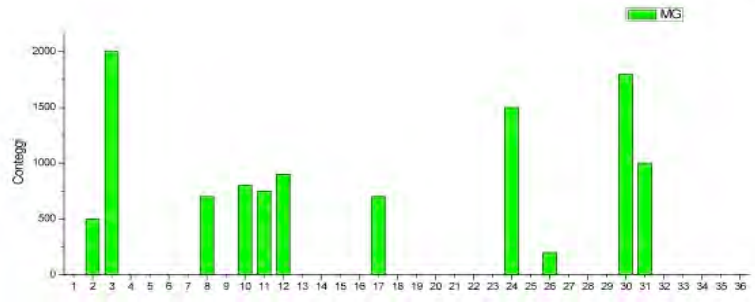

Fig 61: SERS signals of PC3 hPSCA and PC3WT at 50:50 ratio incubated mix (5uL AS1 + 5uL AS2)

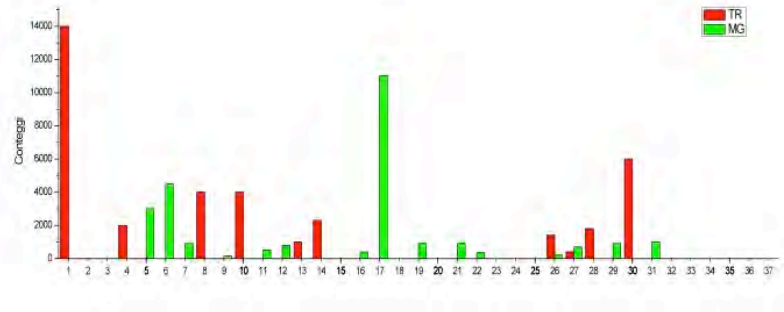

Fig 62: SERS signals of LNCaP and PC3 PSCA at 50:50 ratio incubated with mix (5uL AS1 + 5uL AS2)

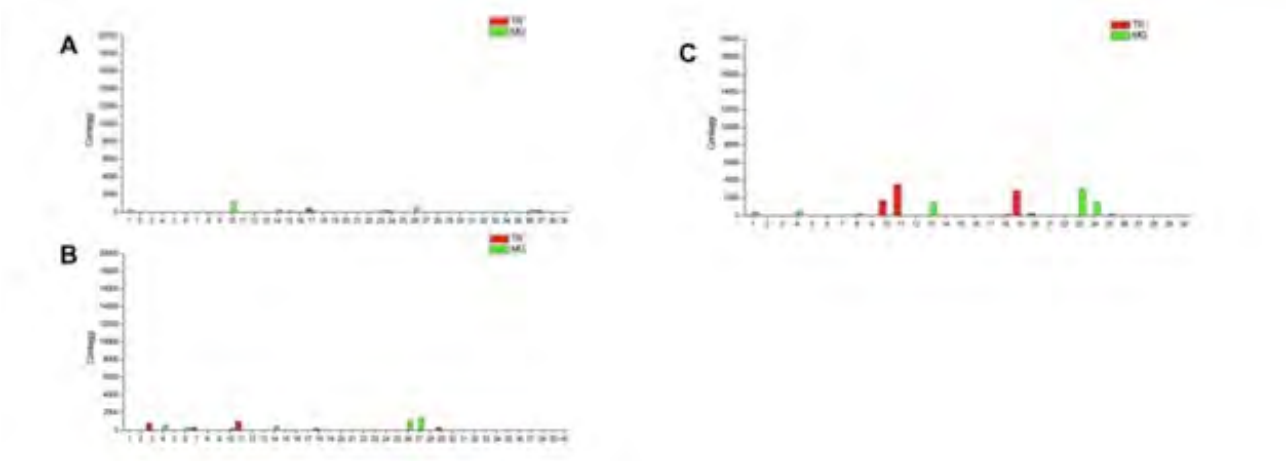

Fig 63: SERS signals recorded on different antigen negative cell lines incubated with preparation mix. A) PC3 WT B) Hela C) A431.

Finally, the mix of the two compounds was also tested on a series of antigen negative cells, in order to further confirm the specificity of targeting (Fig 63). In all cases, the recorded signals

are really low and due to noise. In conclusion, after these experiments, we can say that the two preparations of nanoparticles conjugated to the two different SERS dyes and to the two different antibodies are suitable to be applied in multiplexed imaging analysis.

2.4 Drug loaded Gold Nanoparticles

Another interesting application of nanoparticles is their use as drug carriers for cancer chemotherapy. The advantage of these systems is their selectivity for tumor cells. This nanoparticles increase the effectiveness of therapy and decrease the side effects due to the use of chemotherapic drugs. For this purpose nanosystems of gold nanoparticles have been studied, targeting with monoclonal antibody (D2B) and loading both with a chemotherapic drug and a SERS dye. This aspect of the study of nanoparticles was also carried out in collaboration with the University of Padua (prof. Meneghetti). Doxorubicin is a drug with intercalating properties and it is currently used and studied for its anticancer properties. Unfortunately, doxorubicin presents some side effects including cardiotoxicity. In this case too, the University of Padua synthesized the nanoparticles by LASiS techniques and then monoclonal antibody for the targeting and doxorubicin were added. The dye used as SERS probes is TexasRed. All the preparations were treated with polyethylene glycol with a terminal SH necessary for the gold adhesion.

For this type of study we prepared several batches of nanoparticles loaded with Doxorubicin, going to test the best binding for the maintenance of drug activity. The first preparations were focused exclusively on the study of drug delivery and efficacy: in one preparation the doxorubicin was linked covalently to the particles by thiol linker, attached to the amino group of the carbohydrate. In a second one doxorubicin was adhered to AuNPs particles simply through the interaction of the π system and the aromatic hydroxyl and amino groups. The presence of doxorubicin in these preparations was verified by reading the spectrum from 200 to 800 nm.

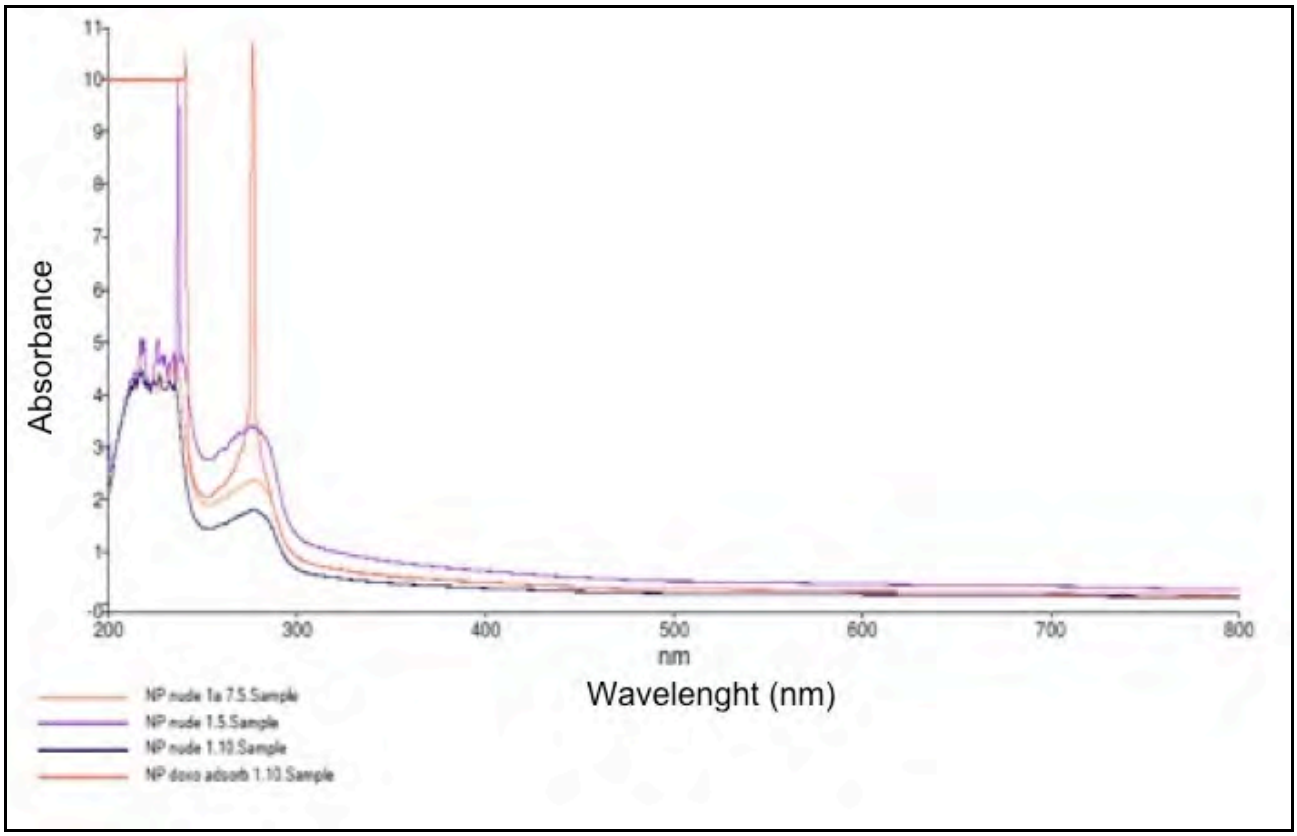

Fig 64: Spectra of different dilutions of naked gold nanoparticles loaded with doxorubicin (dark orange color). Spectra were recorded from 200 to 800 nm. Doxorubicin peak is at 280 nm.

Spectra of figure 64 show a peak at about 280 nm for the drug adsorbed NPs, due to the doxorubicin, on the contrary no signal at this wavelength was recorded for empty AuNPs. When the doxorubicin was covalently loaded on NPs surface, the very low amount of drug did not allow us to record the peak of doxorubicin. These data were confirmed by the fluorimetric analysis: doxorubicin fluorescence was measured applying an excitation light at 480 nm and recording emission at 556 nm. Figure 65 depicts the calibration curve obtained measuring the fluorescence of free doxorubicin in order to extrapolate the concentration of drug loaded on the nanoparticles.

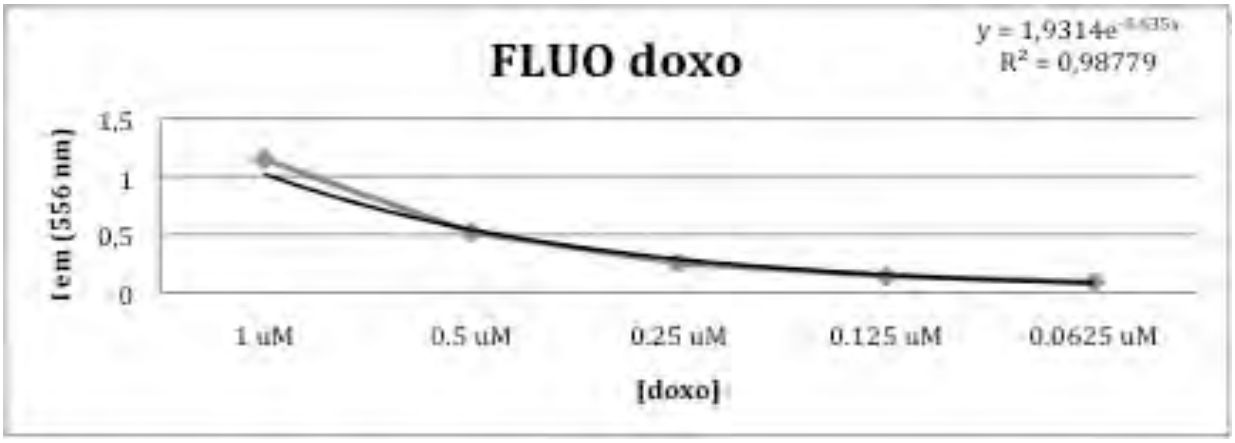

Fig 65: Doxorubicin calibration curve obtained measuring scalar dilution of this drug; fluorimetric measures were recorded using an excitation light at 480 and collecting the emission light at 556 nm. In the Y-axis is reported the Intensity of the fluorescence emission, in the X-axis the doxorubicin concentration.

Doxorubicin concentration in the NPs loaded by adsorption was estimated to be about 4 μM. The NPs batch with doxorubicin covalently linked showed to be inactive when it was assessed in citotoxicity assays on Jurkat cells (fig 66). The non-toxic effect of this batch may be due both to a strong binding of Doxorubicin with a consequent very slow releasing and to the limited amount of drug loaded on the nanosystems.

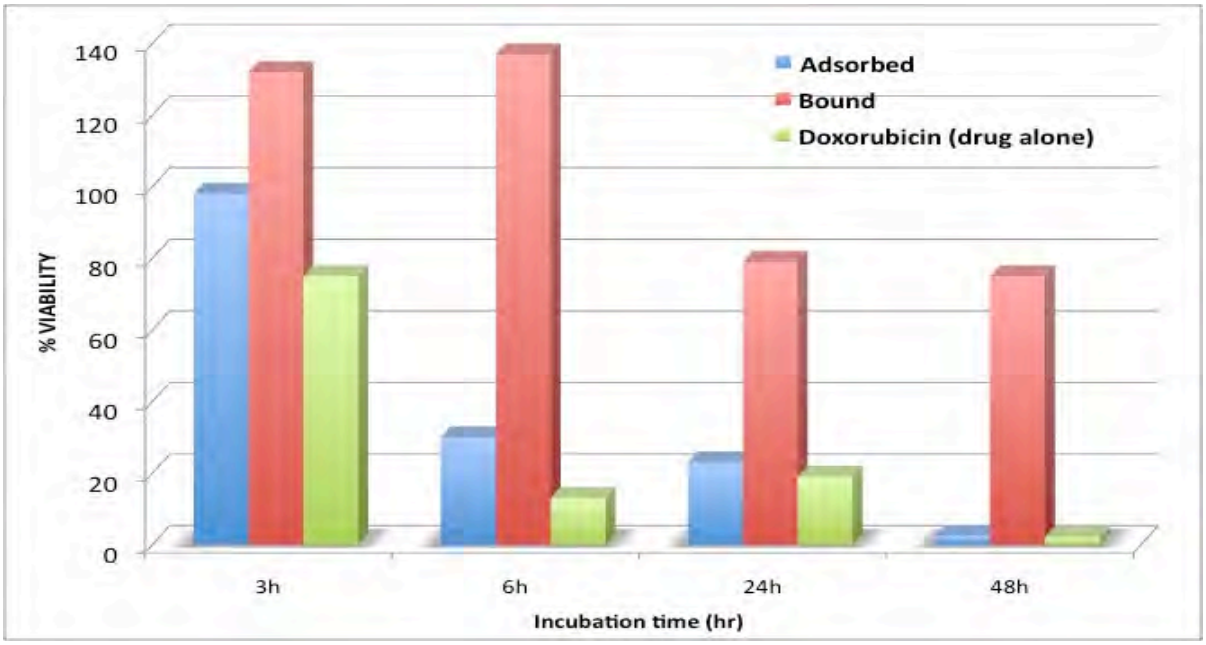

Fig 66: NPs cytotoxicity assay based on 3H thymidine incorporation: the assays were performed on Jurkat cells. The two batches of drug loaded nanoparticles are analyzed and compared to free doxorubicin. The cells were incubated with the samples for different incubation time; this figure shows the percentage of ^{3}HTdR incorporation as a function of the incubation time.

The toxic efficacy of the drug-adsorbed NPs preparation shows to be comparable to free doxorubicin, which was used as control (cytotoxicity assay with an incubation time of 48 hrs). Since this assay shows a low toxicity for the NP batch where the drug was covalently linked (e.g. 75% of cells viability after 48 hrs of incubation), we decided to exploited a new covalent bond which was obtained by means of a cleavable peptide (cleavable by furin enzyme).

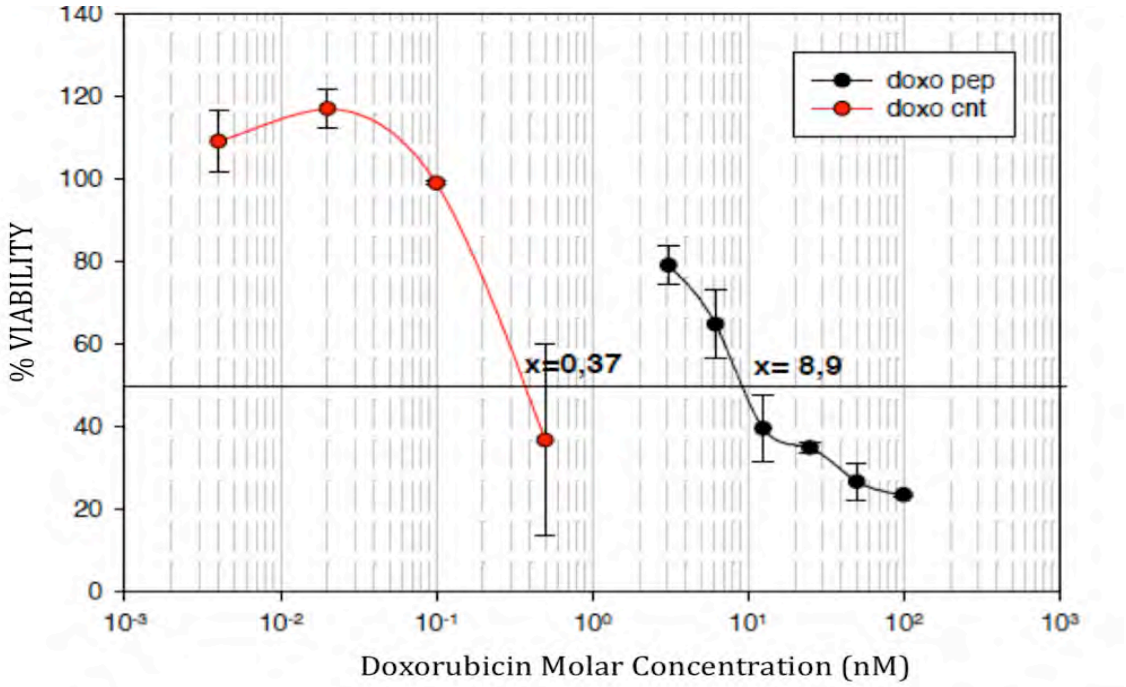

Fig 67 : Cytotoxicity evaluated by 3H thymidine incorporation after treatment with NPs. Assay was performed on PC3 wt cells. Bound doxorubicin (via a cleavable peptide) was compared with free doxorubicin. In the figure is depicted the percentage of ^{3}HRdR incorporation as a function of doxorubicin concentration.

Cytotoxic effects were compared in terms of IC_{50}, which defines the reagent concentration able to inhibit cell proliferation of about 50% respect to untreated control. The new batch of doxorubicin-peptide was less cytotoxic than the free doxorubicin in vitro assays; we estimated that the activity of the drug has decreased about 400 times (Fig 67). The efficacy of doxorubicin is dependent on the cells sensitivity degree to the drug, which is different for each cell line. For this reason in the following cytotoxic assays we have to use a higher concentration of armed gold nanoparticles in order to evoke a toxic effect.

Finally doxorubicin loaded nanoparticle preparation was coupled with the drug delivery aim. This purpose was achieved by linking to the doxorubicin loaded NPs (via cleavable peptide) an anti-PSMA monoclonal antibody (mAb D2B). The last series of batch has been synthesized to test the above mentioned component effect on the cells. We expect that only the samples

loaded with doxorubicin should show toxicity, excluding the harmful effects of the antibody, of the PEG and of the same particles, whereas the Texas Red dye seems to be firmly linked to AuNPs.

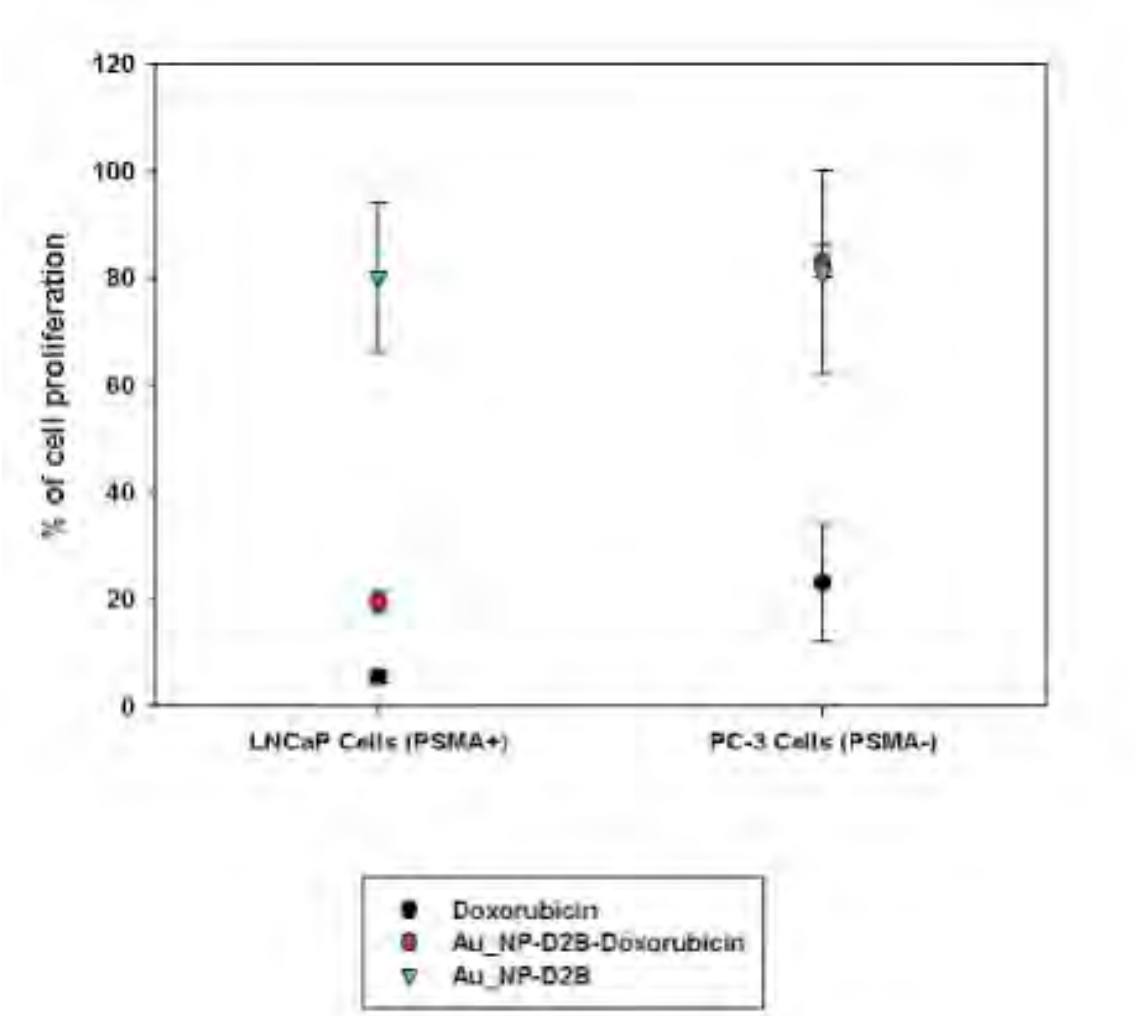

Fig 68 Cytotoxicity assays performed on LNCaP (PSMA+) and PC3 wt (PSMA-) cell lines; the killing efficacy was calculated measuring 3H thymidine incorporation.

Finally PSMA targeted-doxorubicin loaded gold nanoparticles were assessed on PSMA +/- cell to investigate the killing selectivity. Figure 68 summarizes the results obtained in these assays on LNCaP cells (PSMA positive) and PC3 wt (PSMA negative): free doxorubicin shows the same toxicity on both the cell lines. The antibody conjugated nanoparticles have got the same low efficacy on the two cell lines (80% of cell viability on LNCaP and PC3 cells) while the nanoparticles loaded with doxorubicin and PSMA targeted show high toxicity on LNCaP cells (20% of cell viability) and a lower killing capability on PC3 cells (about 80% of viability).

These results demonstrate that it is possible to decrease the non-specific activity of the chemotherapeutic drugs by means of targeted drug loaded nanosystems.

2.5 Synthesis and characterization of conjugated Silica nanoparticles

In this part of my project, I investigated the characteristic of Silica NPs. They have been coated with polyethylene glycol (PEG) in order to increase their biocompatility and preserve them better from immune recognition. The PEG molecules that coat silica NP surface, also prevent possible aggregation phenomena, increase the hydrophilicity and allow us to manipulate their surface by chemical reaction in order to conjugate driving moieties.

Silica NPs coated with PEG-NH2 and loaded with mTHPC (a photosensitizing reagent for PDT therapy, whose fluorescence signal could be detected by APC filter; commercial name: Foscan®) were synthesized in collaboration with Prof. F. Mancin (Organic Chemistry Dept. University of Padova). The size of synthesized nanoparticles was about of 90-110 nm. As reported in literature the NPs with a size ranging between 100 and 400 nm are optimal vehicles for tumor targeting. Smaller nanoparticles are quickly eliminated from the bloodstream by macrophages, especially at the level of the reticuloendothelial system.

At Padua Prof. Mancini's group studied a new one-pot procedure to prepare dense PEG coated organically modified silica nanoparticles (ORMOSIL).

Loading a photosensitizer on nanosystems and then driving the nanodevices with tumor cell specific ligands or antibody may achieve the increasing of mTHPC accumulation in tumor tissue. So we exploited the use of silica nanosystems conjugated to anti PSMA mAb D2B or anti EGFR mAb Cetuximab for a more efficient and selective delivery of Foscan®.

The NPs were conjugated to the mAbs by means of bifunctional cross linkers. Derivatization protocols are the result of several preliminary tests performed using different cross-linkers, different molar ratios between reagents and NPs/antibodies and different incubation times, in order to identify the best combination. Reactivity of amino groups introduced on the NP surface by PEG chains was preliminary assessed by a reaction with NHS-Biotin (Pierce); after this reaction we were able to identify biotin groups on NP surface, incubating with avidin-FITC and analyzing these samples with flow cytometer. Derivatization of PEG-NH_2 NP was performed first using *N*-Succinimidyl 3-(2-pyridyldithio)propionate (SPDP) and after with 3-Maleimidobenzoic acid N-hydroxysuccinimide ester (MBS).

mAb derivatization was obtained by a reaction with 2 iminothiolane performed for 2 hrs at 30°C and o/n at 4°C. We usually were able to introduce about 1,5 SH for mAb molecule.

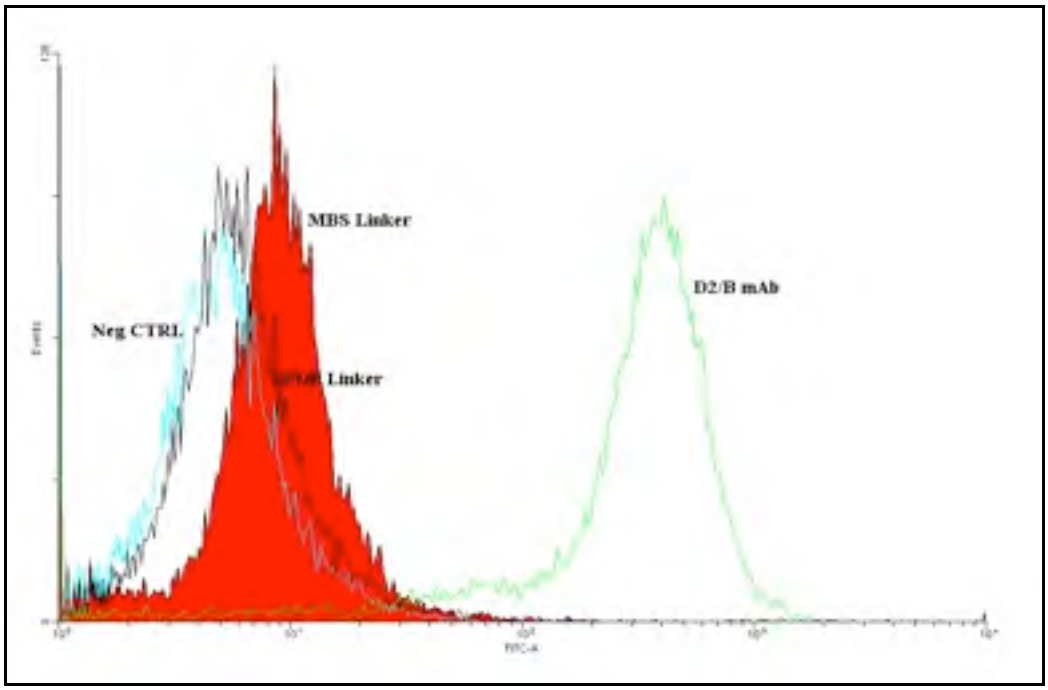

Fig 69: Flow cytometry analysis of the two batches of mAb–conjugated NPs: derivatization methods on LNCaP cell lines. As positive control we used mAb D2B (empty green curve). The full red curve corresponds to NPs conjugated to mAb by MBS. NPs conjugated to mAb by SPDP correspond to empty black curve.

Finally the functionality of our conjugates (e.g. mAb+NPs) was evaluated by flow cytometry on antigen +/- cells. Since the amino groups present on NP surface could be protonated acquiring a positive charge, which should increase their nonspecific uptake by cells (Ag +/-), we decided to create a second negative control, in addition to the naked nanoparticles. As second negative control we synthesized NPs conjugated to the protein BSA.

Fig 69 summarizes the binding results of our nanodevices on Ag + cells; analysis was performed by flow cytometry. We can observe that the MFI value (FITC channel) of the nanoconjugate synthesized using MBS cross linker results higher than the MFI value of the SPDP conjugates. So in our laboratory experience the derivatization with MBS allows creating Ab- driving nanosystems with well targeting capability.

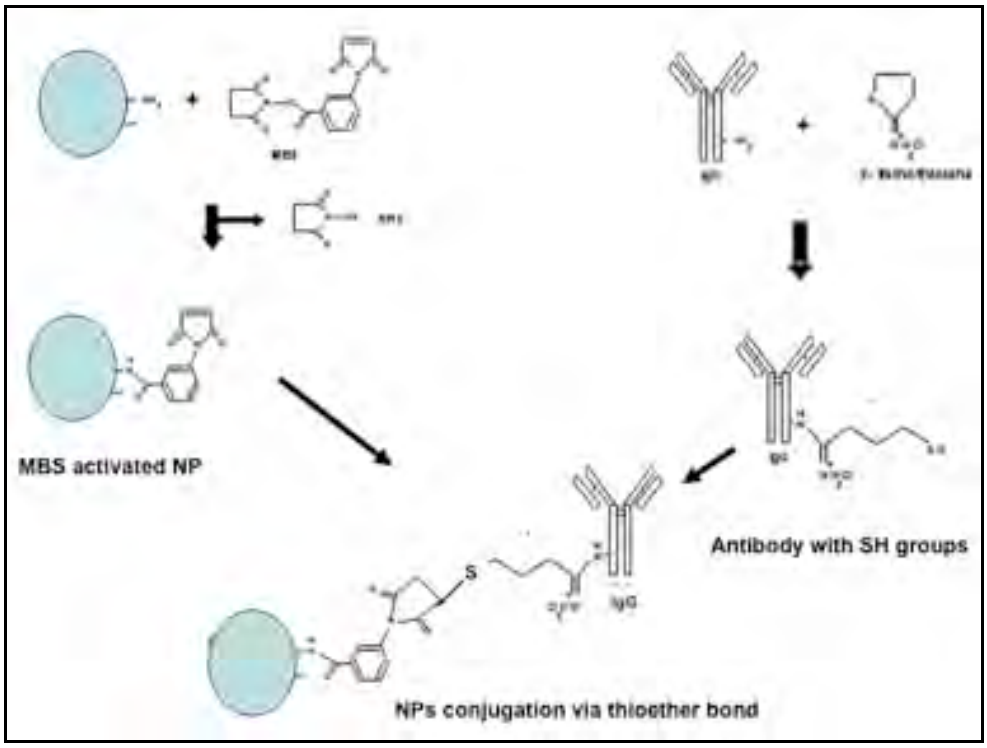

Fig 70: Picture representing our conjugation protocol

To check that our purification protocol worked very well and no traces of free antibody were present in the final product, we developed a western blot assay.

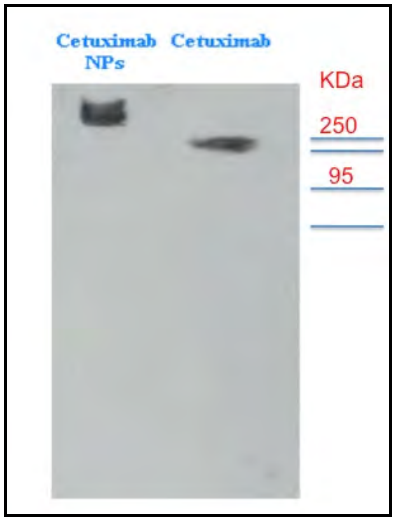

Fig 71: Western blot of silica mAb conjugated nanoparticles stained with goat anti mouse HRP. Free mAb cetuximab was used as positive control

One example of this procedure is depicted in Fig. 71; Ab NPs gives a band at a molecular mass > 250 KDa, while the mAb band appears at about 180 KDa. The absence of free mAb in the lane of the mAb-NPs sample is very important because free mAb can compete with Ab-

conjugated NPs for the same receptor, decreasing the guided NPs internalization/accumulation. Western blot assay also demonstrated that the mAb is stably linked to the NPs. Another check was performed by flow cytometry, in order to analyze the antibody conjugation on nanoparticles surface: we incubated nanocojugates with a secondary antibodies FITC-labelled (goat anti mouse IgG-FITC for D2B-NPs or rabbit anti human IgG-FITC for Cetuximab).

NPs staining can be detected by flow cytometry analysis due to their loading with the photosensitizer Foscan® molecule; whose fluorescence can be analyzed in the APC channel.

Owing to their small size, NPs localize in the cytometry graph region in which cell debris and other spurious events fall (Fig 72 A-B). We decided to put a window on the population that was APC positive. This population corresponds to the nanoparticles (Fig 72 C). In this population, we measured the FITC fluorescence signal due to FITC-conjugated secondary mAb used to detect the presence of mAb on NP surface. In figure 72 C it is shown the increase in the number of events due to the presence of NPs. In Fig 72 D it is shown the FITC signal increasing due to the presence of mAb on NP surface.

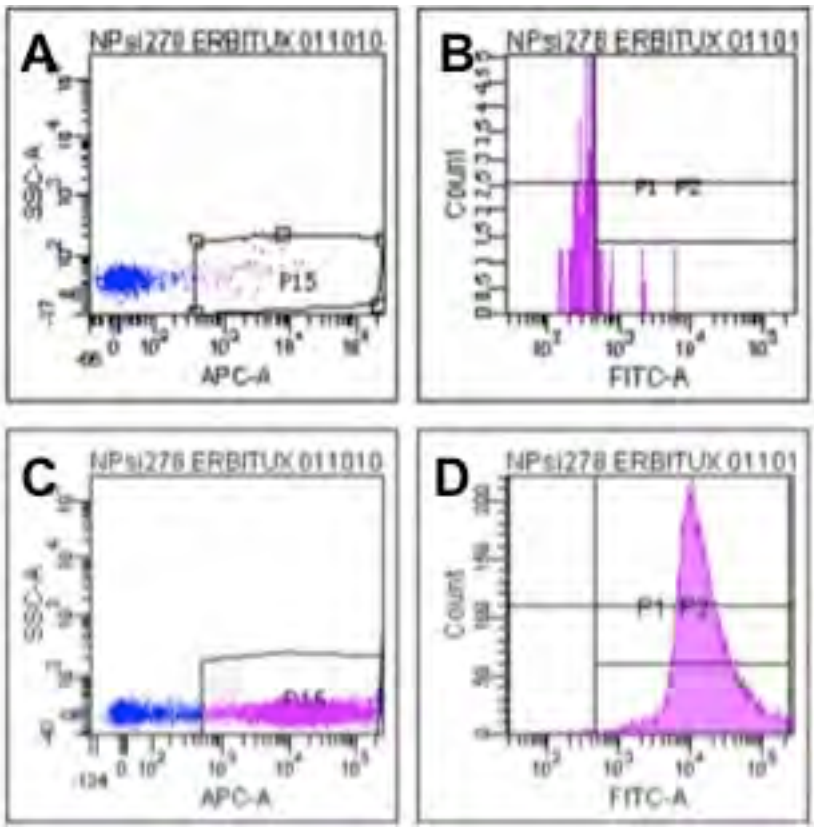

Fig 72: Flow cytometry pannel. A-B): blank sample (we used PBS buffer as blank in order to record the background noise signal of the instrument). C-D): nanoconjugate sample.

D2B functionalized siNP

To check the functionality of our nanoconjugate we evaluated their binding specificity by flow cytometry on different PSMA positive (LNCaP, B16 hPSMA) and negative cell lines (DU145, B16wt). In the analysis it was measured FITC fluorescence due to secondary Ab anti-Human FITC.

Figure summarizes (Fig. 73) the fluorescence histograms obtained incubating our nanosystems at +4°C for 1 hour on Ag +/- cell lines.

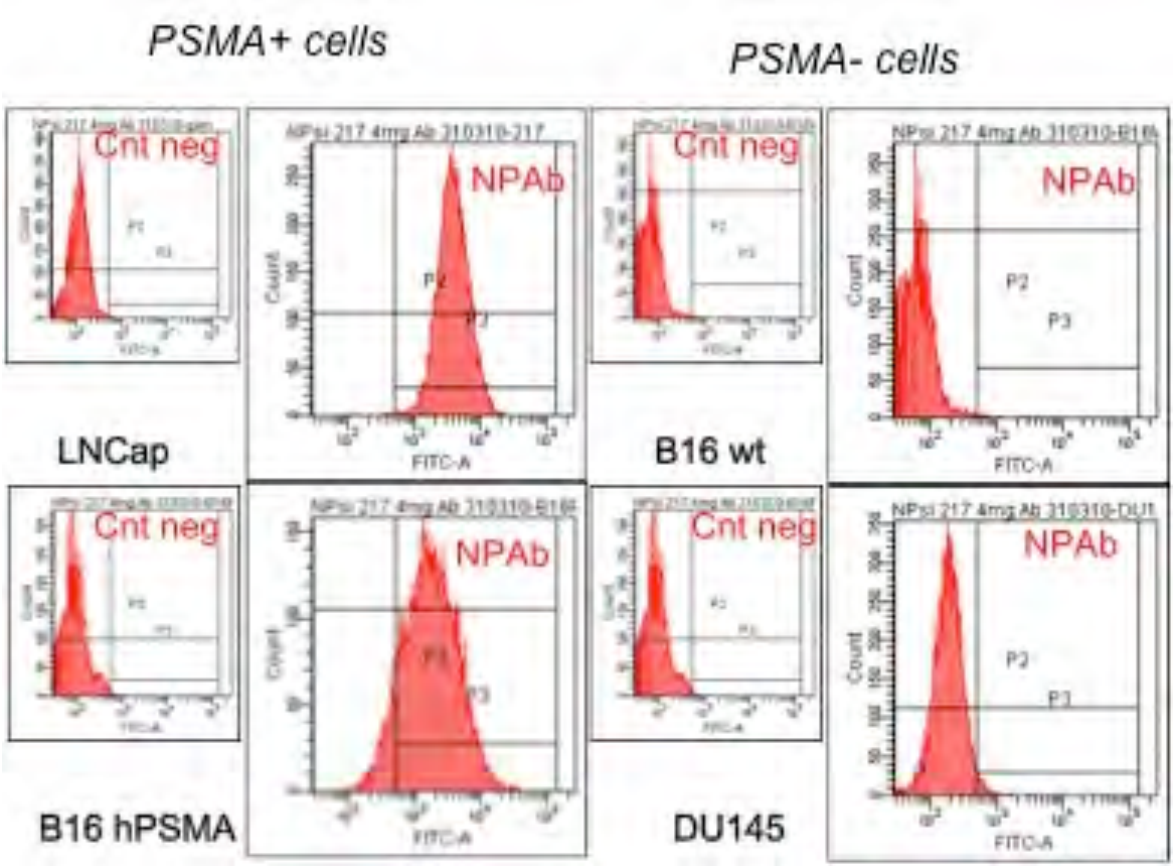

Fig 73 Flow cytometry assay of siNPS D2B performed on different cell lines at 4°C (FITC channel). The concentration of nanoparticles used is 1 μM in Foscan®.

These slides demonstrate that NPs with surface linked antibody molecules acquired specificity for the target antigen positive cells.

These results were also confirmed working with other PSMA+ cell lines as PC3 PIP (PC3 PSMA transfected cells). We analyzed the binding properties of our nanodevices, incubating with antigen positive cells for 3 hrs at +4°C. We used as negative control, silica nanoparticles conjugated with BSA. The graph 74 shows the fluorescence in the channel of the APC, the NPs-

D2B show an increment in APC signal of 5X compared to the APC signal of NPs-BSA. This result proves that the binding of functionalized nanoparticles is specific to antigen-positive cells. The NPs-BSA bind to the cells aspecifically, in a negligible level in comparison to the antibody conjugated nanoparticles.

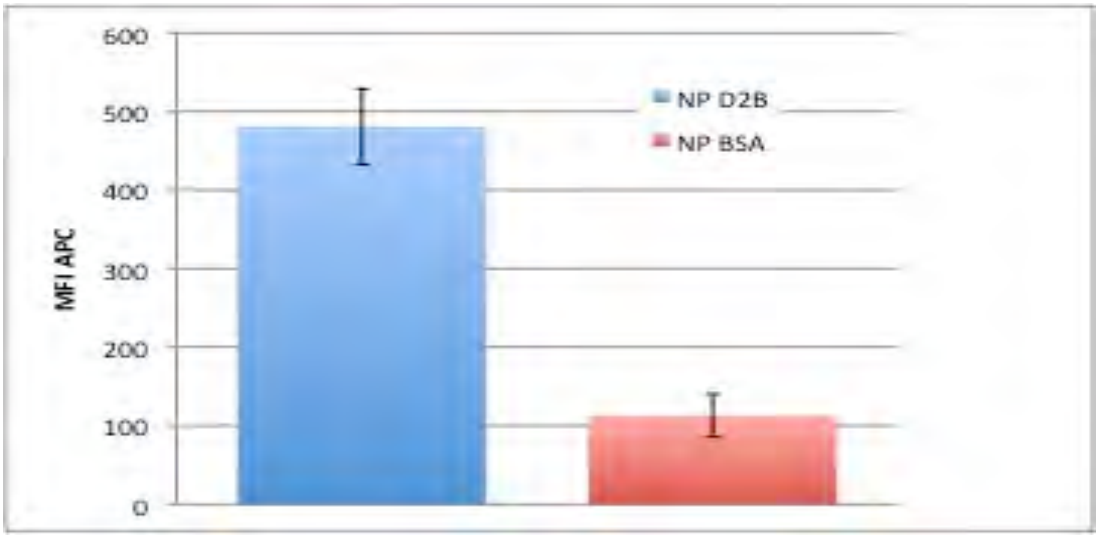

Fig 74: Flow cytometry assay at 4°C on PC3 PIP (PSMA+) to compare binding of NP D2B and NP BSA.

After binding experiments at 4°C we also performed assays at 37 °C, in order to investigate the specific uptake.

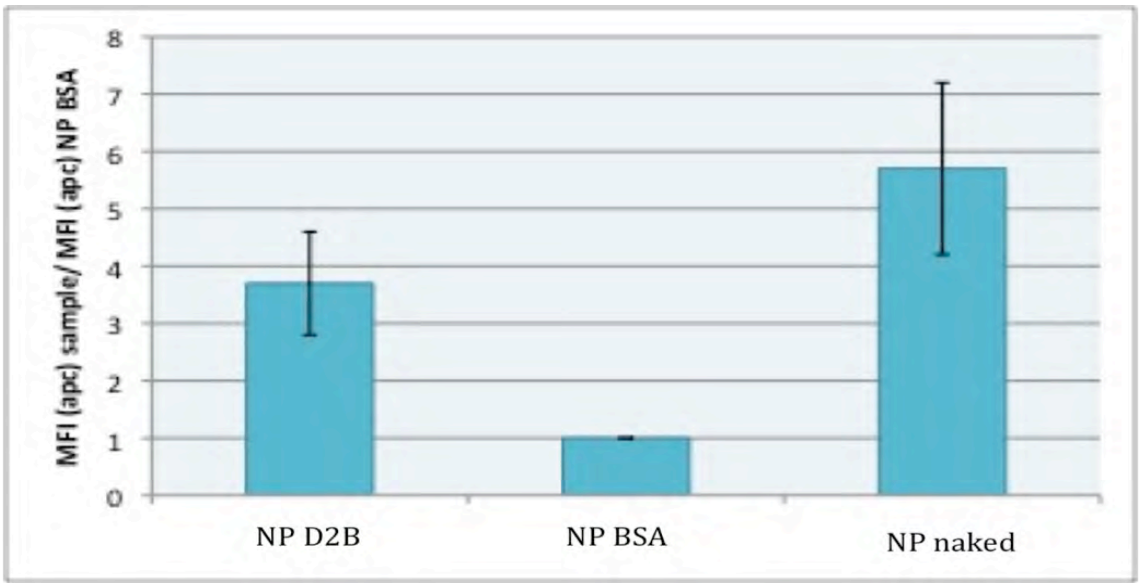

Fig 75: Uptake of conjugated silica nanoparticles at 37°C: results analyzed by flow cytometry. The value of Y axis represent the ratio between MFI samples and MFI NP BSA (APC channel).

The uptake assays were perfomed incubating PC3 PIP (PSMA+) cells with the same amount of nanoconjugate (1μM Foscan®) for 1hr and 30'. To summarize more clearly the results, we have reported in the Bar Graph (see fig 75) the ratio between APC MFI of the samples and APC MFI of NPs-BSA. So we can highlight the increased uptake of antibody conjugated nanoparticles compared with BSA conjugated nanoparticles (used as negative control). The naked nanoparticles show more non-specific uptake probably due to their positive surface charge. Moreover we have studied the time dependent uptake of our D2B guided NPs compared with the BSA conjugated NPs (e.g. negative control). We can appreciate that working with a constant NPs concentration (1μM Foscan®), the specific uptake starts to decrease after 3 hrs of incubation (Fig 76).

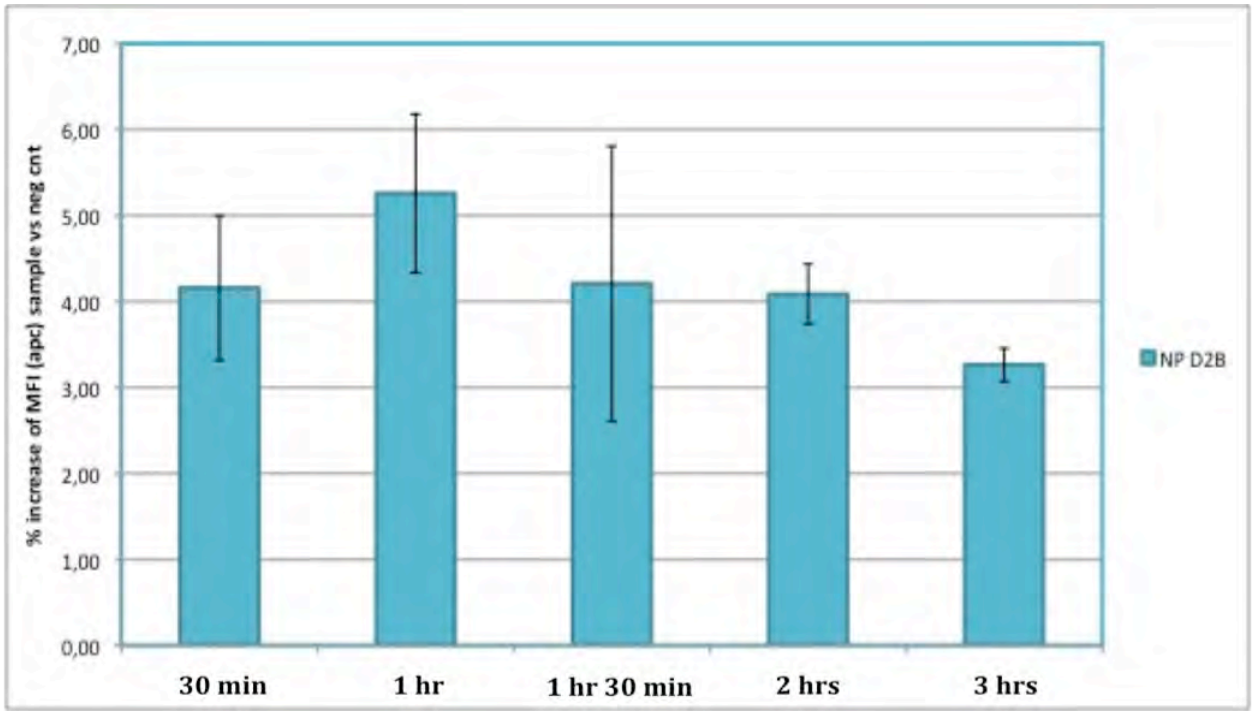

Fig 76: Kinetics uptake performed on PC3 PIP at a constant NPs concentration of 1 μM Foscan®. The results are reported as the ratio between APC MFI of samples and APC MFI of NP BSA.

So we can observe that the trafficking of nanoparticles is probably fast in this system.
To further confirm of the binding specificity of guided nanoparticles, we carried on a competition assay on PSMA positive PC3 PIP cells. After co incubation of mAb driven NPs with a molar excess of free mAb, we demonstrated that, working on PSMA + cells, the binding is specific.
In figure 77, red lines show the decrease of APC MFI. We can appreciate the decrease of nanoparticles uptake only by coincubation of free D2B mAb with both NPs-D2B and NPs-Hemi D2B

but no with NPs-BSA. This result proves definitely that the antibody leads nanoparticles to bind and to internalize specifically in PSMA positive cells.

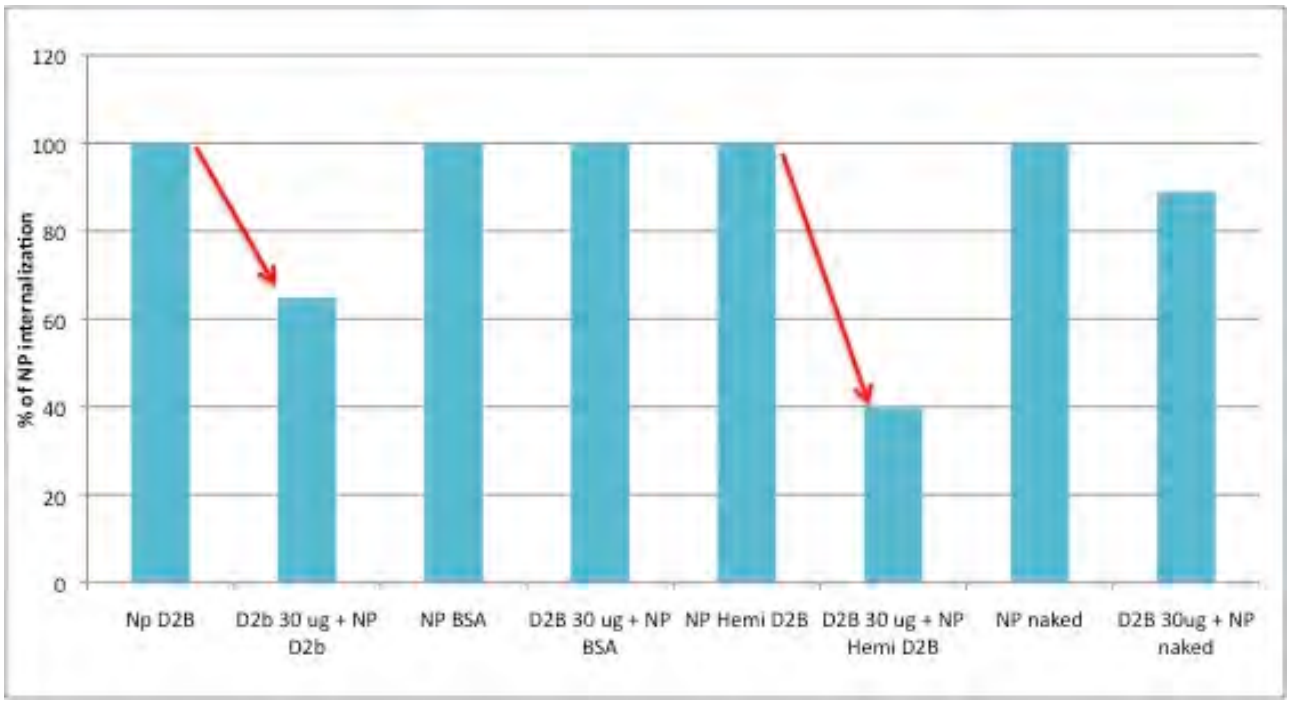

Fig 77: Competition experiment performed on PC3 PIP cells. The results were acquired by flow cytometry (APC channel). We used a NPs concentration of 1μM Foscan®, and 1h30' of incubation.

These experiments were repeated on other PSMA positive cells such as LNCaP, and also on some PSMA negative cells confirming these data.

Saturation assays performed incubating PC3 PIP cells with increasing NP concentrations ranging from 0.06 μM to 5 μM (time 1h 30') suggested that the more specific uptake is obtained using lower Foscan® concentrations. With Foscan® concentration higher than 1 μM, the APC fluorescence recorded at flow cytometer is decreased, and therefore also the cell uptake.

We also applied the confocal microscopy analysis to better appreciate the mAb-driven NP internalization. In these experiments we incubated cells with NPs for 24hrs in presence of complete growth medium. siNPs were detected due to their loading with Foscan® (APC channel fluorescence) whereas the cell membrane was stained with anti CD71-FITC (anti transferrin receptor-FITC) or Concanavallin A-FITC. Confocal microscopy image showed that only mAb guided NPs are localized inside the plasma membrane of LNCaP cells (PSMA+). In DU145 (PSMA-) cells no accumulation was observed inside the cytoplasm. Therefore these

analyses demonstrated that the binding and internalization is also antigen-specific. Moreover no internalization was detected in the same system using BSA-NPs (Fig 78).

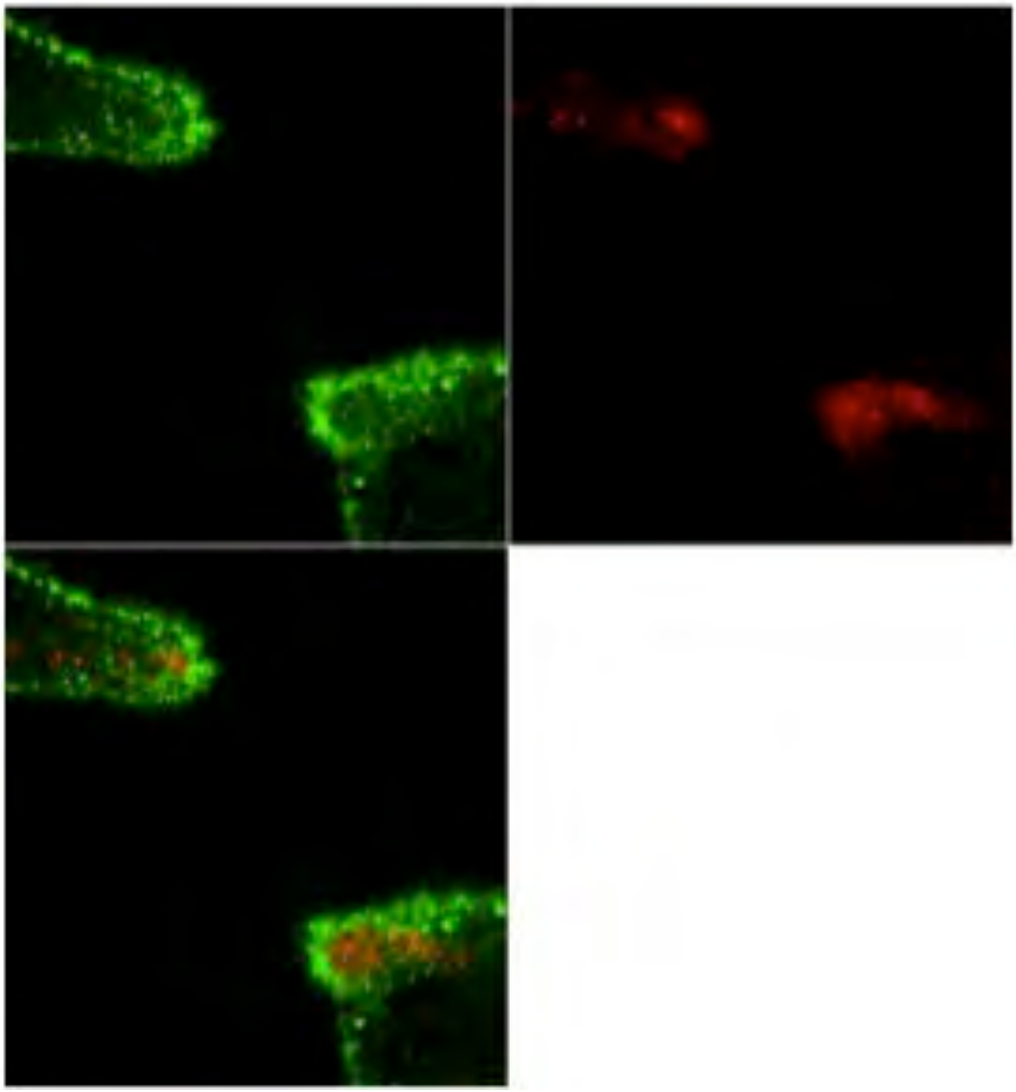

Fig 78: Confocal analysis of mAb guided NPs internalization on LNCaP cells. siNPs are APC labelled (red color in this pictures), cell membrane was detected by FITC conjugated trackers.

We, then, evaluated the stability of our conjugates in presence of human serum. D2B-NPs were pre-incubated for 12hrs in serum at 37°C and than binding properties were analysed by flow cytometry.

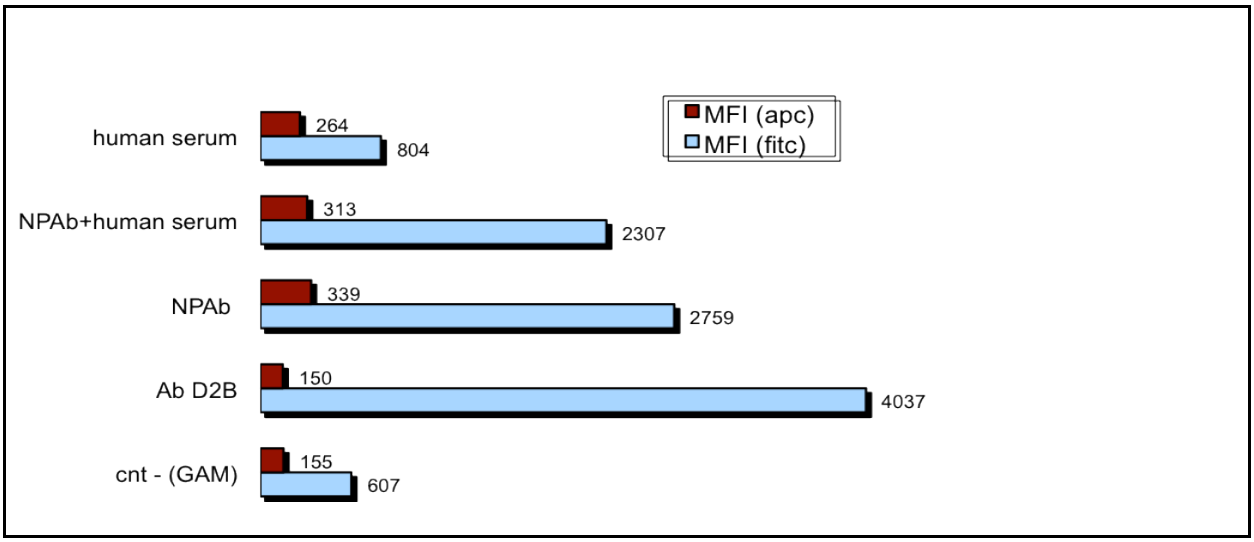

Fig 79: Nanodevice serum stability. After D2B-NP incubation at 37°C for 12 hrs, uptake experiments were performed on PSMA+ cells and data acquired by flow cytometry. We considered APC MFI value (due to NPs) and FITC MFI value (due to the staining of mAb conjugated to NPs with anti mouse IgG FITC)

Figure 79 shows clearly that binding capability does not change if the NPs-Ab are preincubated with human serum.

Since the photodynamic therapy killing is related to the amount of Foscan® molecules accumulated in the target cells, we assessed a multiuptake strategy, incubating cells with nanoconjugates with cells four times, for 1h and 30' with breaks of 4 hrs. During every break the nanoparticles were removed and replaced with complete medium.

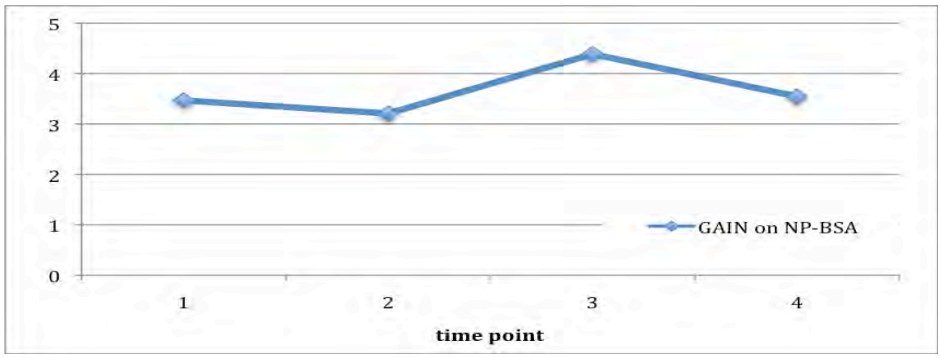

Fig 80: Multiuptake experiment performed on PC3 PIP cells. The results are reported as the MFI APC ratio between samples and NP BSA.

After the third treatment with D2B NPs we can appreciate a very little increasing in the specific uptake compared to BSA NPs (Fig 80).

A cytotoxicity assay was necessary to check that these Foscan® loaded nanoparticles are toxic only when they are subjected to a laser beam. So we carried out toxicity assays: analyzing cell viability after treatment with NPs (e.g. XTT assay and ^{3}HTdR incorporation).
We worked with three NP concentrations: 0,5- 1- 2 μM Foscan®. The NP treated cell viability was superimposable to the untreated cells, showing that nanoparticles are not toxic for the cells. (Fig 81)

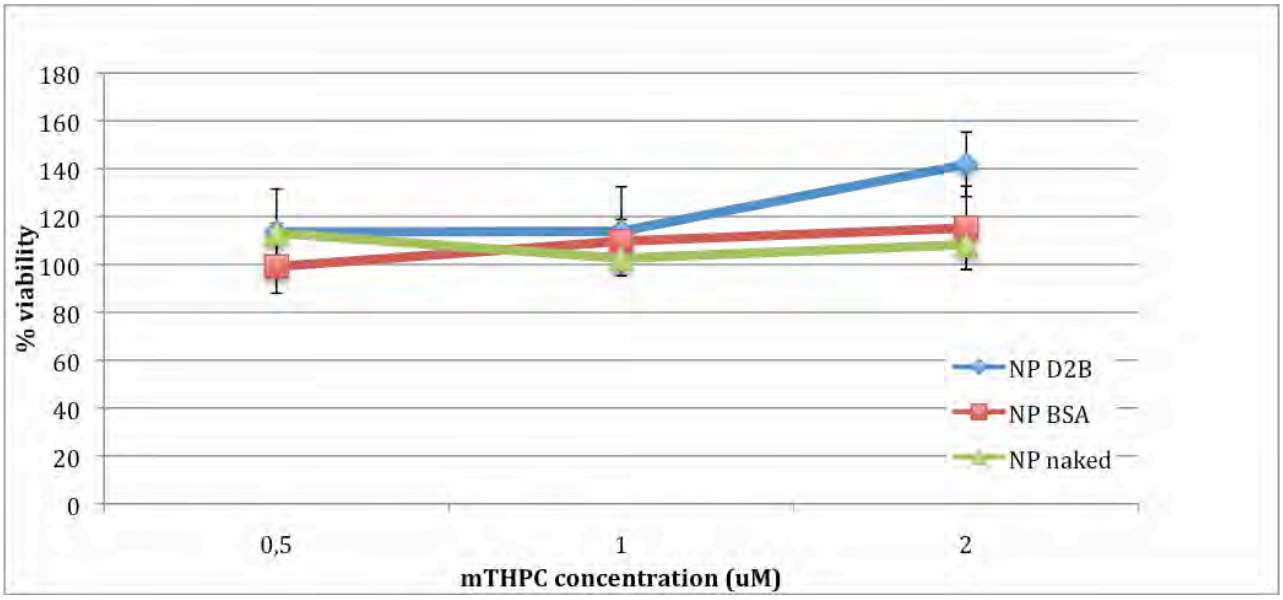

Fig 81: Cytotoxic effect of our nanoparticle preparations. PC3 PIP, PSMA + cells, were incubated with different NP sample (e.g. mAb or BSA conjugated and naked). Viability was calculated by measuring the 3HTdr incorporation compared with mock treated control.

Cetuximab functionalized siNP

After Cetuximab conjugation to siNPs, we carried out the cytometric analysis to demonstrate the binding specificity of these new tools.

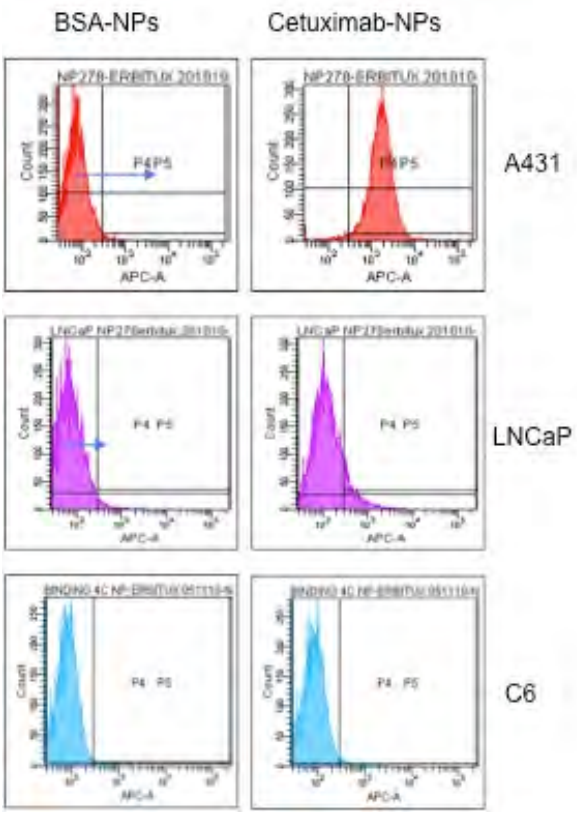

Fig 82: Flow cytometry analysis of NP cetuximab versus NP BSA performed on A431 cells at 4°C. We measured the fluorescence in APC channel due to the Foscan® molecules. A431 and LNCaP cells are EGFR+ cells, C6 cells are EGFR-cells.

We used in these experiments two human EGFR+ cell lines (A431, LNCaP) and a rat cell line C6 (glioblastoma cells), which represents a negative control cell line, due to its expression of the rat isoform of EGFR. It is important to remember that Cetuximab recognition is only against the human isoform of EGFR. In figure 82 the histograms demonstrate that the antibody specificity is not altered after conjugation to the NPs; the ability of the conjugates (Cetuximab-NPs) to bind to A431 cells more than the LNCaP cells was due to the different levels of EGFR expression. The table below shows the different level of EGFR expression described for LNCaP and A431 cells.

CELL LINES	Receptor/cell	Ref
A431	$1*10^6$	Kinzel et al 1990 Cancer Res.
LNCaP	80,000	Yang et al 2002, ASCO

Tabella 11: Receptor number of each cell line, reported in literature.

From the literature we can deduce that A431 cells have an amount of receptor 12.5 times more than LNCaP cells. Our experiments conformed this ratio, showing a ratio of the MFI signal (MFI on A431/MFI on LNCaP) of 11.1. Moreover analyzing the APC MFI of Cetuximab guided versus BSA guided NPs on A431 cells we observed an increasing of the specific uptake of about 17, 5 times; while on LNCaP cells this specificity index increase to 2 times only. Working with C6 cells we demonstrated that no increasing of specificity was measured on human EGFR negative cells.

After the binding analysis we moved to study the specific uptake at 37°C: cells were incubated for 1 hr 30' and then samples were analyzed by flow cytometry (APC channel).

	MFI APC
NP Cetuximab	8,900
NP BSA	200
NP nake	450

Tab 12: Uptake at 37°C on A431 cells, data of flow cytometry analysis (APC channel).

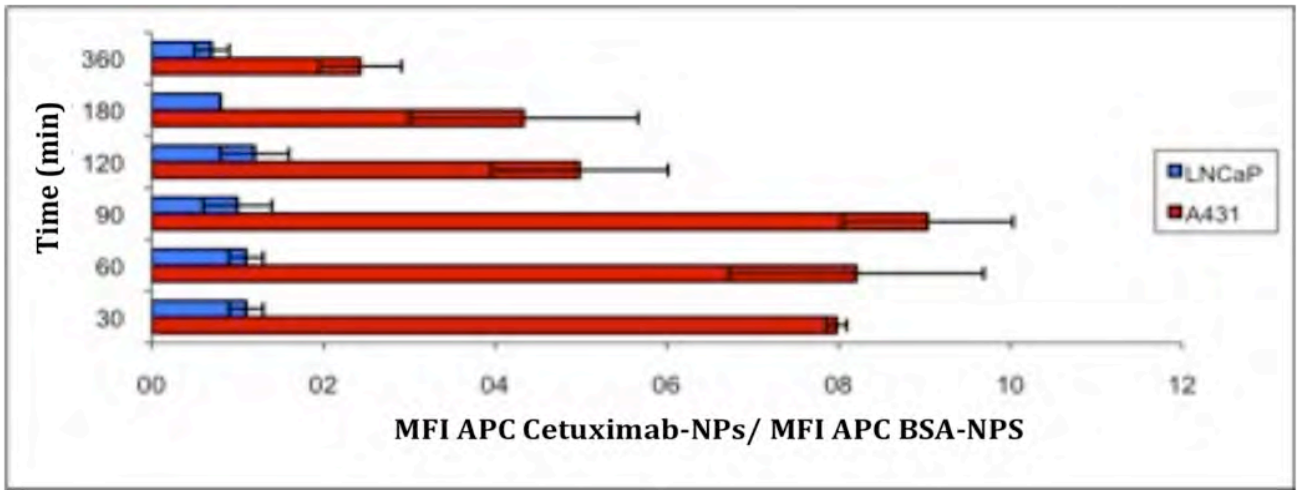

Fig 83: Time dependent uptake of Cetuximab-NPs: MFI sample values were normalized to BSA-NPs MFI.

Then it was assessed the time-dependent accumulation of nanoparticles, using a concentration of Foscan® of 1μM. The data shown in figure 83 confirm what was already observed in binding experiments. There is a specific accumulation in A431 cells and the maximum of specificity was achieved at the shorter times. The Ab conjugated NPs reached a plateau, unlike the naked NPs that have a time linear increasing. All these data show that the accumulation of our conjugates is receptor dependent, unlike the naked NPs that seem accumulate within cells in a nonspecific manner. The high and non-specific accumulation of naked NPs is due to the positive charged surface (e.g. amino group on the PEG shell). BSA-NPs showed less accumulation than both naked NPs and Cetuximab conjugate NPs; indicating that the elimination of amino groups on NP shell by means of conjugation, decreases the "sticky" properties of NPs and therefore their non specific accumulation in the target cells.

The specific binding of these new-guided nanoparticles to the receptor was further confirmed by competition assay using NPs at a concentration of 0.25 μM in Foscan®. When free Cetuximab was added during incubation on A431 cells, we saw a decreasing in Cetuximab NPs uptake. The APC MFI value measured by flow cytometry was reduced from 800 to 200 of MFI. Using BSA-NPs we did not detect any decreasing of the MFI value.

We analyzed A431 cells by confocal microscopy to confirm the uptake on target cells. A431 cells were incubated with a number of NPs corresponding to a concentration of mTHPC 1 μM. Two incubation times were chosen: 2 hours and 15 minutes. Picture 84 show that guided NPs have already accumulated after 15 minutes of incubation and that after 2 hours the accumulation is more clusterized. The BSA-NPs demonstrate in the same experiments very faint signals confirming low accumulation.

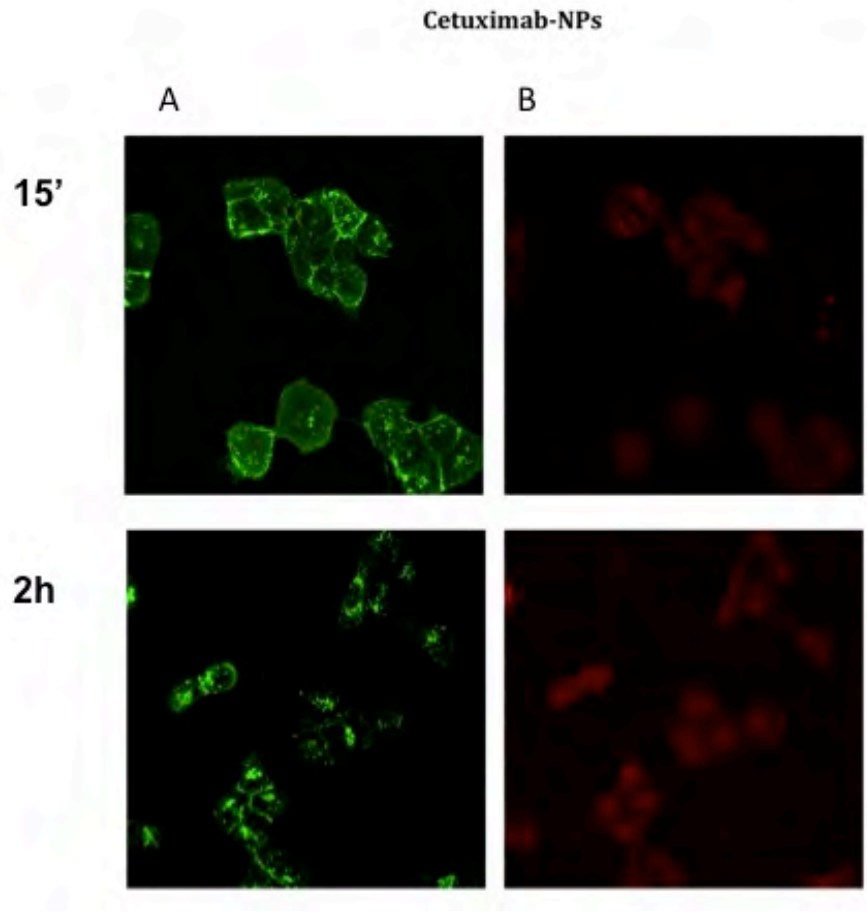

Fig 84: Confocal Microscopy analysis: A431 cells incubated with cetuximab-NPs for 15 minutes and 2 hours; A) FITC fluorescense due to anti human FITC that binds Cetuximab B) APC fluorescence due to Foscan®.

No influence of NP pre-incubation with serum at 37°C was observed when binding and uptake experiments were carried out on A431 cells.

2.6 Photodynamic therapy with Foscan® silica nanoparticles.

Once demonstrated that antibody conjugation to NPs did not decrease its specificity and besides increased target cell uptake, we moved to evaluate the photodynamic therapy efficacy of these new guided Foscan® loaded nanodevices. In collaboration with Prof. Papini of Padua University we conduced several preliminary PDT assays. The cytotoxicity of mTHPC delivered by guided silica nanoparticles was evaluated after exposure to red light. The cells were seeded and incubated (37°C) for 6 hrs with nanoparticles at Foscan® concentration of 1 μM. After in-

cubation, the cells were washed and irradiated with 0.12 Jcm $^{-2}$ of a red light emitted from PTL Penta quarts halogen lamp for 10 minutes. Cell viability was measure 24 hrs later with MTT assay.

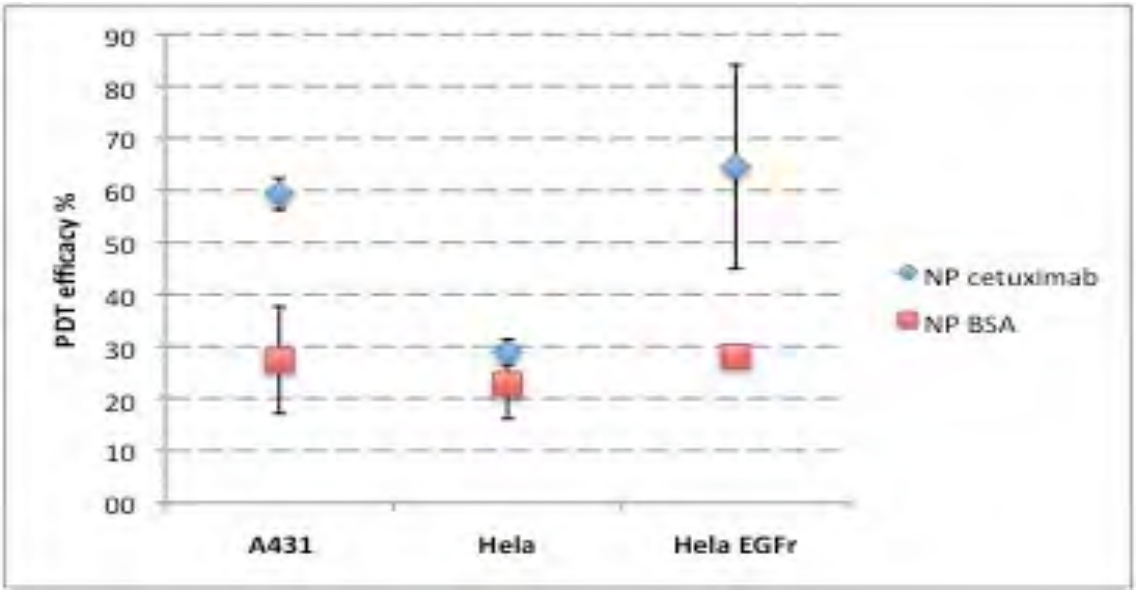

Fig 85: PDT efficacy of NP Cetuximab and NP BSA incubated for 6hrs and irradiated with red light for 10'. The following cell lines were used: A431-Hela and Hela EGFR.

In figure 85 it can be appreciate the difference between the two types of conjugated nanoparticles. On A431 cells, Cetuximab NPs show a PDT efficacy of 60% versus the 28% of NPs BSA. The delivery of mTHPC to the target cells seems to be increased using antibody functionalized nanoparticles. Furthermore, the possibility to assess the nanoconjugates on cell line, with different EGFR levels constitutes the best control to determine the effectiveness of these nanosystems as a specific carrier for photodynamic therapy. For this reason we used a cell line (HeLa) expressing low levels of receptor and a transfected clone expressing a highest levels of receptor (EGFR Hela) obtained at Padua University.

CELL LINES	Receptor/cell	Ref
HeLa	50,000-140,000	Kinzel et al 1990 Cancer Res.
A431	$1*10^6$	Kinzel et al 1990 Cancer Res.
HeLa EGFR	250,000-400,000	Data obtained in our laboratory

Tab 13: EGFR positive cell lines.

The Killing capability of NP BSA in PDT treatment appears quite the same in all three cell lines, thus due to a non specific uptake. As it was already shown in previous binding tests, high Foscan® concentration is correlated to a decrease in cell uptake. All this causes a lower cytotoxic effect due to the smaller concentration of mTHPC inside the cells. (Fig. 86)

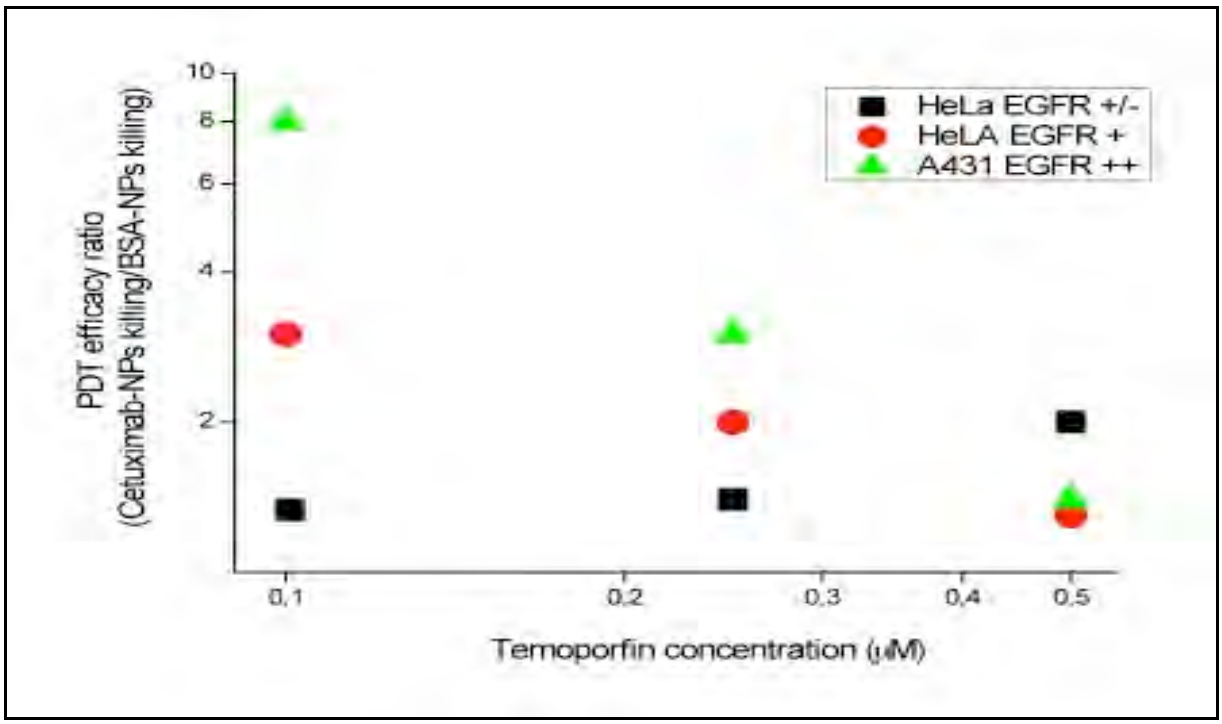

Fig 86: PDT efficacy ratio versus Foscan® concentration. PDT assay performed on A431, HeLa, and HeLa EGFR cell lines, incubating nanoparticles for 6hrs and then irradiating for 10'. The cell viability was evaluated by MTT assay.

In additional experiments the cells were treated as above, but the PDT killing capability was determinated by the human Annexin V-FITC Kit (Bender MedSystems, Wien, Austria). Percentage of annexin positive cells after treatment with cetuximab NPs was of 7% versus 2% of non-irradiated. On the contrary for the treatment with NPs-BSA the percentage varies from 5.2% to 2.7 %.

Discussion

Nanotechnology, developed over the past twenty years, is the meeting point of different disciplines such as biology, material chemistry, chemistry and physics. Medicine is one of the most interesting fields of its application, especially by providing innovative solutions for diagnostic imaging and therapy of tumors.

Thanks to their advantageous chemical-physical properties the NPs are able to accumulate in the tumor site (EPR effects), and due to their small dimensions the NPs can pass through some barriers present in the human body, such as the blood-brain barrier. Firstly, we focalized our attention on the reactivity and on the physical-chemical characterization of nude nanoparticles, and then on "drug loaded" and driven ones.

In clinical oncology both, the diagnostic protocols based on molecular markers and targeted therapies are becoming very important. Nowadays applications of nanotechnology in diagnostic allow to further lower the detection limit of cancer markers [*Ray S. et al, 2011*]. Early detection is particularly important in cancer therapy because early stage diseases are treated with the greatest probability of success. Furthermore, it would also desirable to have non invasive imaging methods with a high signal in order to localize also deep tumors. In this contest, high-throughput and high sensitive methods for biomolecule detection are the main objective of many researchers, and nanotechnology offers a broad spectrum of highly innovative techniques to join this objective.

As regards naked nanoparticles we studied samples made of different materials: gold and iron-magnetic ones. Gold material was chosen because it is widely used in medical application due to its several positive advantages: chemical and biological inertness, resistant to oxidative conditions, no toxicity, facility to direct bind different organic/biological molecules via gold sulphur bond or electrostatic attraction. Particularly gold nanoparticles exhibit a unique phenomenon, known as surface plasmon resonance, when they are exposed to specific wavelenghts. This phenomenon enhances the gold optical properties (absorption and scattering) and depends on the particle size. The light scattering of 80 nm AuNPs is four to five orders of magnitude larger than those of conventional dyes. Moreover, the light scattering signal is resistant to bleaching and not sensitive to the background. Surface enhanced Raman scattering (SERS), achieved by adsorption of specific dye molecules (SERS dye) on particle

surface, can gain a signal enhancement in the order of 10^{14}-10^{15}[*Radwan S.H. et al, 2009*]. Most intense signals are obtained when the molecule is also in resonance with the laser excitation, namely surface enhanced resonant Raman scattering (SERRS)[Kneipp et al, 2006]. Furthermore, the bandwidth of Raman peaks is on the order of few nm and therefore each different molecule exhibits a distinctive Raman fingerprinting. There is a wide series of SERRS labels (e.g. MG, CV, TR, RB, TRITC) [*Amendola V. et al 2011*]; which can be excited at the same time with the same laser wavelength. This feature makes SERS labels promising for multiplexed analysis. All these characteristics offer a great advantage for non invasive trace biodetermination technique. [*Qian, X. M. et al 2008; Nie S. et al, 1997: Kneipp K. et al, 2006; Le Ru E.C. et al, 2007*]

In our work, in collaboration with the Meneghetti's staff, we used naked gold nanoparticles SERS labelled in order to investigate a new quantitative detection method. With this study we demonstrate the correlation between SERS signals and the concentration of SERS labels (based on AuNP amount) for in vitro quantitative biological applications.

The nanoparticles (NPs) with two different Raman active dyes (Cresyl Violet and Malachite Green) were incubated with cells and we analyzed the Raman signals from cell lysates. Finally we correlated these data with the value obtained by ICP-MS (inductively coupled plasma mass spectrometry) on the same samples. The time stability of Raman signal in physiological medium and the reproducibility of the synthesis procedure are crucial parameters for quantitative applications of SERS labels.

The results show a linear correlation between the AuNPs concentration and the SERS signals in physiological medium providing a suitable new analytical approach for ultrasensitive quantitative analysis (down to picomolar concentration) of biolabelling agents in biological samples.

In literature there are already some application examples of this technique, Gambhir and coworkers reported their in vivo multiplexed SERS analysis by using available silica coated AuNP loaded with Raman active dyes. Nie's group demonstrated the reliability of "in vivo" tumor targeting and detection by using pegylated gold nanoparticles functionalized with antibodies selective for the EGFR. [*Keren, S. et al, 2008; Zavaleta, C. L. et al, 2009; Qian, X. et al, 2008*]. A variety of SERS labels were described in the literature, and used for qualitative assays. There are no application examples of quantitative analysis. This new field can be a very interesting analytical objective but it requires the study of SERS label features in order to enhance their sensitivity. It was widely demonstrated the improvement of the Raman signal

strength can be reached increasing nanoparticle diameter: therefore a 20 nm AuNPs exhibit a lower absorption than 80 nm AuNPs. The frequency, intensity of absorption and scattering bands depend on the composition, size and shape of AuNPs. Hu J. at al. demonstrated that SERS effects increase with the nanoparticle bend. A sharp shape would be desirable because in tip closeness the electrical field is gathered. It is well known that SERS signal enhancement is associated mainly with local electrical fields. So that, the highest SERS enhancement factors were obtained by aggregates or clusters (namely hot spots) deriving from gold nanoparticles of 20-60 nm in size. For this reason, in our work we increased the Raman intensity signal of 20 nm AuNPs by controlling the formation of gold nanoparticle aggregates. [*Khoury C.G. et al, 2009; Kneipp K. et al, 2006: Le Ru E.C. et al, 2007; Lombardi J.R. et al, 2009; Kneipp H.et al, 2006*]

The second part of the study on "naked" nanoparticles is concerned with magnetic iron oxide nanoparticles. Magnetic nanoparticles show a unique characteristic compared to other nanoparticles: they obey Coulomb's law and they can be manipulated by an external magnetic field. Thanks to this property and to the intrinsic diffusion of magnetic field into human tissues, magnetic nanoparticles could be directed to target tissue, in this way they open up many interesting medical applications. Magnetic nanoparticles could be used to deliver packages to deep target lesions, such as an anticancer drug or radionuclides. For example Magneto-fluorescent macrophage cells are of great interest in nanomedicine because they can act as carriers of MNPs into deep lesions, aiming at the multimodal magnetic resonance–fluorescence imaging. When functionalized with DNA vectors, MNPs could be used as effective gene transfection systems under external magnetic field (magnetofection). Furthermore they could be used as hyperthermia agents to destroy cancer cells, exploiting their response to a time-varying magnetic field which results in an advantageous energy transfer from the exciting field to the nanoparticles, with a consequent heating of target tissues. [Shubayev, V.I., et al, 2009]

Also iron oxide nanoparticles offer other advantages in comparison to other MNPs due to their good biocompatibility and long term biodegradability. We demonstrated that our FeOx-MNPs do not show any cytotoxic effect, and do not induce apoptosis. We also described the use of fluorescent FeOX-MNPs for label macrophage cells and their sorting and manipulation by external magnetic field.

The efficacy of nanoparticle uptake was performed in macrophage differentiated U937 cells (human non adherent monocyte like cells). Fluorescein conjugated FeOX-MNPs were first incubated with macrophage cells and then assessed by flow cytometry and confocal microscopy.

We found that these fluorescent loaded MNPs can be effectively used for cell sorting and manipulation by a magnetic field without cytotoxic effects. As we have already mentioned, macrophage NP uptake is important because it is well known that macrophage can infiltrate in the tumor lesions and so loaded macrophage can be visualize by MRI and in this way they could also allow a focalized drug release. Moreover we demonstrated the possibility of MNPs used as vehicles to transport theranostic agents into tissues or lesions. Our results indicated that FeOX-MNPs could be an optimal new theragnostic tool for cancer management. The next step in our investigation will be the study of these types of MNPs in *in vivo* mouse model.

After the investigation on naked nanoparticles, our attention was focalized on antibody-driven nanoparticles. These nanoparticles, exploiting active targeting, are able to enhance their tumor accumulation compared with healthy tissues. In the second part of my thesis I evaluated the feasibility of in vitro and ex vivo targeting of tumor cells by antibody guided NPs with the goal of developing immunodiagnostic and immunotherapeutic devices. Key points for the success of our investigation were the availability of high affinity monoclonal antibodies recognizing tumor associated antigens and appropriate in vivo mouse models for the assessment of the immunogenic and immunotherapeutic potential of these targeted NPs.

In the latest years cancer therapy becomes even more specific and personalized, in this contest tumor associated antigens play a central role. Tumor Associated Antigens or biomarkers can be proteins, fragments of protein, DNA or RNA. Generally, TAA are proteins over expressed in tumor tissues, and present at low level in healthy tissues. Several reviews have summarized the progresses made in this field: many TAA have been described, against which monoclonal antibodies were produced and assessed for cancer treatment.

Our first objective was the investigation of functionalized gold nanoparticles used for cancer cell detection. The ability of detecting very low concentration of tumor biomarkers can be very useful for predicting tumor staging and its metastatic potential. Furthermore, functionalization can be made with different monoclonal antibodies and in this way we could be able to detect simultaneously multiple proteins, in a single tissue sample without enzymatic amplification. This application is called multiplexing analysis and could improve greatly the diagnosis and the possibility of personalized medicine. In this section we have therefore investigated the binding properties of gold-NPs conjugated to mAbs recognizing prostate specific antigens (PSMA and PSCA) and loaded with two different SERS labels: Texas Red and Malachite Green. PSMA for its wide distribution in prostate tumor (about 70-80% of patient tumors are PSMA+) is an important biomarker in the management of this malignancy using

targeted drugs. PSMA is also ectopic-expressed on the vasculature of many solid tumours, making it a more general applicable target in oncology. PSCA is highly expressed by a large fraction of human prostate, pancreatic and bladder tumors, including metastatic and hormone refractory prostate cancer, but it has a limited expression in normal issue. [*Li, Y. et al, 2010*]

We analysed the binding specificity and the internalization in antigen positive cells of our mAb functionalized gold NPs by flow cytometry and confocal microscopy analysis. We recorded also the specific SERS signals using a Raman microscopy. Finally we evaluated the potential use of these nanoparticles in "*in vivo"* mouse model. We found that the length of PEG coating plays a key role in the antibody binding functionality: it can be thought that the movable chain of PEG hides the antibody binding site, preventing in this way its capability to recognize and bind the target antigen. For this reason, we have investigated several PEG chains for NP coating. Finally we decided for a PEG length between 3,000 and 5,000 MW. Our data show that mAb guided nanoparticles have a good ability to specifically target antigen positive cells and to produce intense SERS signals. This feature is most advantageous for their imaging-diagnostic applications. Furthermore, in vivo experiments on a syngeneic tumor mouse model (C57/BL6 mice injected ev and/or sc with mouse B16hPSMA cells) showed nanoparticle stability in physiological conditions. All these evidences supported our ideas to use mAb targeted NPs to enhance the transport of toxic drugs at the tumor sites and confirmed the possibility to apply these devices in tumor imaging and therapy.

It is important to highlight the innovation of our approach compared to others: the achievement of targeting and detection in a single step. Lee K. et al. performed a similar study, but they exploited gold nanoparticle network formed by DNA Hybridization in order to detect CD44+/CD24- subpopulation of breast cancer stem cells. The particle network enhanced SERS signal [Lee K. et al, 2011]. In the literature it is described other nanoparticles used in multiplexing imaging: the composite organic inorganic nanoparticles (COIN). They consist of nanoclusters formed by aggregation of silver nanoparticles and Raman active molecule. COIN provides higher Raman intensity signal, but the measurement suffered from auto fluorescence and spectral fitting was necessary [*Sun L. et al, 2007*]

In the future there is still much progress that could be done in this field, for instance it is desirable to increase the penetration depth of the laser used for particle irradiation (NIR wavelengths are the most penetrable). All these improvements are necessary if we want to move these compounds into the clinic.

Once evaluated the feasibility of functionalized gold nanoparticles in imaging/diagnostic applications, we also investigated the possibility to apply these nanoparticles in therapeutical applications. It is well known that nanoparticle drug delivery enhances therapeutic effectiveness and reduces side effects of the drug payloads by improving their pharmacokinetics. For this purpose we used gold nanoparticles, targeted with mAbs and loaded with doxorubicin. Doxorubicin is a chemotherapeutic drug commonly used in treatment of a wide range of cancer, but it exhibits some side effects, the most serious is life-threatening heart damage. Due to this reason, we propose an alternative mechanism for the specific accumulation of doxorubicin in the tumor sites.

Our preliminary in vitro results prove a lower cytotoxic effect of loaded-driven nanoparticles than the doxorubicin alone. At the same time, our experiments show a selective effect of nanoparticles driven and loaded with the drug only versus antigen positive cell. The driving/specificity was obtained thanks to the use of a targeting moiety: a monoclonal antibody that recognizes a tumor associated antigen (PSMA). In this way we have an effective system that could be assessed in *in vi*vo assays.

Nanoparticle drug incorporation is new drug delivery modalities that can also suppress/reduce chemoresistence. The simultaneously delivery of different drug has several positive implications: it joins together the pharmacokinetics of different drugs, and so it converts the slower one to the more effective one. The efficacy could be further increased, due to the delivery of sequential combinatory drug. A multi-target approach, using multiple drugs, could raise the genetic barrier due to cancer cell mutation (the cancer adaptation process) and could be more effective thanks to the synergistic action of multiple drug versus the same cellular pathway [*Hu C.M.J. et al, 2010*]. Furthermore, using nanocarriers, the drug release in the target tissue can be regulated, involving another interesting characteristic: the drug tumor priming. This phenomenon is characterized by the promotion of the transport and the penetration in the deep tissues of solid tumors thanks to a temporal drug release. At the first, released drug induces partial cancer apoptosis and expands the interstitial space of solid tumors. Then the NPs can diffuse deeper into the tumor and release the second drug for a more effective cancer treatment.

Thanks to all these reasons the delivery of multiple therapeutic agents with a single nanocarrier is the aim of several researches.

In the last part of the work we studied silica nanoparticles loaded with a photosensitizer drug and guided by means of a mAb. These types of nanoparticles can be used in photodynamic

therapy (PDT) for the selective killing of neoplastic cells. PDT is suited for the treatment of early cancer because, by means of a localised fibre-optic light delivery, it allows a high accurate thermoablation of localized metastasis (it is possible to treat the whole of the prostate using PDT, and since the prostate cancer can be diagnosed at early stage this is a particularly promising application). PDT treatment modality involves the simultaneous presence of light, oxigen and a light activable chemical drug called photosensitizer, to achieve a cytotoxic effect. Once activated by red light, the photodynamic agents are able to promote photosensitised reactions with the release of singlet oxygen, which leads to the tumor killing. Furthermore photodynamic agents allow tumor mass visualization thanks to their fluorescent emission.

We used the Foscan® (metatetrahydroxyphenyl-chlorin), which is one of the most potent photosensitizer available for PDT clinical applications, distribuited by Biolitec. This drug produces a satisfactory tumor response at both very low drug doses (0,1 mg/kg) and light irradiation energy (10j/cm^2). Despite these favourable characteristics, Foscan® shows variable clinical results, due to its variable selective accumulation in malignant tissues. This is probably explained by the fact that, as demonstrated by experimental studies, the tumoricidal effects of Foscan®-PDT are largely mediated by vascular damage and the efficacy of the treatment does not correlate with the tumour levels of Foscan® at the time of irradiation but rather with its plasma level [*Cramers*, *P. et al*, *2003*]. Furthermore the low specific accumulation requires an interval between drug administration and light irradiation of four days to avoid considerable damage in normal tissues.

All these considerations suggests the necessity of a suitable delivery system able to modulate Foscan® biodistribution and to improve the efficacy and selectivity of PDT. Increasing the selective accumulation we could have high treatment efficiency with lower drug doses. In this way we reduce the sensitivity to light, the unavoidable side effect associated to the administration of photosensitizing drugs.

In this doctoral thesis we investigated as carrier silica nanosystems conjugated with targeting moieties, mAbs recognizing EGFR and PSMA. The primary aim was to define the efficiency of cell internalisation mediated by the specific receptor through in vitro studies with appropriate cell lines. In addition experimental PDT studies aimed to demonstrate the improved efficacy and selectivity of these treatments, with NPs functionalized on their surface with mAbs A further goal will be to demonstrate the usefulness of this targeted Foscan® NPs for tumor imaging by monitoring the red fluorescence of Foscan®.

The choice of silica material allows to prepare nanoparticles with the desired size, shape and porosity. The porosity of their matrix is essential for the singlet oxygen diffusion, which carries out the toxic function. Using SiO_2 NPs, the photosensitized drug is entrapped into the NPs and it can exerts its phototoxic effects without being released from the carrier. In this way the phototoxic effects in the skin and eye caused by non specific accumulation of free drug could be reduced. The use of silica particles loaded with a photosensitizer drug (2-devinyl-2-(1 hexyloxyethyl) pyropheophorbide, HPPH) for PDT has been already proposed by Prasad and co-workers [*Roy I. et al*, *2003*]. They demonstrated cellular uptake and retained in vitro PDT activity of the nanocarriers. Recently, Kopelman and co-workers proposed another related example [*Gao D. et al, 2007*], in which they entrapped Foscan® into 2-3 nm hydrogel particles and demonstrated that the PDT activity is retained. Beyond silica nanoparticles, also liposomes were particularly useful for their capability to solubilize these molecules in their phospholipid bilayer [*Ferrari M. et al, 2005*]: on the contrary such particles do not appear to be an ideal candidates for Foscan® delivery, as due to their very small size that permits the inclusion of only one or two photosensitizer molecule per particle. As for metal nanoparticles, surface of silica nanoparticles can be coated with polyethylene glycol (PEG) in order to obtain stealth particles with enhanced circulation time in the bloodstream. We increased both efficiency and selectivity of Foscan® loaded NPs through the conjugation to ligands that specifically bind to receptors that are preferentially over expressed on tumor cells, such as PSMA and EGFR (this receptor is over-expressed on various carcinoma including those from the head and neck, lung, colon and prostate).

SiNPs were synthesized by Prof. Mancini's Staff (Padua University) and they show on the surface a limited number of amino groups. Exploiting this amino group, we chemically linked the mAb-targeting moieties. To select and test the best conjugation conditions required a lot of time, and here we cannot describe all the steps. Briefly, targeting protocols were carried out considering two important parameters: the number of ligands (antibody molecules for particle) and length of PEG spacer, both of them can affect the efficiency of specific binding and endocytosis in the targets cells. We assessed each silica nanoconjugate batch on appropriate tumor cell lines: LNCaP for PSMA guided NPs, and A431 or HeLa-EGFR for Cetuximab NPs by flow cytometry and by confocal microscopy. All the results confirmed the binding specificity of our targeted nanoparticles for antigen positive cells, and their accumulation into the cells after incubation at 37°C.

Kinetic analysis showed that the differential uptake between mAb or BSA targeted NPs decreased with the increasing of the time, with a peak between 1 and 2 hrs. The specific uptake decreased also treating cells with increased NPs concentration due to the saturation of the receptor mediated endocytosis mechanism.

Serum stability was investigated to analyze possible hindrance effects and degradations due to serum proteins and enzymes; we discovered that mAb-NP binding capability is unchanged after their incubation at 37°C in serum from healthy donor or PCa patients. Furthermore PDT experiments showed that Foscan® loaded NPs, when guided by mAbs, can selectively kill target cells decreasing non specific effects. It is mandatory to investigate new chemical conjugation protocol for Foscan®-NP binding in order to improve the Foscan® photoactivation.

One of the ideal properties of a photosensitising agent is low toxicity in absence of light laser pulse, therefore we tested the dark toxicity in the absence of light. We demonstrated that mTHPC can cause cell death without irradiation at rather low concentration.

Obviously the behaviour of the Foscan®-NPs reported here does not necessarily apply to any other nanocarrier, as it depends on the nanoparticle chemical composition, surface properties, size and targeting moiety. [*Villanueva A, et al, 2009*]. Furthemore, the covalent binding of Foscan® to NPs may be an advantage, allowing the visualization of nanoparticle pathway, once injected into a biological system. This property could have interesting implications in diagnosis and imaging application. On the contrary, the linkage may be an obstacle for Foscan® efficacy in therapy, preventing its release once NP is entered into the cell [*Ohulchanskyy T Y, et al 2007*]. Another possible obstacle for the effectiveness of Foscan® NPs in therapy is the block of the singlet oxygen inside the cell, limiting its toxic action.

The conjugates showing the highest efficiency of cell specific uptake in vitro will be tested also in vivo using suitable tumour models. The in vivo studies will include pharmacokinetic studies for defining blood circulation half-life, uptake and clearance from various normal tissues and tumour in order to evaluate the efficacy and the selectivity of targeted PDT.

Key role in this type of therapy is carried out by the toxic action of the singlet oxygen, for this reason an opportunity to increase the effectiveness of PDT may be to combine the treatment with substances that increase the singlet oxygen half life (such as Deuterium oxide [*Athar M et al, 1988*]). Combination of PDT with a secondary treatment is a common way to improve its effectiveness. Furthermore another important effect of PDT is hypoxia due to the oxygen consumption and vasculature damage. A number of reports described unexpected pro-oxidant

properties of the anti oxidants, which are considered chemopreventive agents against cancer. Buettner and co workers demonstrated that in the presence of metal traces, ascorbate combined with photofrin/PDT enhanced the production of radicals and decrease cell survival.

A second approach to increase PDT efficacy is a combinatory treatment with antiangiogenic drug in order to reduce angiogenic responses, caused by PDT. PDT act on the vasculature, producing divergent effects in that the expression of some angiogenic factors may be enhanced. Ferrario et al. have demonstrated an improved treatment response by combining photofrin®-mediated PDT with antiangiogenic drugs. The same group evaluated the anti tumor activity of PDT followed by administration of a potent synthetic metalloproteinase inhibitor, and they showed a significant difference in long term cure rate compared to PDT alone. [*Postiglione I. et al, 2011*]

PDT followed by the administration of an angiogenic inhibitor, abolished the VEGF increase and reduce local tumor growth. Therefore the direct inhibition of VEGF secretion could enhance both PDT and antiangiogenic treatment. [Kosharskyy et al, 2006]

The secondary treatments may act also increasing the susceptibility of tumor cells to PDT, by pre-weakening the tumor cells [*Verma, S. et al 2007*].

For the first time in 1990, Kennedy and Pottier introduced the use of topical 5-aminolevulinic acid (ALA), a potent endogenous photosensitizer. The introduction of this molecule and its topical administration represented a turning point in dermatological PDT, since this'' prodrug" has the property to easy penetrate and focusing in many epithelial tumors and other skin lesions. This effect is selective because the surrounding healthy skin, covered with a normal stratum corneum, is waterproof to ALA. In this way the susceptibility of tumor cells to PDT is increased. All these studies are significant step towards improving PDT application both in local and metastasis tumor. Another exciting area of research is looking at the use of PDT along with current therapy to make it more effective. One way to do this may be to use PDT during surgery to help keep cancer from coming back on large surface areas inside the body, such as the pleura (lining of the lung) and the peritoneum (lining of the belly or abdomen). These are common sites of spread for some types of cancer. Someday PDT may be used to help treat larger solid tumors, too. A technique known as *interstitial therapy* involves using imaging tests (such as CT scans) to guide fiber optics directly into tumors using needles. This may be especially useful in areas that would require major surgery. Early results of studies of interstitial therapy in head and neck, liver, prostate, and pancreas tumors have been promising. [*www-cancer.org*].

Bibliography

Adams, G. P., Weiner, L. M. (2005). Monoclonal antibody therapy of cancer. *Nature Biotechnology*: 23 (9): 1147-1157.

Amendola, V. and Meneghetti M. (2011) Exploring how to increase the brightness of surface enhanced raman spectroscopy nanolabels: the effect of the raman active molecules and of the label size. *Adv. Funct. Mater*. Vol 22 (2) 353-360.

Amendola, V., Meneghetti, M., Granozzi, G., Agnoli, S., Polizzi, S., Riello, P., Boscaini, A., Anselmi, C., Fracasso, G., Colombatti,M., Innocenti, C., Gatteschi, D., and Sangregorio, C. (2011). Top down synthesis of multifunctional Iron Oxide nanoparticles for macrophage labelling and manipulation. *Journal of Materials Chemistry*; Vol 21, 3803-3813

Amendola, V., Meneghetti, M., Fiameni, S., Polizzi, S., Fracasso, G., Boscaini, A., Colombatti, M. (2011).SERS labels for quantitative assay: application to the quantification of gold nanoparticles uptaken by macrophage cells; *The Journal of Physical Chemistry*; vol 3 -849-856

Akerman, M.E. et al. (2002). Nanocrystal targeting in vivo. *Proc. Natl. Acad. Sci. U. S. A*. :99, 12617-12621

Arayne, M.S. and Sultana N. (2006). Nanopartcles in drug delivery for the treatment of cancer. *Pak.J.Pharm.Sci*: Vol 19(3), 258-268

Athar, M., Mukhtar, H., Bickers, DR. (1988). Differential role of reactive oxygen intermediates in photofrin-I- and photofrin-II-mediated photoenhancement of lipid peroxidation in epidermal microsomal membranes. *J. Invest. Dermatol* :90(5) 652-7.

Ballou, B. et al. (2004). Noninvasive imaging of quantum dots in mice. *Bioconjug. Chem*: 15, 79-86

Bander,N.H., Trabulsi,E.J. , Kostakoglu L. , et al. (2003). Targeting metastatic prostate cancer with radiolabeled monoclonal antibody J591 to the extracellular domain of prostate specific membrane antigen*. J Urol*: 170:1717-1721

Bharat Bhushan. (2010). Introduction to Nanotechnology. *Springer Handbook of Nanotechnology.*

Brannon-Peppas, L., Blanchette, J.O. (2004). Nanoparticle and targeted systems for cancer therapy. *Advanced Drug Delivery Reviews* 56 1649- 1659

Brigger, I., Dubernet, C., Couvreur, P. (2002). Nanoparticles in cancer therapy and diagnosis. *Advanced Drug Delivery Reviews:* 54, 631-651

Chan W.H. et al. (2006) CdSe quantum dots induce apoptosis in human neuroblastoma cells via mitochondrial-dependent pathways and inhibition of survival signals*. Toxicol. Lett.* : 167, 191-200

Chang, J.S., Chang, K.L., Hwang, D.F., Kong, Z.L. (2007). In vitro cytotoxicitiy of silica nanoparticles at high concentrations strongly depends on the metabolic activity type of the cell line. *Environ Sci Technol*.: 41:2064-2068

Chang, S., Reuter, V. et al (2001). Comparison of AntiProstate Specific Membrane Antigen Antibodies and other Immunomerkers in Metastatic Prostate Carcinoma. *Urology*;57(6).

Chang, S.S. et al. (2004). Overview of Prostate Specific Membrane Antigen. *Reviews in Urology*, vol 6 suppl. 10.

Chang, S.S., O'Keefe, D.S., Bacich, D.J., Reuter, V.E., Heston, W.D.W. and Gaudin P.B. (1999) Prostate specific membrane antigen is produced in tumor associated neovascolature. *Clin Cancer Res*.: 5:2674-2681.

Chang, S.S., Reuter, V.E. et al. (1999). Five Different Anti Prostate Specific Membrane Antigen (PSMA) Antibodies Confirm PSMA Expression in Tumor-associated Neovascolature. *Cancer Research* 59, 3192-3198.

Cramers, P., Ruevvekamp, M., Oppelaar, H., Dalesio, O., Baas, P., Stewart F.A. (2003). Foscan® uptake and tissue distribution in relation to photodynamic efficacy. *Br. J. Cancer* 88: 283-290.

Cho, K., Wang, X., Nie, S., Chen, Z. and Shin, D.M. (2008). Therapeutic Nanoparticles for Drug Delivery in Cancer. *Clin Cancer Res*;14 (5)

Choi, Y.E., Kwak, J.W. and Park, J.W. (2010). Nanotechnology for Early Cancer Detection. *Sensors*, 10, 428-455

Colombatti M, Grasso S, Porzia A, Fracasso G, Scupoli MT, Cingarlini S, Poffe O, Naim HY, Heine M, Tridente G, Mainiero F, Ramarli D. (2009). The prostate specific membrane antigen regulates the expression of IL-6 and CCL5 in prostate tumour cells by activating the MAPK pathways. *PLoS One*: 4(2):e4608.

Connor, E. E., Mwamuka, J., Gole, A., Murphy,C. J. and Wyatt M. D. (2005). Gold nanoparticles are taken up by human cells but do not cause acute cytotoxicity. *Small*: 1:325-327

Dan Peer et al. (2007). Nanocarriers as an emerging platform for cancer therapy. *Nature nanotechnology*: Vol 2, December.

David Conrad. (2006). Tumor Seeking Nanoparticles. NCI Alliance for Nanotechnology in Cancer: Monthly Feature, September.

Davis, M.I., Bennett, M.J. et al (2005). Crystal structure of Prostate Specific Membrane Antigen, a tumor marker and peptidase. *PNAS* April, vol 102, no. 17, 5981-5986

Davis,M.E., Chen, Z. & Shin, D.M. (2008). Nanoparticle therapeutics: an emerging treatment modality for cancer. *Nature Reviews Drug Discovery* 7, 771-782.

Dolmans, D.E., Fukumura, D., Jain, R.K. (2003). Photodynamic therapy for cancer. *Nat Rev Cancer*: 3:380-7

Dufort, S., Sancey, L., Coll, J.L. (2011).Physico-chemical parameters that govern nanoparticles fate also dictate rules for their molecular evolution. *Adv. Drug Deliv. Rev*., doi:10.1016/j.addr.2011.09.009

El-Sayed, I.H., Huang X., El-Sayed, M.A. (2005). "Surface plasmon resonance scattering and absorption of anti-EGFR antibody conjugated gold nanoparticles in cancer diagnostics: applications in oral cancer" *Nano Lett*: 5, 829-834

El-Sayed, I.H., Huang, X., El-Sayed, M.A. (2006). Selective laser photo-thermal therapy of epithelial carcinoma using anti-EGFR antibody conjugated gold nanoparticles. *Cancer Letters* 239, 129-135

Epenetos, A., Snook, D., Durbin, H., et al. (1986). Limitations of radiolabelled monoclonal antibodies for localisation of human neoplasms. *Cancer Res*: 46: 3183-3191

Fabrizio Gelain. (2007) Le nanotecnologie: mercato ed investimenti. Tinconzero No. 71.

Farokhzad, O.C. and Langer, R. (2009). Impact of Nanotechnology on Drug Delivery. *ACS NANO* vol 3 no1.

Ferlay,J., Parkin, D.M., Steliarova-Foucher, E. (2010). Estimates of cancer incidence and mortality in Europe in 2008. *EUROPEAN JOURNAL OF CANCER* 46, 765 -781.

Ferrari M.(2005). Cancer nanotechnology: opportunities and challenges. *Nature reviews*: Vol 5 March.

Fischer, H.C. and Chan, W.C. (2007) Nanotoxicity: the growing need for in vivo study. *Curr. Opin. Biotechnol:* 18, 565-571

Gao, Feng & Guo (2010). Antibody engineering promotes nanomedicine for cancer treatment. *Nanomedicine*: 5(8), 1141-1145

Gao, D., Xu, H., Philbert, M.A., Kopelman, R. (2007). Ultrafine hydrogel nanoparticles: synthetic approach and therapeutic application in living cells. *Angew. Chem. Int. Ed*. 46: 2224-2227

Ghosh, A. et al (2005). Novel Role of Prostate Specific Membrane Antigen in suppressing Prostate Cancer Invasiveness. *Cancer Research* :65 (3).

Gopee, N.V. et al. (2007) Migration of intradermally injected quantum dots to sentinel organs in mice. *Toxicol. Sci*. 98, 249-257

http://en.Wikipedia.org, Enciclopedia multimediale

Hu, C-M. J., Aryal, S., Zhang, L. (2010) Nanoparticle assisted combination therapies for effective cancer treatment. *Therapeutic Delivery* vol 1(2), 323-334

Hu, J.; Wang, Z.; Li, J. (2007) Gold nanopaticles with Special shake: Controlled Synthesis, Surface enhanced Raman Scattering and the Application in Biodetection. *Sensor, 7, 3299-3311.*

Ismail A.M. Ibrahim et al (2010). Preparation of spherical silica nanoparticles: Stober silica. *Journal of American Science*; 6(11)

Israeli, R.S., Thomas Powell, C. et al (1994). Expression of the Prostate Specific Membrane Antigen. *Cancer Research* 54, 1807-1811, April.

Jeremy Ramsden (2009). Essentials of Nanotechnology. Ramsden & Ventus Publishing ApS.

Jeremy Ramsden. (2009). Applied nanotechnology: the conversion of research results to products. Elsevir.

Jia, G. et al. (2005) Cytotoxicity of carbon nanomaterials: single-wall nanotube, multi-wall nanotube, and fullerene. *Environ. Sci. Technol.* 39, 1378-1383

Jin, Y., Kannan, S., Wu, M., Zhao, J.X. (2007). Toxicity of luminescent silica nanoparticles to living cells. *Chem Res Toxicol* : 20:1126-1133

Juarranz, A., Jaén, P., Sanz-Rodríguez, F., Cuevas, J., González, S., (2008). Photodynamic therapy of cancer. Basic principles and applications. *Clin Transl Oncol :* 10:148-154

Keren, S., Zavaleta, C., Cheng, Z., de La Zerda, A., Gheysens, O., Gambhir, S. S.. (2008). Noninvasive molecular imaging of small living subjects using Raman spectroscopy. *Proc Natl Acad Sci US*: 105, 5844- 5849

Khoury,C.G., Norton, S.J., Vo-Dinh, T. (2009). Plasmonics of 3-D Nanoshell Dimers Using Multipole Expansion and Finite Element Method, *ACS NANO* vol 3 no 9.

Kinzel V., Kaszkin M., Blume A., Richards J., (1990). Epidermal Growth Factor Inhibits Transiently the Progression from G2-Phase to Mitosis: A Receptor-mediated Phenomenon in Various Cells. *Cancer Research*, 50: 7932-7936.

Kipp, R.T., McNeel, D.G. (2007). Immunotherapy for Prostate Cancer- Recent Progress in Clinical Trials. *Clinical Adv Hematology Oncology*; 5(6):465-74-9.

Kneipp H. and Moskovits M. (2006) Surface-Enhanced Raman Scattering: Physics and Applications, Springer Verlag.

Kneipp, J., Kneipp,H., McLaughlin, M., Brown, D. and Kneipp K. (2006). In Vivo Molecular Probing of Cellular Compartments with Gold Nanoparticles and Nanoaggregates. *NANO Letters*: Vol 6, No 10 2225-2231.

Kneipp, K., Kneipp, H., Kneipp, J. (2006). Surface Enhanced Raman scattering in Local Optical Fields of Silver and Gold Nanoaggregates- From Single-Molecule Raman Spectroscopy to Ultrasensitive Probing in Live cells. *Acc. Chem. Res.* vol *39*, 443-450;

Köhler, G., Milstein, C. (1975).Continuous cultures of fused cells secreting antibody of predefined specificity. *Nature*: Aug 7;256(5517):495-7.

Kosharskyy, B., Solban, N., Chang, S.K., Rizvi, I., Chang, Y., Hasan, T. (2006). A mechanism-based combination therapy reduces local tumor growth and metastasis in an orthotopic model ofprostate cancer. *Cancer Res* ; 66: 10953-10958.

Kumar,A.P., Depan, D., Tomer, N.S., Singh, R.P., (2009). Nanoscale particles for polymer degradation and stabilization. Trends and future perspectives. *Progress in Polymer Science*: Volume 34, Issue 6, June, Pages 479-515

L.L.Green (1999). Antibody engineering via genetic engineering of the mouse: XenoMouse strains are a veicle for the facile generation of therapeutic human monoclonal antibodies. *Journal of Immunological Methods* 231, 11-23.

Lafky, J.M., Wilken, J.A., Baron, A.T., Maihle, N.J., (2008). Clinical implications of the ErbB/epidermal growth factor (EGF) receptor family and its ligands in ovarian cancer. *Biochimica et Biophysica Acta*, 1785: 232-265

LaRocque, J., Bharali, D.J. et al. (2009). Cancer Detection and Treatment: The Role of Nanomedicines*. Mol Biotechnol*: 42:358-366

Lei Sun et al, (2007). Composite organic inorganic nanoparticles as raman labels for tissue analysis. *Nano letters*, vol 7 no 2 351-356

Le Ru, E. C., Blackie, E., Meyer, M., Etchegoin, P. G. (2007). Surface Enhanced Raman scattering enhancement Factors: A Comprehensive Study. *J. Phys. Chem. C* vol *111*, 13794-13803;

Lee, K., Vladimir P. Drachev, V.P., and Irudayaraj, J. (2011). DNA-Gold Nanoparticle Reversible Networks Grown on Cell Surface Marker Sites: Application in Diagnostics. *ACS NANO* vol 5 no 3;

Lee, Y.S. et al. (2006). Nanoparticle Probes with Surface Enhanced Raman Spectroscopic Tags for Cellular Cancer Targeting. *Anal. Chem*. 78, 6967-6973

Li,Y., Cozzi, P.J., Russel, P.J. (2009) Promising Tumor Associated antigens for Future Prostate Cancer Therapy. *Medical Research Reviwes*, Vol 30 No 1, 67-101

Lin, W., Huang, Y.W., Zhou, X.D., Ma, Y. (2006). In vitro toxicity of silica nanoparticles in human lung cancer cells. *Toxicol Appl Pharmacol*: 217:252-259

Lin, Y.S. and Haynes, C.L. (2010). Impacts of Mesoporous Silica Nanoparticle Size, Pore Ordering, and Pore Integrity on Hemolytic Activity. *J. Am. Chem*. Soc. 132, 4834-4842

Little, M., Kipriyanov S.M. et al. (2006). Of mice and man: hybridoma and recombinant antibodies. *Immunology Today*: 364, vol 21, no 8.

Liu, Y., Miyoshi, H. and Nakamura M. (2007). Nanomedicine for drug delivery and imaging: A promising avenue for cancer therapy and diagnosis using targeted functional nanoparticles. *Int. J. Cancer*: 120, 2527-2537.

Lombardi, J. R.; Birke, R. L. (2009) A Unified View of Surface Enhanced Raman Scattering. *Acc. Chem. Res.* vol 42, 734-742

Lovric _, J. et al. (2005) Differences in subcellular distribution and toxicity of green and red emitting CdTe quantum dots. *J. Mol. Med*. 83, 377-386

Lovric, J. et al. (2005) Unmodified cadmium telluride quantum dots induce reactive oxygen species formation leading to multiple organelle damage and cell death. *Chem. Biol.* 12, 1227-1234

M. Eghtedari et al. (2009). Engineering of Hetero-Functional Gold Nanorods for the in vivo Molecular Targeting of Breast Cancer Cells. *Nano Lett.* :9, 287-291

McAteer, M.A. et al. (2007) In vivo magnetic resonance imaging of acute brain inflammation using microparticles of iron oxide. *Nat. Med.* 13, 1253-1258

McNeil S.E. (2005). Nanotechnology for the biologist. *Journal of Leukocyte Biology* Volume 78.

Mohanraj, V.J. and Chen, Y. (2006). Nanoparticles - A Review. *Tropical Journal of Pharmaceutical Research*; 5 (1): 561-573

Nel, A., Xia, T., Madler, L., Li, N. (2006) Toxic potential of materials at the nanolevel. *Science* 311, 622-667

Nie, S., Emory, S. R. (1997). Probing Single Molecules and Single Nanoparticles by Surface Enhanced Raman Scattering. *Science*, vol 275, 1102;

Nie, S., Xing,Y., Kim, G.J. and Simons, J.W. (2007). Nanotechnology Applications in Cancer. *Annu. Rev. Biomed. Eng.* .9:257-88

Oberdorster, G., Oberdorster, E.,Oberdorster. J. (2005) Nanotoxicology: an emerging discipline evolving from studies of ultrafine particles. *Environ. Health Perspect*. 113, 823-839

Ohulchanskyy, T.Y., Roy, I., Goswami, L.N., Chen, Y., Bergey, E.J., Pandey, R.K., Oseroff, A. R. and Prasad, P. N. (2007). Organically modified silica nanoparticles with covalently incorporated photosensitizer for photodynamic therapy of cancer. *Nano Lett.* 7(9) 2835-42.

Pan, Y., Neuss, S., Leifert, A. , Fischler, M. , Wen, F., Simon, U., Schmid, G. , Brandau, W. and Jahnen-Dechent, W. (2007). Size-dependent cytotoxicity of gold nanoparticles. *Small* 3:1941-1949

Pankhurst, Q. A., Connolly, J., Jones, S. K. and J Dobson (2003). Applications of magnetic nanoparticles in biomedicine. *J. Phys. D: Appl. Phys*. :36 R167-R181

Parveen,S., Misra,R., Sahoo, S.K. (2011). Nanoparticles: a boon to drug delivery, therapeutics, diagnostics and imaging. *Nanomedicine*: doi:10.1016/j.nano.2011.05.016

Pastan, I., Hassan, R., FitzGerald, D. J., Kreitman, R. J. (2006). Immunotoxin therapy of cancer. *Nature Reviews in cancer* 6: 559-565.

Patra, C.R., Bhattacharya, R., Mukhopadhyay, D. and Mukherjee, P. (2010) Fabrication of Gold Nanoparticles for targeted therapy in pancreatic cancer. *Adv Drug Deliv Rev*: March 8; 62(3): 346-361

Perner,S., Hofer, M.D. et al. (2007). Prostate Specific Membrane Antigen expression as a predictor of Prostate Cancer Progression. *Human Pathology*, 38,696-701.

Pernodet, N. et al. (2006) Adverse effects of citrate/gold nanoparticles on human dermal fibroblasts. *Small* 2, 766-773

Pisanic, T.R., II et al. (2007) Nanotoxicity of iron oxide nanoparticle internalization in growing neurons. *Biomaterials* 28, 2572-2581

Portney, N.G., Ozkan, M. (2006). Nano-oncology: drug delivery, imaging, and sensing. *Anal Bioanal Chem* 384: 620-630

Postiglione, I., Chiaviello, A., Palumbo, G., (2011). Enhancing Photodynamyc Therapy Efficacy by Combination Therapy: Dated, Current and Oncoming Strategies. *Cancer* 3, 2597-2629.

Qian, X. M.; Nie, S. M. (2008). Single molecule and single nanoparticle SERS: from fundamental mechanism to biomedical applications. *Chem. Soc. Rev*. Vol 37, 912-920;

Qian, X.; Peng, X. H.; Ansari, D. O.; Yin-Goen, Q.; Chen, G. Z.; Shin, D. M.; Yang, L.; Young, A. N.; Wang, M. D.; Nie, S. (2008) In vivo tumor targeting and spectroscopic detection with surface enhanced Raman nanoparticle tags. *Nat. Biotechnol.* vol 26, 83-90

Radwan, S.H. and Azzazy, H.M.E (2009). Gold nanoparticles for molecular diagnostics. *Expert Rev. Mol. Diagn*. 9(5), 511-524.

Raj Bawa. (2008). Nanoparticles-based therapeutics in Humans: a Survey Nanotechnology. Law & Business-Summer.

Ray, S., Reddy, P.J., Choudhary, S., Raghu, D., Srivastava, S. (2011). Emerging nanoproteomics approaches for disease biomarker detection: a current perspective. *Journal of Proteomics* (74)12.

Ratner, M., Ratner, D. (2002). Nanotechnology: A Gentle Introduction to the Next Big Idea. Prentice Hall, November 08

Ravi Kumar, M.N.V., Sameti, M., Mohapatra, S.S., Kong, X., Lockey, R.F., Bakowsky, U., Lindenblatt, G., Schmidt, C.H., Lehr, M. (2004). Cationic Silica Nanoparticles as Gene Carriers: Synthesis, Characterization and Transfection Efficiency In vitro and In vivo. *Journal of Nanoscience and Nanotechnology*, 4:876-881

Reichert, J.M., Rosensweig, C.J., Faden, L.B., Dewitz, M.C.(2005). Monoclonal antibody successes in the clinic. *Nat Biotechnol*. ;23(9):1073-8.

Reichert, J.M., Valge-Archer, V.E.(2007). Development trends for monoclonal antibody cancer therapeutics. *Nat Rev Drug Discov*. ;6(5):349-56.

Reiter, R.E., Gu, Z., Watabe, T., Thomas, G., Szigeti, K., Davis, E., Wahl, M., Nisitani,S., Yamashiro, J., Le Beau, M., Loda, M., Witte, O. (1998) Prostate stem cell antigen: a cell surface marker overexpressed in prostate cancer. *Proc. Natl. Acad. Sci. USA* 95:1735-1740

Robbins (1999). Pathologic basis of disease. Sixth Edition, W. B. Saunders Company, Philadelphia, Pennsylvania, USA .

Ron, R., Allison, M.D., Sibata, C.H. PhD (2010). Oncologic photodynamic therapy photosensitizers: A clinical review*. Photodiagnosis and Photodynamic Therapy*: 7, 61-75

Roque, A.C. et al (2004). Antibodies and Geneti cally Engineered Related Molecules: Production and Purification. *Biotechnology Progr.* : vol 20, no 3.

Roy, I., Ohulchanskyy, T.Y., Pudavar, H.E., Bergey, E.J., Oseroff, A.R., Morgan, J., Dougherty, T.J., Prasad, P.N. (2003). Ceramic-based nanoparticles entrapping water-insoluble photosensitzing anticancer drugs: a novel drug-carrier system for photodynamic therapy. *J. Am. Chem. Soc.* 125: 7860-7865

Rozanova, N. and Zhang, J.Z. (2009).Photothermal ablation therapy for cancer based on metal nanostructures. *Sci China Ser B-Chem* :vol. 52, no. 10,1559-1575

Sanvicens, N. and Marco, M.P. (2008). Multifunctional nanoparticles -properties and prospects for their use in human medicine. *Trends in Biotechnology* Vol.26 No.8

Sato, J.D., Kawamoto, T., Le, A.D., Mendhelson, J., Polikoff, J., Sato, G.H., (1983). Biological effects in vitro of monoclonal antibodies to human epidermal growth factor receptors. *Mol Biol Med*, 1: 511-529.

Sayes, C.M. et al. (2005) Nano-C60 cytotoxicity is due to lipid peroxidation. *Biomaterials* 26, 7587-7595

Schrama, D., Reisfeld, R.A., Becker, J.C. (2006). Antibody targeted drugs as cancer therapeutics. *Nat Rev Drug Discov*. Feb;5(2):147-59.

Sharkey, R. M., Goldenberg, D. M. (2006). Targeted therapy of cancer: new prospects for antibodies and immunoconjugates. *CA Cancer J. Clin*. 56: 226-243

Sharkey, R. M., Goldenberg, D. M. (2008). Use of antibodies and immunoconjugates for the therapy of more accessible cancers. *Advanced Drug Delivery Reviews*. 60: 1407-1420.

Shubayev, V.I., Pisanic, T.R., Jin, S. (2009). Magnetic nanoparticles for theragnostics. *Advanced Drug Delivery Reviews* 61, 467-477

Silva, G.A., M.Sc., (2004). Introduction to Nanotechnology and Its Applications to Medicine. Surg Neurol ;61:216-20

Singh, R., Lillard Jr, J.W. (2009). Nanoparticle-based targeted drug delivery. *Experimental and Molecular Pathology* 86 215-223

Sinha, R., Kim, G.J., Nie, S. and Shin, D.M. (2006) Nanotechnology in cancer therapeutics: bioconjugated nanoparticles for drug delivery. *Mol Cancer Ther*;5 (8). August.

Stricker, N., Li, M. et al. (2001). Phage Display Technologies. Encyclopedia of life sciences.

Thariat, J., Milas ,L., Ang, K., (2007). Integrating radiotherapy with epidermal growth factor receptor antagonists and other molecular therapeutics for the treatment of head and neck cancer. *Int Radiation Oncology Biol Phys*, 69 (4): 974-984

Tsoli, M., H. Kuhn, W. Brandau, H. Esche, and G. Schmid. (2005). Cellular uptake and toxicity of Au55 clusters. *Small* 1:841-844

Verma, S., Watt, G.M., Mai, Z., and Hasan, T. (2007). Strategies for Enhanced Photodynamic Therapy Effects. *Photochemistry and Photobiology*, 83: 996–1005

Villanueva, A., Ca˜nete, M., Roca, A. G., Calero, M., Veintemillas-Verdaguer, S., Serna, C. J., del Puerto Morales, M. and Miranda, R. (2009), The influence of surface functionalisation on the enhanced internalisation of magnetic nanoparticles in cancer cells. *Nanotechnology* 20:115103.

Vinogradov, S.V., Batrakova, E.V. and Kabanov, A.V. (2004). Nanogels for Oligonucleotide Delivery to the Brain. *Bioconjug Chem*; 15(1): 50-60

Voura, E.B. et al. (2004) Tracking metastatic tumor cell extravasation with quantum dot nanocrystals and fluorescence emission-scanning microscopy. *Nat. Med*. 10, 993-998

Wang, A.Z., Gu , F. , Zhang , L., Chan , J.M., Radovic-Moreno , A., Shaikh M.R. & Farokhzad O.C.(2008). Biofunctionalized targeted nanoparticles for therapeutic applications. *Expert Opin. Biol. Ther:* 8(8):1063-1070

Weissleder, R., Moore, A., Mahmood, U., Bhorade, R., Benveniste, H.,Chiocca, E.A. and Basilion J.P. (2000). In vivo magnetic resonance imaging of transgene expression. *Nature Medicine*, vol 6, no 3.

Wu, A. M., Senter, P. D. (2005). Arming antibodies: prospects and challenges for immunoconjugates*. Nature Biotechnology* 23 (9): 1137-1146.

www.fda.gov/Drugs

Yang X.D., Wang P., Fredlin P., Davis C.G., (2002). ABX-EGF, a fully human anti-EGF receptor monoclonal antibody: inhibition of prostate cancer in vitro and in vivo. *ASCO Annual Meeting*.

Zavaleta, C. L.; Smith, B. R.; Walton, I.; Doering, W.; Davis, G.; Shojaei, B.; Natan, M. J.; Gambhir, S. S. (2009). Multiplexed imaging of surface enhanced Raman scattering nanotags in living mice using noninvasive Raman spectroscopy. *Proc. Natl. Acad. Sci. USA* Vol *106*, 13511-13516;

Zhang, L., Gu, F.X., Chan, J.M., Wang, A.Z., Langer R.S. and Farokhzad O.C. (2008). Nanoparticles in Medicine: Therapeutic Applications and Developments. *Clinical pharmacology and therapeutics*: vol 83, n. 5.

Zimmermann, M., Zouhair, A., Azria, D., Ozsahin, M., (2006). The epidermal growth factor receptor in head and neck cancer: its role and treatment implication. *Radiat. Oncol*, 1:11